Molecular mechanism of protein translocation across the mitochondrial outer membrane

タンパク質のミトコンドリア外膜透過の分子機構の解析

2001 Ph. D. Thesis

Masatoshi Esaki

江崎 雅俊

報告番号	甲第 4928 号

Molecular mechanism of protein translocation across the mitochondrial outer membrane

タンパク質のミトコンドリア外膜膜透過の分子機構の解析

2001 Ph.D. Thesis

Masatoshi Esaki

江崎雅俊

Department of Chemistry

Graduate School of Science

Nagoya University

I wish to express my greatest gratitude to Professor Toshiya Endo

for his continuous guidance and kind encouragement throughout the present study.

I am grateful to Drs. Shuh-ichi Nishikawa and Takashi Kanamori

for their valuable advice and their encouragement over the past six years.

I am deeply indebted to Dr. Tohru Yoshihisa

for his helpful advice and discussions.

Also, I express my thanks

to Drs. Peter G. Schultz and Injae Shin (University of California, Berkeley)

for providing materials used in amber suppressor tRNA method;

to Dr. Takahiro Hohsaka (Okayama University)

for his advice on the synthesis of BPA.

I also thank Hayashi Yamamoto and Tomoko Ono

for providing mutant yeast strains lacking TOM22C, TOM5, TOM6, and/or TOM7.

And I thank all the members of Prof. Endo's laboratory

for technical assistance and helpful discussions.

Masatoshi Esaki

Masatoshi Esaki

February 2001

CONTENTS

ABBREVIATIONS

The following abbreviations were used in this thesis

BPA	DL-2-amino-5-(*p*-benzoylphenyl)pentanoic acid
BSA	bovine serum albumin
CCCP	carbonyl cyanide *m*-chlorophenylhydrazone
DHFR	mouse dihydrofolate reductase
DTT	dithiothreitol
$\Delta\Psi$	membrane potential
EDTA	ethylenediaminetetraacetic acid
HBD	heme binding domain
IMS	mitochondrial intermembrane space
kDa	kilodalton
Mops	3-[*N*-morpholino]propanesulfonic acid
MPP	matrix processing peptidase
mtHsp70	heat shock protein 70 in the mitochondrial matrix
MTX	methotrexate
NADH	β-nicotinamide adenine dinucleotide reduced form
NADPH	β-nicotinamide adenine dinucleotide phosphate reduced form
PAGE	polyacrylamide gel electrophoresis
SDS	sodium dodecyl sulfate
TIM	translocase of the inner mitochondrial membrane
TOM	translocase of the outer mitochondrial membrane
Tom22C	C-terminal domain of Tom22
Tris	tris(hydroxymethyl)aminomethane

Chapter 1

General introduction

1-1 Introduction

Eukaryotic cells are subdivided into membrane-bound compartments called organelles that play unique roles in growth and cellular metabolism. Each organelle contains unique sets of proteins that catalyze requisite chemical reactions, transfer metabolites, protect cells and organelles against stresses, etc. Almost all of these proteins are encoded by the nuclear genes and synthesized on the cytosolic ribosomes. Therefore, newly made proteins must be localized to their specific destinations including organelle interiors by crossing biological membranes (Fig.1-1). Each organelle membrane contains a specific pore complex through which proteins can traverse the membrane. Although proteins can move through a pore complex in both directions, the actual protein translocation occurs in only one direction. How do proteins move across the membrane from one side to the other side in a unidirectional manner?

1-2 Unidirectional translocation

Several mechanisms for the unidirectionality of the protein movement across the membrane have been proposed. Protein translocation across the bacterial membrane is typically mediated by the SecYEG complex and SecA (1). The SecYEG complex forms a hydrophilic pore, through which proteins can be transported from the cytoplasm to the periplasm. SecA is a peripheral membrane protein located on the cytoplasmic side and functions as a translocation motor that pushes proteins across the membrane in an ATP-dependent manner. In the case of the post-translational translocation across the membrane of the endoplasmic reticulum (ER), proteins move through the Sec61 complex with the aid of ER luminal Hsp70, BiP, which utilizes the energy of ATP hydrolysis to achieve the unidirectionality of the translocation (2, 3). In the case of the co-translational protein translocation across the ER membrane, the energy provided by the protein synthesis reaction may well generate the driving force

for the unidirectional protein translocation (3). Mitochondria consist of two membranes (see below). The protein translocation across the mitochondrial inner membrane utilizes the membrane potential ($\Delta\Psi$) across the inner membrane and the energy of the ATP hydrolysis by Hsp70 in the matrix to achieve unidirectionality of the protein movement (2). Chloroplasts are surrounded by two envelope membranes and contain the thylakoid membranes in their interiors. The translocation across the chloroplast envelope membranes requires the energy of both ATP and GTP hydrolysis, and that across the thylakoid membrane depends on ATP and/or ΔpH across the thylakoid membrane (4). These energies may well drive the unidirectional protein movement across the membranes.

Thus in many cases, unidirectional protein translocation is achieved by coupling transport to the ATP/GTP hydrolysis or to the utilization of the $\Delta\Psi/\Delta$pH across the membranes. However, there are a few exceptional cases in which apparently no energy is required to generate a vectorial driving force for protein translocation. For example, protein translocation across the mitochondrial outer membrane does not depend on ATP or GTP and there is no membrane potential or proton gradient across the outer membrane. Then what drives the unidirectional protein translocation across the mitochondrial outer membrane? The present study has focused on this question in particular with respect to the mechanism of protein translocation and the roles of the translocation channel in the translocation process.

1-3 Mitochondria

Mitochondria are essential organelles that carry out oxidative phosphorylation, thereby producing most of the ATP molecules in eukaryotic cells. A mitochondrion is made up of two membrane systems that subdivide the organelle into two aqueous subcompartments, the intermembrane space, IMS, between the outer and the inner membranes, and the matrix, which is enclosed by the inner membrane. While the

mitochondrion has its own genome and a system for protein synthesis, only about ten proteins are encoded by the mitochondrial genome. The majority of mitochondrial proteins are encoded by the nuclear genes and synthesized in the cytosol.

1-4 Targeting of proteins to mitochondria

Mitochondrial proteins contain sufficient information for targeting to mitochondria and sorting to intramitochondrial compartments (5, 6). Many mitochondrial proteins are synthesized with an N-terminal extension, a presequence, which contains the matrix targeting signal and is removed proteolytically by matrix processing protease (MPP) in the matrix (7). Other mitochondrial proteins synthesized without a cleavable presequence have targeting/sorting information within their internal sequences (8).

In principle, protein import into mitochondria can take place in a post-translational manner and require coordinated actions of factors outside the mitochondria as well as those inside the mitochondria. In some cases, cytosolic factors are involved in protein targeting to mitochondria. Two chaperones in the cytosol, Hsp70 and mitochondrial import stimulation factor (MSF), have been shown to bind to some precursor proteins and to prevent misfolding or aggregation of the proteins during or following the completion of their synthesis (9-11). In *in vivo* situation, translation and translocation of some mitochondrial proteins can be at least kinetically coupled. The nascent polypeptide-associated complex (NAC) may facilitate this co-translational protein import (12).

1-5 Translocase of the outer membrane

The mitochondrial outer membrane contains a translocase complex, TOM. In yeast *Saccharomyces cerevisiae*, nine proteins constituting the TOM complex have been identified (Fig. 1-2). The major subunits are Tom70, Tom40, Tom22, Tom20, Tom7,

Tom6, and Tom5, with the number indicating the monomeric molecular mass (in kDa) of the protein (13). Tom72, a poorly expressed homologue of Tom70, and Tom37, a proposed partner of Tom70, have also been identified (14-16). Among these proteins, only Tom40 and Tom22 are essential proteins for cell viability (17, 18). Tom70 and Tom20 are anchored to the membrane by their N-terminal hydrophobic segments and expose the large C-terminal domains to the cytosol which are involved in recognition of mitochondrial targeting signals (19-21). Tom20 serves as a receptor preferentially for precursor proteins with a presequence, whereas Tom70 binds to proteins bearing internal targeting signal (22). The N-terminal domain of Tom22 exposed to the cytosol are rich in acidic residues and may help the receptor function of Tom20 by binding to the mitochondrial targeting signals of precursor proteins (23). Tom5 contains a single membrane anchor and a small hydrophilic domain exposed to the cytosol, and facilitates protein transfer from the receptors to the channel (24). The membrane-embedded protein Tom40 forms a hydrophilic channel through which proteins traverse the outer membrane (25, 26). Other small proteins, Tom7 and Tom6, seem to play indirect roles in protein translocation by modulating the dynamics of the assembly of the TOM complex; Tom6 promotes the assembly of the TOM subunits, and Tom7 promotes their disassembly (27).

1-6 Translocase of the inner membrane

The mitochondrial inner membrane contains at least two translocase complexes mediating the translocation of nuclear-encoded proteins across the inner membrane (Fig. 1-2). The Tim23 complex mainly mediates the translocation of presequence-bearing proteins into the matrix and the Tim22 complex mediates the insertion of presequence-less proteins into the inner membrane (28). The Tim23 complex consists of Tim23, Tim17, and Tim44. The integral membrane proteins Tim23 and Tim17 probably form a protein-conducting channel of the inner membrane

(29-31). The hydrophilic peripheral membrane protein Tim44 is associated with both Tim23 and Tim17 on the matrix side and functions as an anchor for the matrix chaperone, mitochondrial Hsp70 (mtHsp70), which supplies the driving force for the unidirectional polypeptide translocation (30-32). The Tim22 complex consists of at least three integral membrane proteins, Tim22, Tim54, and Tim18, and mediates the integration of the members of the carrier protein family including ADP/ATP carrier and phosphate carrier into the inner membrane (33-36). Five small proteins in the IMS, Tim8, Tim9, Tim10, Tim12, and Tim13, are also involved the translocation of the inner membrane proteins. These small soluble proteins form complexes with each other and mediate transfer of the proteins from the TOM complex to the TIM complexes (37). On the other hand, the translocation of the mitochondrial genome-encoded inner membrane proteins is mediated by the Oxa1 complex, which consists of Oxa1p and unidentified components (38).

1-7 Energy requirement for the translocation across the mitochondrial membranes

Protein import into the mitochondrial matrix requires both $\Delta\Psi$ across the inner membrane and ATP hydrolysis in the matrix. The precise role of $\Delta\Psi$ is still open, but it is required for the presequence to enter the TIM channel and to move across the inner membrane (39). The energy of ATP hydrolysis is used by mtHsp70 for the subsequent translocation of the rest part of the protein across the inner membrane, although the precise mechanism of this process is controversial (2, 40).

In contrast to the translocation across the inner membrane, translocation across the outer membrane occurs independently of $\Delta\Psi$ or ATP. Indeed, a membrane potential across the outer membrane does not exist, and an ATP-dependent chaperone like Hsp70 has not been found in the IMS. In order to reveal the mechanism for the vectorial protein translocation across the outer membrane without coupling to any energy sources, I used cytochrome b_2 as a model precursor protein. Cytochrome b_2 is a

soluble protein localized in the IMS, and the translocation of the cytochrome b_2 precursor consists of two steps. The first step is driven by $\Delta\Psi$ across the inner membrane and by ATP-dependent mtHsp70, but the second step is independent of $\Delta\Psi$ and mtHsp70. Therefore, I analyzed the late $\Delta\Psi$- and mtHsp70-independent step as a model case for the energy-independent protein translocation across the outer membrane. I show in the next chapter that the translocation of the mature part of cytochrome b_2 is driven by two distinct mechanisms.

1-8 New features of subunits of the TOM complex

If the driving force for the unidirectional protein translocation across the outer membrane is provided by the mechanisms which are independent of the functions of the TOM complex, what are the roles of the TOM complex in protein translocation? Does the TOM complex merely function as a receptor for mitochondrial proteins and provide a passive protein-conducting channel? In Chapters 3 and 4, I focused on these questions.

In Chapter 3, I tried to characterize the nature of the TOM complex channel, which mainly consists of Tom40. Systematic analyses of site-specific photocrosslinking of cytochrome b_2 fusion proteins in transit across the outer membrane revealed that Tom40 tends to interact with unfolded segments of the translocating polypeptide chain. This suggests that Tom40 functions not only as a protein-conducting channel but also as a chaperone for unfolded translocating proteins.

In Chapter 4, I analyzed the roles of presequence binding sites of the TOM complex in translocation of the presequence part of the mitochondrial proteins across the mitochondrial membranes. Previous studies showed that the TOM complex contains binding sites for the presequence on both side of the outer membrane, the '*cis* site' on the cytosolic side and the '*trans* site' on the IMS side (41). The cis site most likely consists of receptor proteins including Tom20. On the other hand, components

constituting the trans site have not been previously determined and their roles in protein translocation across the mitochondrial membranes have not been resolved clearly. In the present study, I revealed that Tom40, the IMS domain of Tom22, and Tom7 constitute or are close to the trans site of the TOM complex. By using mutant mitochondria lacking both Tom7 and the IMS domain of Tom22, I showed that both Tom7 and the IMS domain of Tom22 are important for the presequence transfer from the TOM complex to the Tim23 complex.

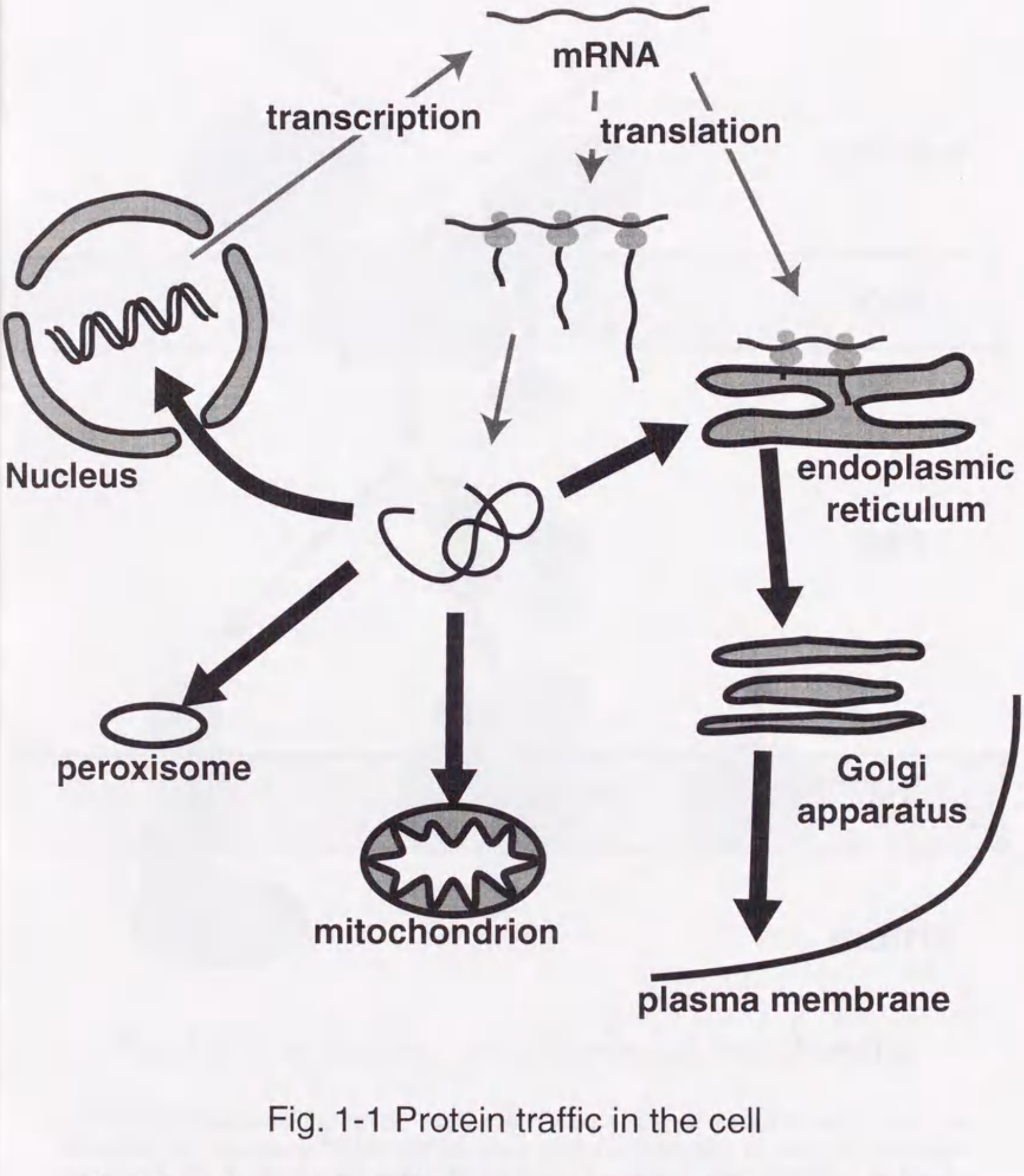

Fig. 1-1 Protein traffic in the cell

Almost all proteins are synthesized in the cytosol and transferred to their correct destinations.

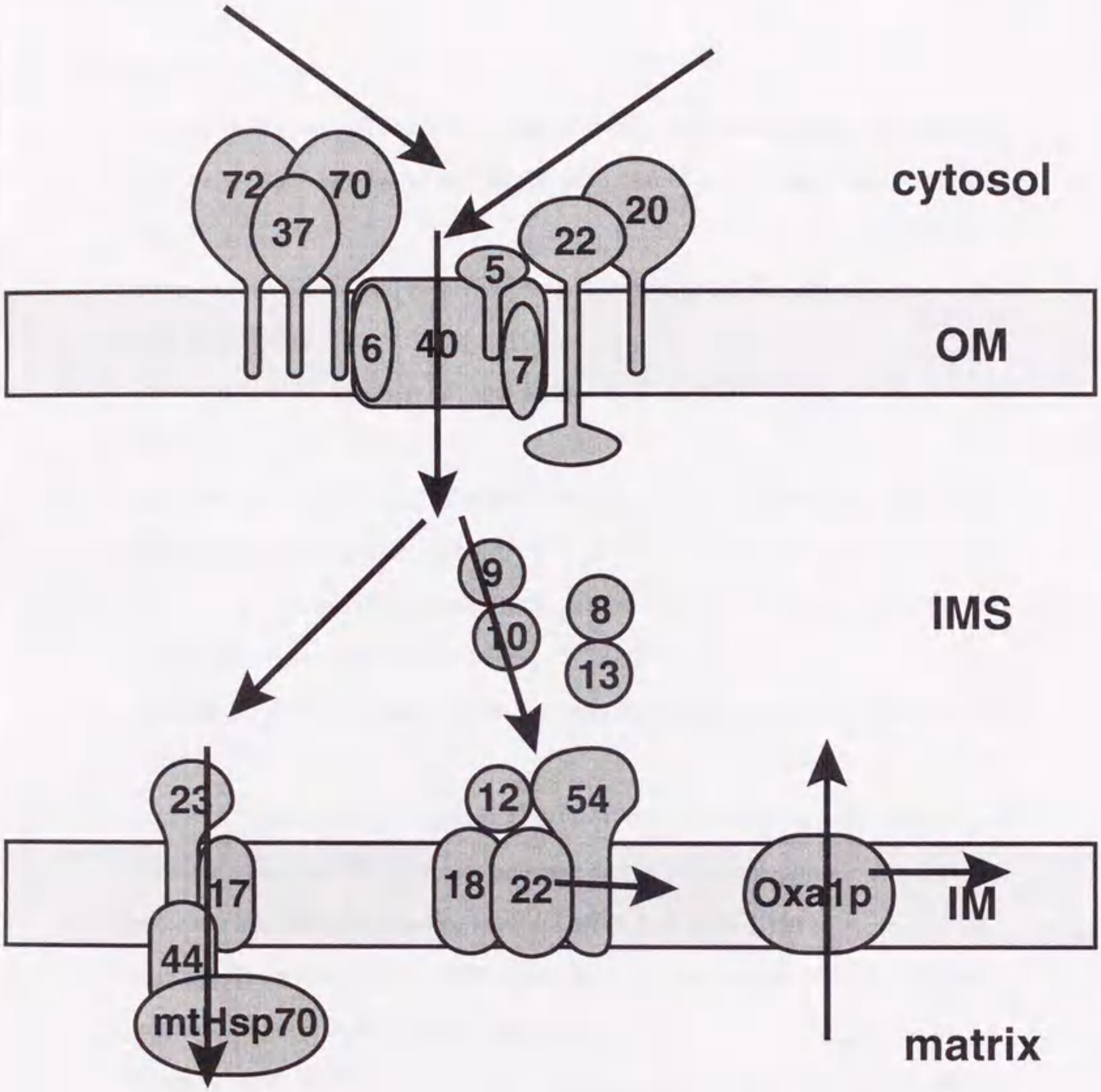

Fig. 1-2 Translocation machineries of mitochondria

Many components of the protein translocation machineries of the outer and of the inner mitochondrial membranes (TOM and TIM, respectively) are identified in yeast *Saccharomyces cerevisiae*. These proteins are named Tom for proteins in the outer membrane or Tim for proteins in the intermembrane space or in the inner membrane with specific numbers representing thier molecular weights. OM, outer membrane; IMS, intermembrane space; IM, inner membrane.

References

1. Dalbey, R. E. and Robinson, C. (1999) Protein translocation into and across the bacterial plasma membrane and the plant thylakoid membrane. *Trends Biochem. Sci.*, **24**, 17-22
2. Pilon, M. and Schekman, R. (1999) Protein translocation: How Hsp70 pulls it off. *Cell*, **97**, 679-682
3. Matiack, K. E. S., Mothes, W., and Rapoport, T. A. (1998) Protein translocation: Tunnel vision. *Cell*, **92**, 381-390
4. Keegstra, K. and Cline, K. (1999) Protein import and routing systems of chloroplasts. *Plant Cell*, **11**, 557-570
5. Pfanner, N., Craig, E. A., and Hönlinger, A. (1997) Mitochondrial preprotein translocase. *Annu. Rev. Cell Dev. Biol.*, **13**, 25-51
6. Neupert, W. (1997) Protein import into mitochondria. *Annu. Rev. Biochem.*, **66**, 863-917
7. Hurt, E. C., Pesold-Hurt, B., and Schatz, G. (1984) The amino-terminal region of an imported mitochondrial precursor polypeptide can direct cytoplasmic dihydrofolate reductase into the mitochondrial matrix. *EMBO J.*, **3**, 3149-3156
8. Pfanner, N and Neupert, W. (1987) Distinct steps in the import of ADP/ATP carrier into mitochondria. *J. Biol. Chem.*, **262**, 7528-7536
9. Deshaies, R. J., Koch, B. D., Werner-Washburne, M., Craig, E. A., and Schekman, R. (1988) A subfamily of stress proteins facilitates translocation of secretory and mitochondrial precursor polypeptides. *Nature*, **332**, 800-805
10. Endo, T., Mitsui, S., Nakai, M., and Roise, D. (1996) Binding of mitochondrial presequences to yeast cytosolic heat shock protein 70 depends on the amphiphilicity of the presequence *J. Biol. Chem.*, **271**, 4161-4167
11. Hachiya, N., Mihara, K., Suda, K., Horst, M., Schatz, G., and Lithgow, T. (1995) Reconstitution of the initial steps of mitochondrial protein import. *Nature*, **376**,

705-709

12. Fünfschilling, U. and Rospert, S. (1999) Nascent Polypeptide-associated complex stimulates protein import into yeast mitochondria. *Mol. Biol. Cell*, **10**, 3289-3299

13. Pfanner, N., Douglas, M. G., Endo, T., Hoogenraad, N. J., Jensen, R. E., Meijer, M., Neupert, W., Schatz, G., Schmitz, U. K., and Shore, G. C. (1996) Uniform nomenclature for the protein transport machinery of the mitochondrial membranes. *Trends Biochem. Sci.*, **21**, 51-52

14. Bömer, U., Pfanner, N., and Dietmeier, K. (1996) Identification of a third yeast mitochondrial Tom protein with tetratrico peptide repeats. *FEBS lett.*, **382** 153-158

15. Schlossmann, J., Lill, R., Neupert, W., and Court, D. A. (1996) Tom71, a novel homologue of the mitochondrial preprotein receptor Tom70. *J. Biol. Chem.*, **271**, 17890-17895

16. Gratzer, S., Lithgow, T., Bauer, R. E., Lamping, E., Paltauf, F., Kohlwein, S. D., Haucke, V., Junne, T., Schatz, G., and Horst, M. (1995) Mas37p, a novel receptor subunit for protein import into mitochondria. *J. Cell Biol.*, **129**, 25-34

17. Kevin, P. B., Schaniel, A., Vestweber, D., and Schatz, G. (1990) A yeast mitochondrial outer membrane protein essential for protein import and cell viability. *Nature*, **348**, 605-609

18. Nakai, M. and Endo, T. (1995) Identification of yeast *MAS17* encoding the functional counterpart of the mitochondrial receptor complex protein MOM22 of *Neurospora crassa*. *FEBS lett.*, **357**, 202-206

19. Söllner, T., Griffiths, G., Pfaller, R., Pfanner, N., and Neupert, W. (1989) MOM19, an import receptor for mitochondrial precursor proteins. *Cell*, **59**, 1061-1070

20. Ramage, L., Junne, T., Hahne, K., Lithgow, T., and Schatz, G. (1993) Functional cooperation of mitochondrial protein import receptors in yeast. *EMBO J.*, **12**, 4115-4123

21. Schlossmann, J., Dietmeier, K., Pfanner, N., and Neupert, W. (1994) Specific

recognition of mitochondrial preproteins by the cytosolic domain of the import receptor MOM72. *J. Biol. Chem.*, **269**, 11893-11901

22. Brix, J., Dietmeier, K., and Pfanner, N. (1997) Differential recognition of preproteins by the purified cytosolic domains of the mitochondrial import receptors Tom20, Tom22, and Tom70. *J. Biol. Chem.*, **272**, 20730-20735
23. Mayer, A., Nargang, F. E., Neupert, W., and Lill, R. (1995) MOM22 is a receptor for mitochondrial targeting sequences and cooperates with MOM19. *EMBO J.* **14**, 4204-4211
24. Dietmeier, K., Hönlinger, A., Bömer, U., Dekker, P. J. T., Eckerskorn, C., Lottspeich, F., Kübrich, M., and Pfanner, N. (1997) Tom5 functionally links mitochondrial preprotein receptors to the general import pore. *Nature*, **388**, 195-200
25. Vestweber, D., Brunner, J., Baker, A., and Schatz, G. (1989) A 42K outer-membrane protein is a component of the yeast mitochondrial protein import site. *Nature*, **341**, 205-209
26. Künkele, K-P., Heins, S., Dembowski, M., Nargang, F. E., Benz, R., Thieffry, M., Walz, J., Lill, R., Nussberger, S., and Neupert, W. (1998) The preprotein translocation channel of the outer membrane of mitochondria. *Cell*, **93**, 1009-1019
27. Dekker, P. J. T., Ryan, M. T., Brix, J., Müller, H., Hönlinger, A., and Pfanner, N. (1998) Preprotein translocase of the outer mitochondrial membrane: Molecular dissection and assembly of the general import pore complex. *Mol. Cell. Biol.*, **18**, 6515-6524
28. Koehler C. M. (2000) Protein translocation pathways of the mitochondrion. *FEBS lett.*, **476**, 27-31
29. Blom, J., Dekker, P. J. T., and Meijer, M. (1995) Functional and physical interactions of components of the yeast mitochondrial inner-membrane import machinery (MIM). *Eur. J. Biochem.*, **232**, 309-314
30. Berthold, J., Bauer, M. F., Schneider, H-C., Klaus, C., Dietmeier, K., Neupert, W.,

and Brunner, M. (1995) The MIM complex mediates preprotein translocation across the mitochondrial inner membrane and couples it to the mt-Hsp70/ATP driving system. *Cell*, **81**, 1085-1093

31. Moro, F., Sirrenberg, C., Schneider H-C., Neupert, W., and Brunner, M. (1999) The TIM17•23 preprotein translocase of mitochondria: composistion and function in protein transport into the matrix. *EMBO J.*, **18**, 3667-3675
32. Schneider, H-C., Berthold, J., Bauer, M.F., Dietmeier, K., Guiard, B., Brunner, M., and Neupert, W. (1994) Mitochondrial Hsp70/MIM44 complex facilitates protein import. *Nature*, **371**, 768-774
33. Sirrenberg, C., Bauer, M. F., Guiard, B., Neupert, W., and Brunner, M. (1996) Import of carrier proteins into the mitochondrial inner membrane mediated by Tim22. *Nature*, **384**, 582-585
34. Kerscher, O., Holder, J., Srinivasan, M., Leung, R. S., and Jensen, R. E. (1997) The Tim54p-Tim22p complex mediates insertion of proteins into the mitochondrial inner membrane. *J. cell Biol.*, **139**, 1663-1675
35. Kerscher, O., Sepuri, N. B., and Jensen, R. E. (2000) Tim18p is a new component of the Tim54p-Tim22p translocon in the mitochondrial inner membrane. *Mol. Biol. Cell*, **11**, 103-116
36. Koehler, C. M., Murphy, M. P., Bally, N. A., Leuenberger, D., Oppliger, W., Dolfini, L., Junne, T., Schatz, G., and Or, E. (2000) Tim18p, a new subunit of the TIM22 complex that mediates insertion of imported proteins into the yeast mitochondrial inner membrane. *Mol. Cell. Biol.*, **20**, 1187-1193
37. Leuenberger, D., Bally, N. A., Schatz, G., and Koehler, C. M. (1999) Different import pathways through the mitochondrial intermembrane space for inner membrane proteins. EMBO J., 18, 4816-4822
38. Hell, K., Herrmann, J. M., Pratje, E., Neupert, W., and Stuart, R. A. (1998) Oxa1p, an essential component of the N-tail protein export machinery in mitochodria. *Proc.*

Natl. Acad. Sci. USA, **95**, 2250-2255

39. Martin, J., Mahlke, K., and Pfanner, N. (1991) Role of an energized inner membrane in mitochondrial protein import: $\Delta\Psi$ drives the movement of presequence. *J. Biol. Chem.*, **266**, 18051-18057
40. Jensen, R. E. and Johnson, A. E. (1999) Protein translocation: Is Hsp70 pulling my chain? *Curr. Biol.*, **9**, R779-R782
41. Mayer, A., Neupert, W., and Lill, R. (1995) Mitochondrial protein import: Reversible binding of the presequence at the trans side of the outer membrane drives partial translocation and unfolding. *Cell*, **80**, 127-137

Chapter 2

Two distinct mechanisms drive protein translocation across the mitochondrial outer membrane in the late step of the import of cytochrome b_2

2-1 INTRODUCTION

Many mitochondrial proteins are synthesized in the cytosol and imported into mitochondria. The matrix-targeting proteins traverse the mitochondrial outer and the inner membranes through the TOM complex and the Tim23 complex, respectively, in a $\Delta\Psi$- and ATP-dependent manner. On the other hand, the route for the import of protein into the IMS has been a matter of debate.

Cytochrome b_2 is a soluble protein of the IMS, and has a heme binding domain (HBD) in the N-terminal region, which can fold tightly and independently of the other part of the molecule (1, 2). Cytochrome b_2 is synthesized in the cytosol with a presequence, which is composed of two domains. The first part of the presequence directs the attached protein to mitochondria and is removed by matrix processing peptidase (MPP) in the matrix to yield a processing intermediate-size protein. The second part of the presequence is required for the transport of the protein to the IMS and is cleaved off by inner membrane protease 1 (Imp1p) on the IMS side of the inner membrane to yield a mature-size protein (3). Two possible pathways for cytochrome b_2 from the cytosol to the IMS have been proposed (Fig. 2-1; ref. 4, 5). According to the 'conservative sorting model', the entire precursor protein is imported into the matrix through the mitochondrial outer and the inner membrane. Following the cleavage of the N-terminal targeting signal part, the processing intermediate-size protein is re-exported from the matrix to the IMS across the inner membrane. Alternatively, according to the 'stop-transfer model', although the N-terminal targeting signal part of the presequence is imported into the matrix, the second part of the presequence arrests further translocation across the inner membrane. Then the mature part traverses the outer membrane from the cytosol into the IMS directly. In both models, the translocation of the first part of the presequence requires $\Delta\Psi$ across the inner membrane and the ATP hydrolysis in the matrix, which is coupled with the translocation of the

HBD across the outer membrane (2, 3, 6, 7). Once the HBD has passed the outer membrane, subsequent translocation of the following C-terminal part takes place independently of $\Delta\Psi$ and ATP (2, 6, 7). Then, what drives the $\Delta\Psi$- and ATP-independent translocation of the C-terminal part of cytochrome b_2?

In the present study, I showed that cytochrome b_2 is imported into the IMS along the pathway which is consistent with the stop-transfer model, but not with the conservative sorting model. Then, I analyzed the late $\Delta\Psi$- and ATP-independent step in the transport of cytochrome b_2 to the IMS. The import of cytochrome b_2 fusion proteins containing two domains linked by a spacer sequence was arrested at a state, at which the N-terminal and the C-terminal domains folded on the IMS side and on the cytosolic side, respectively, of the outer membrane. The mature-size forms of the translocation intermediates were found to move across the outer membrane in both directions, and the directionality of the movement depends on the balance of the stabilities of the two domains. On the other hand, the processing intermediate-size forms of the translocation intermediates, which are anchored to the inner membrane by their presequence, was transported only to the IMS side independently of the stability of the domain on the IMS. On the basis of these results I propose that two distinct mechanisms, the Brownian ratchet mechanism and the anchor diffusion mechanism, drive protein translocation across the outer membrane for the mature-size form and for the processing intermediate-size form, respectively.

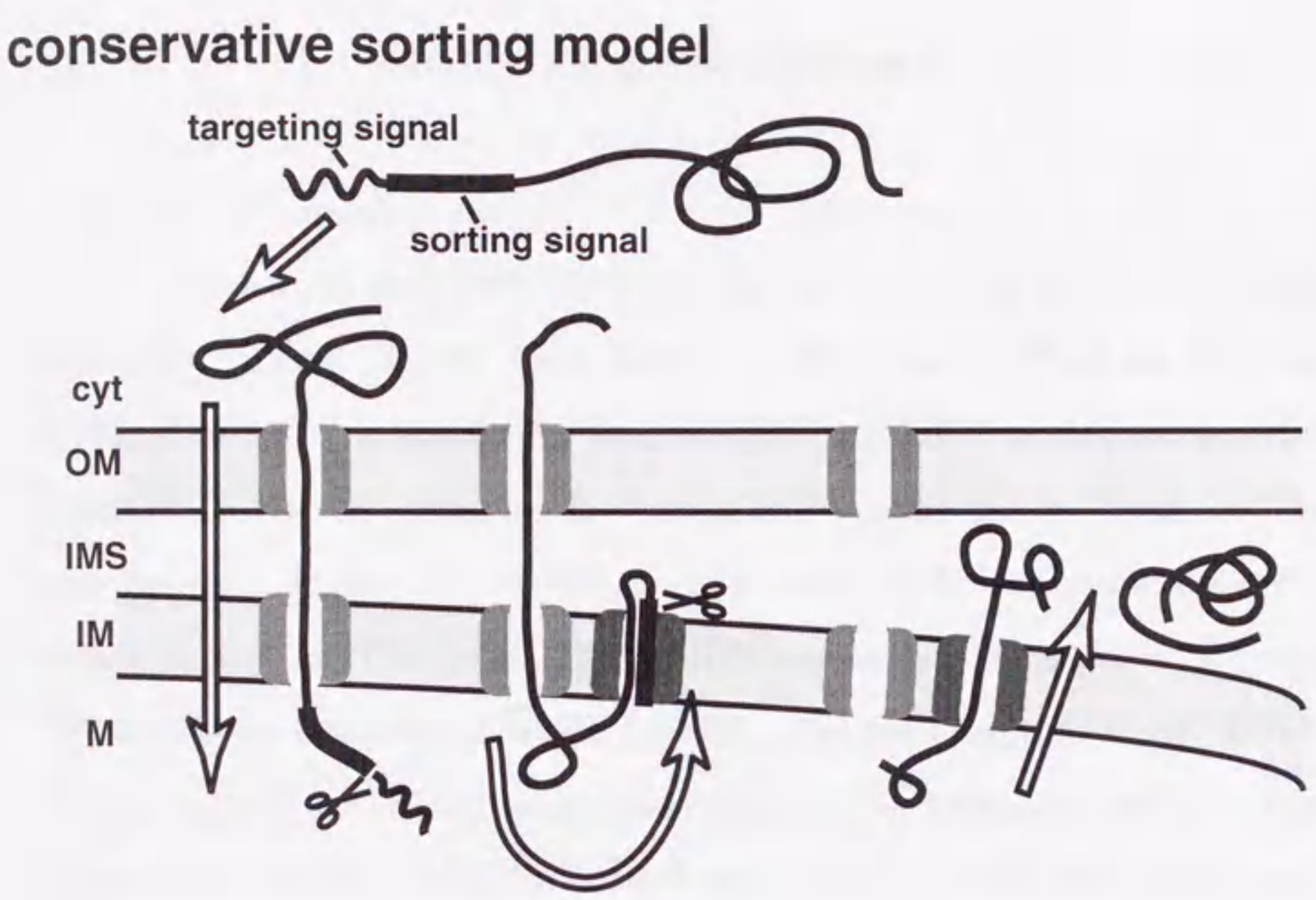

Fig. 2-1 Two sorting models for cytochrome b_2

Two models have been proposed for the import route of cytochrome b_2 into the IMS. cyt, cytosol; OM, outer membrane; IMS, intermembrane space; IM, inner membrane; M, matrix.

2-2 MATERIALS and METHODS

Construction of plasmids

The genes for $pb_2(220)^{dc1}$-DHFR and $pb_2(220)^{dc2}$-DHFR were derived from that of $pb_2(220)^{WT}$-DHFR (8). In brief, codons for His^{123} and His^{146} of the gene for $pb_2(220)^{WT}$-DHFR were replaced by those for Leu^{123} and Leu^{146} to yield the gene for $pb_2(220)^{dc1}$-DHFR, and codons for Phe^{142} and Glu^{143} by those for Pro^{142} and Pro^{143} to yield the gene for $pb_2(220)^{dc2}$-DHFR by oligonucleotide-directed mutagenesis (9). Codons for Asn^{80} and Glu^{81} of $pb_2(220)^{WT}$-DHFR were replaced by those for Ala^{80} and Ala^{81} to yield the gene for $pb_2AA(220)^{WT}$-DHFR. The genes for $pb_2AA(220)^{dc1}$-DHFR and $pb_2AA(220)^{dc2}$-DHFR were constructed by replacing the DNA segments for the first 85 amino-acid residues of $pb_2(220)^{dc1}$-DHFR and $pb_2(220)^{dc2}$-DHFR, respectively, with that taken from the $pb_2AA(220)^{WT}$-DHFR gene. For constructing the gene for $pb_2(260)^{WT}$-HBD, the *Spe*I site and the TAA stop codon were introduced at the 5'-end and at the 3'-end, respectively, of the DNA fragment encoding residues 81-189 of cytochrome b_2 by PCR. The amplified fragment was inserted into the cytochrome b_2 gene at the *Spe*I site, which had been introduced at the codons for residues 259 and 260 with the concomitant replacement of Ile^{259} by Thr^{259}. The genes for $pb_2(260)^{dc1}$-HBD, $pb_2(260)^{dc2}$-HBD, $pb_2AA(260)^{WT}$-HBD, $pb_2AA(260)^{dc1}$-HBD, and $pb_2AA(260)^{dc2}$-HBD were constructed by replacing the DNA segment for the first 200 amino-acid residues of $pb_2(260)^{WT}$-HBD with those taken from the genes for $pb_2(220)^{dc1}$-DHFR, $pb_2(220)^{dc2}$-DHFR, $pb_2AA(220)^{WT}$-DHFR, $pb_2AA(220)^{dc1}$-DHFR, and $pb_2AA(220)^{dc2}$-DHFR, respectively.

Import of cytochrome b_2 *fusion proteins into mitochondria*

The fusion proteins were synthesized in a cell-free translation system with rabbit reticulocyte lysate in the presence of [^{35}S]methionine and 20 μM hemin.

Mitochondria were isolated from the yeast strain D273-10B (10). The radiolabeled fusion proteins were incubated with mitochondria in import buffer (250 mM sucrose, 10 mM Mops-KOH, pH 7.2, 80 mM KCl, 5 mM $MgCl_2$, 2.5 mM KPi, 5 mM DTT, 2 mM methionine, 1% BSA, 2 mM ATP, 2 mM NADH) at 25°C. The import reaction was stopped by adding valinomycin to 10 µg/ml. The mitochondria were reisolated by centrifugation, and proteins were analyzed by SDS-PAGE and radioimaging with a Storm 860 image analyzer (Amersham Pharmacia Biotech).

Methotrexate-arrest of the pb_2(220)-DHFR fusion proteins and chase reactions

The translation products (5%) containing radiolabeled pb_2(220)-DHFR fusion proteins were incubated with 0.5 µM methotrexate (MTX) and 1 mM NADPH in import buffer for 15 min on ice, and were subsequently incubated with isolated yeast mitochondria for 20 min at 25°C. The mitochondria were reisolated by centrifugation, and were washed once with import buffer containing 0.5 mM recombinant DHFR as a trap for MTX. The mitochondria were resuspended in import buffer without BSA and ATP but containing 3 µM hemin, and were incubated at 25°C. The mitochondria were divided into halves and were incubated with or without 100 µg/ml proteinase K for 30 min on ice. Mitochondria were reisolated by centrifugation, and the proteins in the supernatant without protease treatment were precipitated with trichloroacetic acid.

Kinetic arrest of the pb_2(260)-HBD fusion proteins and chase reactions

The radiolabeled pb_2(260)-HBD fusion proteins were incubated with isolated yeast mitochondria in import buffer for 10 min at 25°C. The mitochondria were reisolated by centrifugation, were resuspended in import buffer without BSA (and hemin), and were incubated at 25°C. The mitochondria were divided into halves and were incubated with or without 100 µg/ml proteinase K for 30 min on ice. Mitochondria were reisolated by centrifugation, and the proteins in the supernatant

without protease treatment were precipitated with trichloroacetic acid.

Purification of the pb_2(220)-DHFR fusion proteins

pb_2(220)-DHFR and pb_2AA(220)-DHFR were expressed in *Eschericia coli* cells. The cells were collected by centrifugation, and suspended in 50 mM Tris-HCl, pH 7.5, 100 mM NaCl, 2 mM EDTA. The cell suspensions were frozen in liquid nitrogen, and were thawed at the room temperature. The cells were disrupted by sonication on ice for 3 min (2 s on/ 1 s off pulsed periods, 40% duty cycle, Astorason XL2020 sonicator with a micro tip). The cell lysates were cleared by centrifugation at 15,000×*g* for 10 min. The pellet containing the fusion proteins were washed twice with 20 mM Tris-HCl, pH 7.5, 50 mM KCl, 2 mM EDTA, 2 M Urea, 0.5% Triton X-100, and were solubilized with 6 M Urea, 20 mM Tris-HCl, pH 7.5, 50 mM KCl, 2 mM EDTA, 2 mM DTT. Insoluble materials were removed by centrifugation at 200,000×*g* for 30 min. The proteins were stored at -80°C until use.

Blue-native PAGE

50 μg/ml pb_2(220)-DHFR and pb_2AA(220)-DHFR were preincubated with 1 μM MTX and 1 mM NADPH in import buffer containing 3 μM hemin for 10 min on ice, and were subsequently incubated with mitochondria (0.5 mg/ml protein) for 20 min at 30°C. The mitochondria were reisolated by centrifugation, and were washed once with 250 mM sucrose, 10 mM Mops-KOH, pH 7.2, 80 mM KCl, 1 μM MTX. The mitochondria were solubilized with ice-cold digitonin buffer (1.25% digitonin, 20 mM Tris-HCl, pH 7.4, 0.1 mM EDTA, 50 mM NaCl, 10% glycerol, 1 mM PMSF), and were subjected to blue-native PAGE and Western blotting, as described previously (11).

2-3 RESULTS

2-3-1 Cytochrome b_2 is imported into the IMS along the pathway consistent with the stop transfer model

I analyzed the sorting pathway for the precursor protein for cytochrome b_2 by using a fusion protein $pb_2(220)$-DHFR, which is composed of the first 220 amino-acid residues of the precursor for yeast cytochrome b_2 and mouse dihydrofolate reductase (DHFR). In $pb_2(220)$-DHFR, residues 1-80 and residues 81-180 correspond to the presequence and the HBD, respectively. Since the wild-type HBD folds tightly upon binding to the heme group (Fig. 2-2; ref. 1, 2), I introduced mutations in the HBD part to destabilize the tertiary structure. In $pb_2(220)^{dc1}$-DHFR, His^{123} and His^{146}, which are ligands for the heme group, are replaced with leucine residues so that the heme group cannot coordinate with the HBD (Fig. 2-2 and 2-3A). In $pb_2(220)^{dc2}$-DHFR, Phe^{142}-Glu^{143}-Pro^{144} is replaced by Pro^{142}-Pro^{143}-Pro^{144} so that the α-helix located in the internal region of the HBD tertiary structure is destroyed (Fig. 2-2 and 2-3A). The fusion proteins were synthesized in rabbit reticulocyte lysate with [^{35}S]methionine, and were subjected to digestions with various concentrations of proteinase K. The protease resistant HBD fragment was generated for $pb_2(220)^{WT}$-DHFR (Fig. 2-3B). On the other hand, the HBDs of $pb_2(220)^{dc1}$-DHFR and $pb_2(220)^{dc2}$-DHFR were highly sensitive to the digestion with proteinase K (Fig. 2-3B). Therefore, the tertiary structures of the HBDs of $pb_2(220)^{dc1}$-DHFR and $pb_2(220)^{dc2}$-DHFR are significantly destabilized as compared with that of $pb_2(220)^{WT}$-DHFR.

When incubated with isolated yeast mitochondria, the radiolabeled $pb_2(220)$-DHFR fusion proteins were imported into mitochondria and were sorted to the IMS correctly *in vitro* (8). The rates of import of $pb_2(220)^{dc1}$-DHFR and $pb_2(220)^{dc2}$-DHFR were nearly the same as that of $pb_2(220)^{WT}$-DHFR (Fig. 2-4A and B). However, the second processing of $pb_2(220)^{dc1}$-DHFR and $pb_2(220)^{dc2}$-DHFR by Imp1p to yield the

mature-size form was significantly retarded as compared with that of $pb_2(220)^{WT}$-DHFR (Fig. 2-4C).

Because the translocation across the mitochondrial membranes requires the unfolding of the translocating protein, methotrexate (MTX), which is a ligand for the DHFR, stabilizes the tertiary structure of the DHFR and blocks the translocation of the DHFR part, resulting in the generation of the translocation intermediate (12, 13). In the MTX-arrested intermediates, the DHFR part remained outside the mitochondrial outer membrane, whereas the N-terminal part reached the IMS. According to the stop-transfer model (12), the translocation intermediate spans only the outer membrane, because the length between the HBD and the DHFR part is about 50 amino acid residues, which is sufficient for spanning a single membrane. This topology allows the HBD of $pb_2(220)^{WT}$-DHFR to fold in the IMS. On the other hand, in case of the conservative sorting model (13), the translocation intermediate spans three membranes looping through the matrix, so that the HBD part must form the loop and cannot fold in the IMS. I found that the MTX-arrested translocation intermediates of $pb_2(220)^{dc1}$-DHFR and $pb_2(220)^{dc2}$-DHFR did not receive the second processing by Imp1p after 40 min of incubation, whereas the MTX-arrested intermediate of $pb_2(220)^{WT}$-DHFR was processed by Imp1p to yield the mature-size form within 5 min (Fig. 2-5A and B). Since it has been shown that the folding of the HBD in the IMS is necessary for the second processing (2), these results indicate that the HBD of the MTX-arrested $pb_2(220)^{WT}$-DHFR is folded in the IMS even when the DHFR part still remains on the cytosolic side of the outer membrane. These results are consistent with the stop-transfer model but not with the conservative sorting model.

2-3-2 The mature-size form of the MTX-arrested translocation intermediate is associated only with the TOM complex, whereas the intermediate-size form is associated not only with the TOM complex but also with an unidentified complex

in the inner membrane

When the import of $pb_2(220)^{WT}$-DHFR is arrested by MTX, the HBD of the fusion protein has already passed the outer membrane while the DHFR part stays outside the mitochondria. The stop-transfer model predicts that, in the MTX-arrested intermediate, N-terminus of the mature-size form is free in the IMS, whereas that of the intermediate-size form is anchored to the inner membrane (7, 12). To confirm this prediction, chemical amounts of the MTX-arrested $pb_2(220)^{WT}$-DHFR and $pb_2AA(220)^{WT}$-DHFR fusion proteins were accumulated in the isolated mitochondria. The mitochondria with the intermediate were solubilized with digitonin and were subjected to blue-native PAGE. $pb_2AA(220)^{WT}$-DHFR are imported into the IMS but do not virtually receive the second processing by Imp1p because the amino acids at the processing site are mutated (see Fig. 2-10). In the absence of the fusion proteins, Tom40 and Tim23/Tim17 were found at the 440-kDa complex and mainly at the 90-kDa complex, respectively (Fig. 2-6, ref. 11). After the accumulation of $pb_2(220)^{WT}$-DHFR in the presence of methotrexate and the solubilization of the mitochondria, a part of Tom40 was found at 500-kDa and 600-kDa complexes (Fig. 2-6). When probed with the anti-DHFR antibodies, the bands of 500 kDa and 600 kDa were also observed, indicating that the MTX-arrested $pb_2(220)^{WT}$-DHFR is in the 500-kDa and the 600-kDa complexes. In the case of $pb_2AA(220)^{WT}$-DHFR, a part of Tom40 was found at the 600-kDa complex but not at the 500-kDa complex (Fig. 2-6). On the other hand, the accumulation of $pb_2(220)^{WT}$-DHFR or $pb_2AA(220)^{WT}$-DHFR did not cause a molecular-weight shift of the complexes containing Tim23 and Tim17. Since only the intermediate-size form is generated from $pb_2AA(220)^{WT}$-DHFR, the 600-kDa complex contains the intermediate-size form of 45 kDa. Therefore, the intermediate-size form is likely associated with not only 440-kDa Tom40 complex but also with a 100-kDa unidentified complex without Tim23/Tim17. The 500-kDa complex is found for accumulated $pb_2(220)^{WT}$-DHFR, but not for accumulated $pb_2AA(220)^{WT}$-DHFR,

suggesting that the mature-size form is contained in the 500-kDa complex. Since the molecular weight of the mature-size form is 40 kDa, it is probably associated only with the 440-kDa Tom40 complex.

2-3-3 The MTX-arrested translocation intermediates can be chased into the IMS when MTX is removed

I then tested whether the mature-size form of the MTX-arrested $pb_2(220)$-DHFR fusion proteins complete their translocation when MTX is removed. This chase reaction of the translocation intermediates corresponds to the late step of the translocation mechanism of cytochrome b_2, which takes place independently of $\Delta\Psi$ across the inner membrane and ATP hydrolysis in the matrix. $pb_2(220)^{WT}$-DHFR, $pb_2(220)^{dc1}$-DHFR, and $pb_2(220)^{dc2}$-DHFR were incubated with isolated mitochondria with MTX to generate translocation intermediates. The mitochondria were reisolated, were washed once with fresh import buffer without MTX, and were subjected to further incubation. Thirty-eight percents of the MTX-arrested mature-size form of the wild-type protein were chased into the IMS during the incubation for 20 min (Fig. 2-7B, in/WT). Moreover, I noticed that a small portion of the MTX-arrested mature-size form of the wild-type protein was recovered in the post-mitochondrial supernatant (Fig. 2-7B, out/WT), indicating that it was translocated back across the outer membrane to the cytosol. I also found that, the stability of the HBD affected the efficiency of the forward translocation vs. the retrograde translocation. The MTX-arrested intermediates of the HBD-destabilized mutants, $pb_2(220)^{dc1}$-DHFR and $pb_2(220)^{dc2}$-DHFR, are chased into the IMS less efficiently than that of $pb_2(220)^{WT}$-DHFR (Fig. 2-7B, in). On the other hand, the MTX-arrested $pb_2(220)^{dc1}$-DHFR and $pb_2(220)^{dc2}$-DHFR were released from the mitochondria more efficiently than $pb_2(220)^{WT}$-DHFR (Fig. 2-7B, out).

2-3-4 The translocation of the mature-size protein depends on the stability of the protein domains on both sides of the membrane

Next I prepared the $pb_2(260)$-HBD fusion proteins, which composed of the first HBD (HBD1, wild-type HBD or the mutated HBD), followed by 80 spacer segment and the second wild-type HBD (HBD2) (Fig. 2-8A). When incubated with mitochondria, $pb_2(260)^{WT}$-HBD, $pb_2(260)^{dc1}$-HBD, and $pb_2(260)^{dc2}$-HBD were processed to the mature-size form or the intermediate-size form in a $\Delta\Psi$-dependent manner (Fig. 2-8B), indicating that N-terminal presequence of the $pb_2(260)$-HBD fusion proteins entered the matrix. Treatment of the mitochondria with protease resulted in the formation of two major degradation products of 27 kDa and 23 kDa (Fig. 2-8B). The fragment sizes of 27 kDa and 23 kDa correspond to those of HBD1 attached to the spacer segments of the intermediate-size and of the mature-size forms, respectively. These results indicate that HBD1 has been efficiently translocated across the outer membrane, whereas HBD2 still remained outside the mitochondria. This kinetically arrested fusion protein, in which the two HBDs were on both sides of the outer membrane, allowed me to further characterize the protein translocation across the outer membrane.

The mitochondria containing the partially translocated intermediate of $pb_2(260)^{WT}$-HBD were suspended in fresh import buffer and were further incubated. A part of the accumulated mature-size form of the wild-type protein was transported into the IMS (Fig. 2-9B, in/WT) while a similar amount of the mature-size protein was released to the cytosolic side of the membrane (Fig. 2-9B, out/WT). The accumulated $pb_2(260)^{dc1}$-HBD and $pb_2(260)^{dc2}$-HBD were released from the mitochondria more efficiently than they were imported into the IMS (Fig. 2-9B, in/dc1 and dc2, out/dc1 and dc2).

These findings can be explained by the simplest version of the Brownian ratchet mechanism (14, 15). The translocating polypeptide chain of the mature-size protein would move in both directions in the TOM channel in the outer membrane by

the Brownian thermal motion. When the protein domain of the translocation intermediate on the IMS side is unfolded, the protein will move toward the cytosolic side. On the other hand, when the domain on the cytosolic side is unfolded, the translocation intermediate will move toward the IMS side. Therefore, the translocation of the mature-size protein depends on the stabilities of the tertiary structures of the domains on the cytosolic side and on the IMS side. The accumulation of these fluctuating movements would result in the net displacement of the polypeptide segment in the TOM channel. The translocation intermediate containing the mutated HBD in the IMS would thus move toward the cytosolic side more efficiently than that containing the wild-type HBD.

2-3-5 The translocation intermediate of the processing intermediate is chased into the IMS independently of the stability of the domain in the IMS

Finally, I compared the kinetics of the translocation of the mature-size form with that of the processing intermediate-size form, which is still anchored to the inner membrane by its sorting-signal segment (7, 8, Fig. 2-6). For this purpose, I used the pb_2AA(220)-DHFR and pb_2AA(260)-HBD fusion proteins (Fig. 2-10A and 2-11A) to prevent the second processing of the presequence by Imp1p. In contrast to the pb_2(220)-DHFR fusion proteins, the MTX-arrested $pb_2AA(220)^{WT}$-DHFR, $pb_2AA(220)^{dc1}$-DHFR, and $pb_2AA(220)^{dc2}$-DHFR were transported into the IMS with nearly the same kinetics when MTX was removed (Fig. 2-10B). Similarly, the kinetically arrested $pb_2AA(260)^{WT}$-HBD, $pb_2AA(260)^{dc1}$-HBD, and $pb_2AA(260)^{dc2}$-HBD were also chased into the IMS with the similar kinetics one another (Fig. 2-11B). These results indicate that the translocation of the processing intermediate-size form across the outer membrane does not depend on the stability of the tertiary structure of the N-terminal HBD in the IMS. In other words, the mechanism for the translocation of the processing intermediate-size form is different from that for the mature-size form.

Since the processing intermediate-size form is anchored to the inner membrane, the lateral diffusion of the sorting signal in the inner membrane may well drive the translocation of the rest of the polypeptide chain across the outer membrane ("anchor diffusion mechanism") (16).

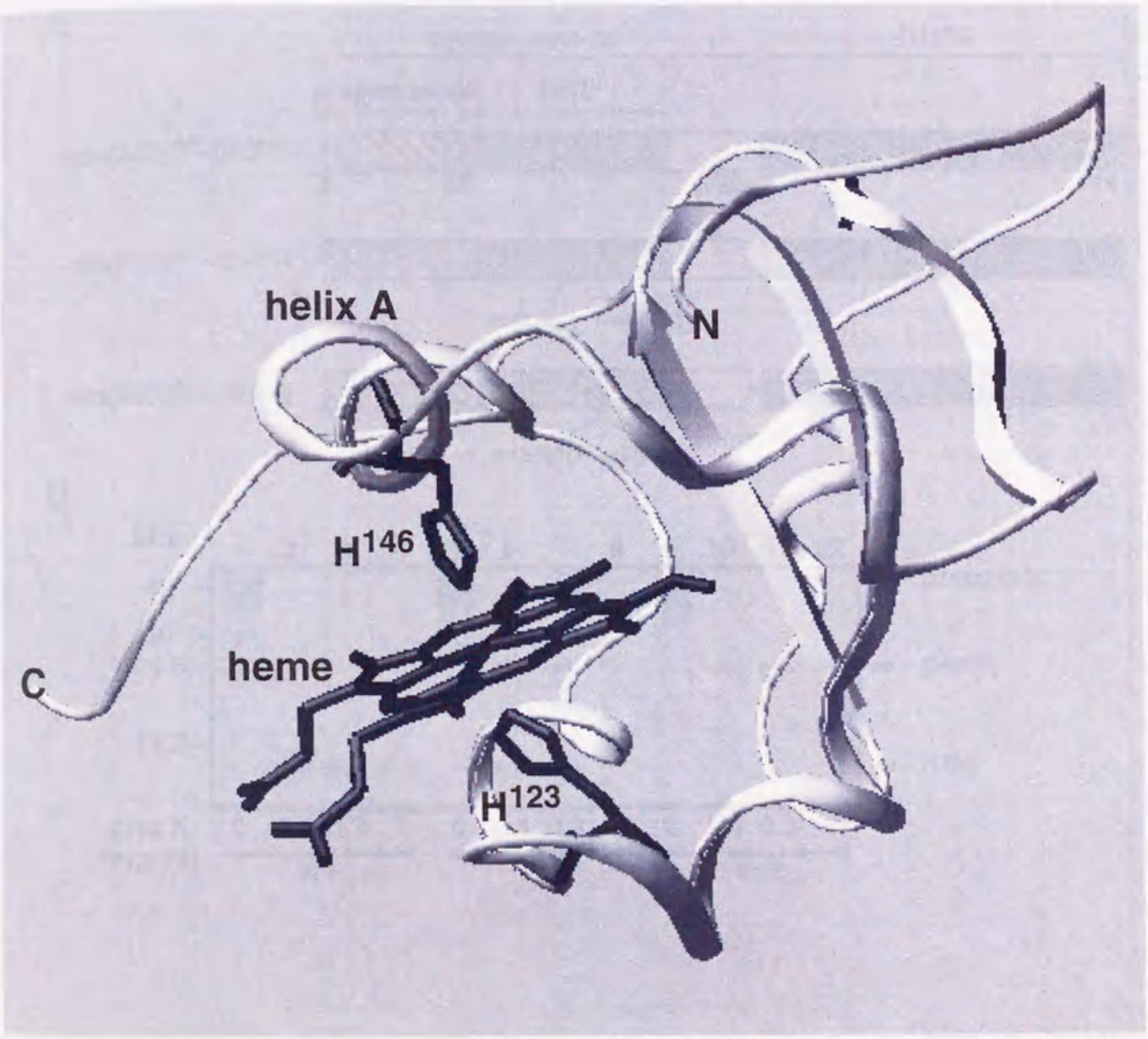

Fig. 2-2 Tertiary structure of the HBD

The tertiary structure of residues 81-180 of the precursor for cytochrome b_2 is shown (PDB accession #1FCB, ref. 1). In HBD^{dc1}, His^{123} and His^{146} are replaced with alanine residues. In HBD^{dc2}, three tandem proline residues are introduced in helix A.

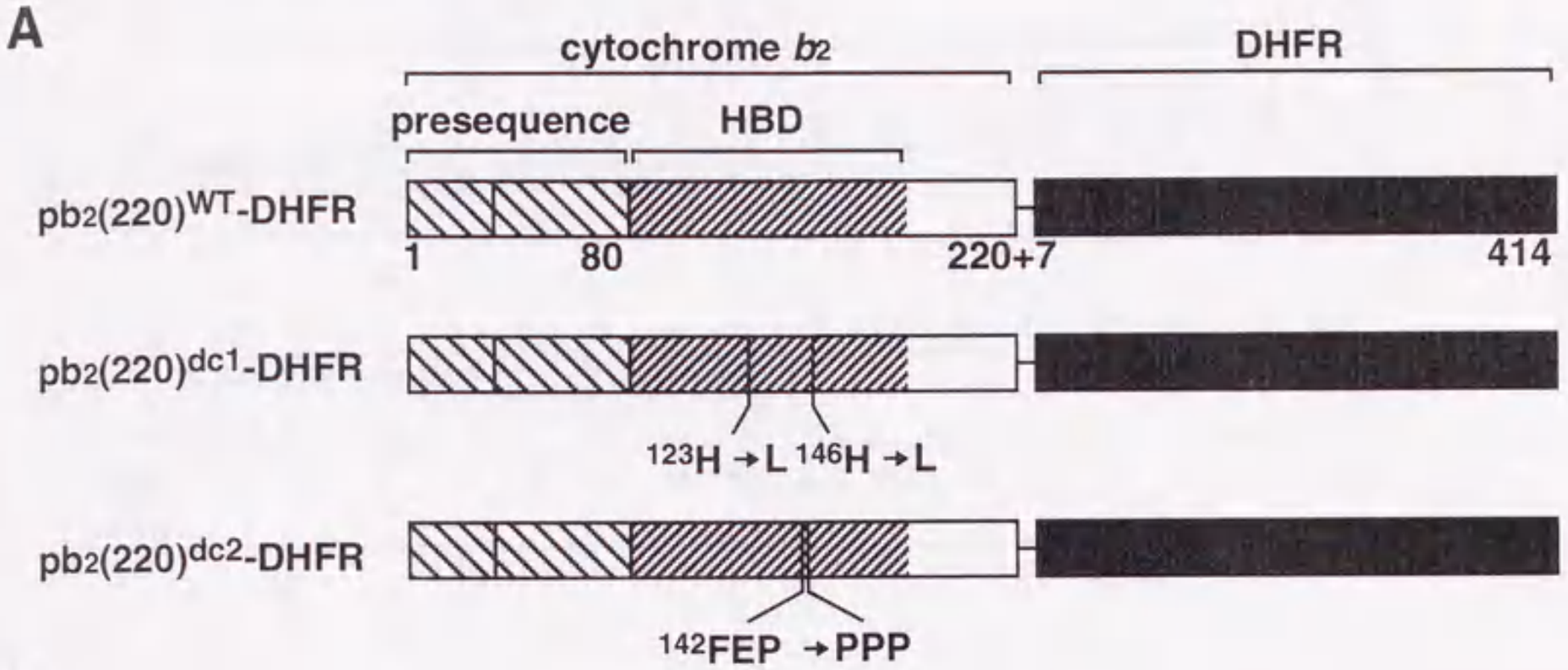

Fig. 2-3 The HBD are destabilized by mutations

A, $pb_2(220)$-DHFR fusion proteins.

B, proteinase K digestions of the $pb_2(220)$-DHFR fusion proteins. $pb_2(220)^{WT}$-DHFR (WT), $pb_2(220)^{dc1}$-DHFR (dc1), and $pb_2(220)^{dc2}$-DHFR (dc2) were synthesized with [^{35}S]methionine in rabbit reticulocyte lysate. The radiolabeled fusion proteins were diluted 100-fold with 250 mM sucrose, 10 mM Mops-KOH, pH 7.2, 80 mM KCl, 2 mM cold methionine, 4 μM hemin, and were treated with various concentrations of proteinase K (prot K) for 10 min at 25°C. The reactions were stopped by the addition of 1 mM phenylmethylsulfonyl fluoride (PMSF), and the proteins were precipitated by trichloroacetic acid and were analyzed by SDS-PAGE and radioimaging.

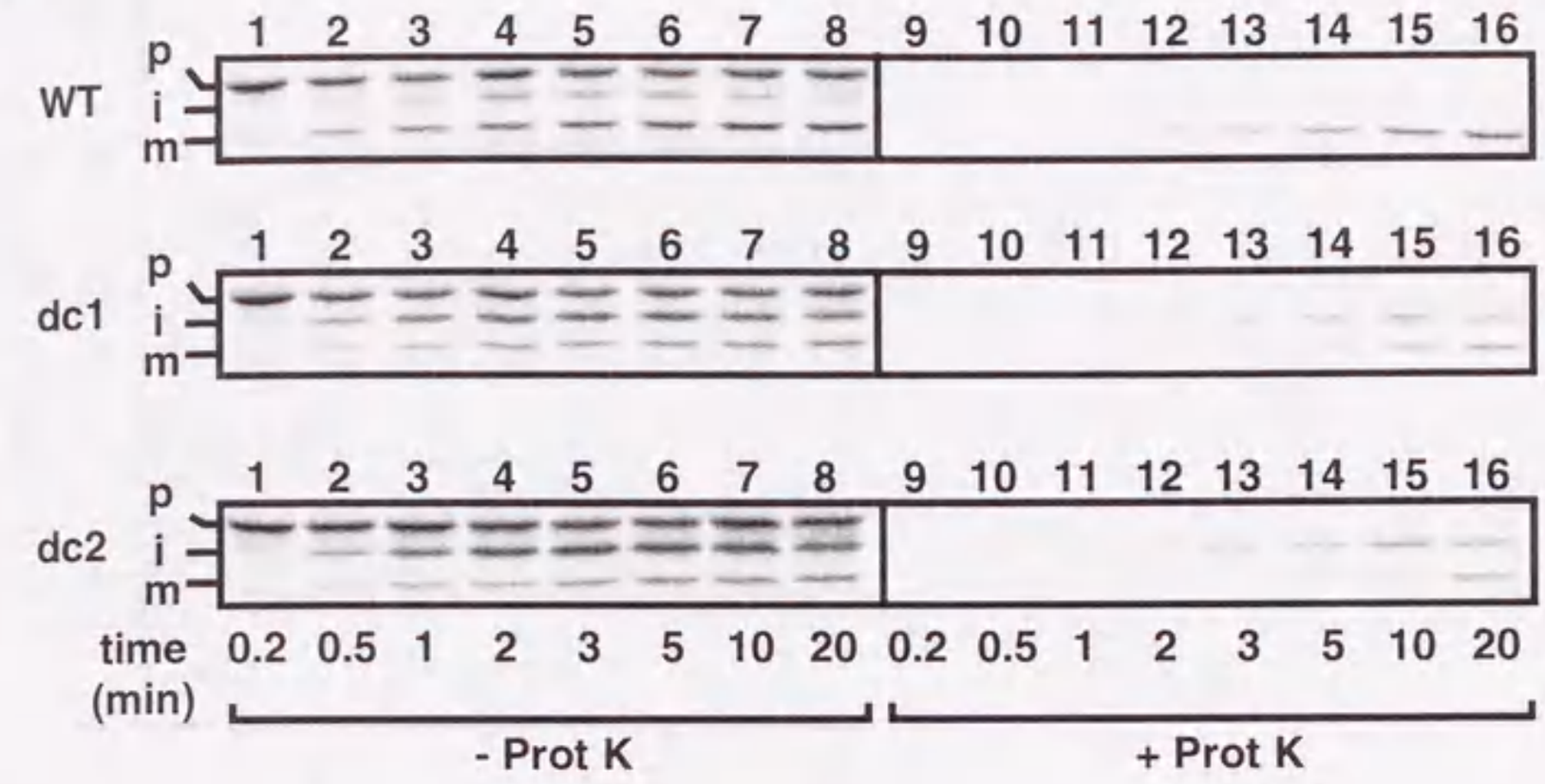

Fig. 2-4 The rate of imoprt of $pb_2(220)$-DHFR fusion proteins is independent of the HBD stability

A, Radiolabeled $pb_2(220)^{WT}$-DHFR (WT), $pb_2(220)^{dc1}$-DHFR (dc1), and $pb_2(220)^{dc2}$-DHFR (dc2) were incubated with yeast mitochondria at 25ºC for indicated times. The mitochondria were treated with (lanes 9-16) or without (lanes 1-8) 100 μg/ml proteinase K on ice for 30 min. p, precursor; i, intermediate-size form; m, mature-size form.

B, Amounts of the protease-protected intermediate- and mature-size forms (A, lanes 9-16) are plotted against incubation times. The amounts of the fusion proteins added to each reaction are set to 100%. Squares, WT; triangles, dc1; circles, dc2.

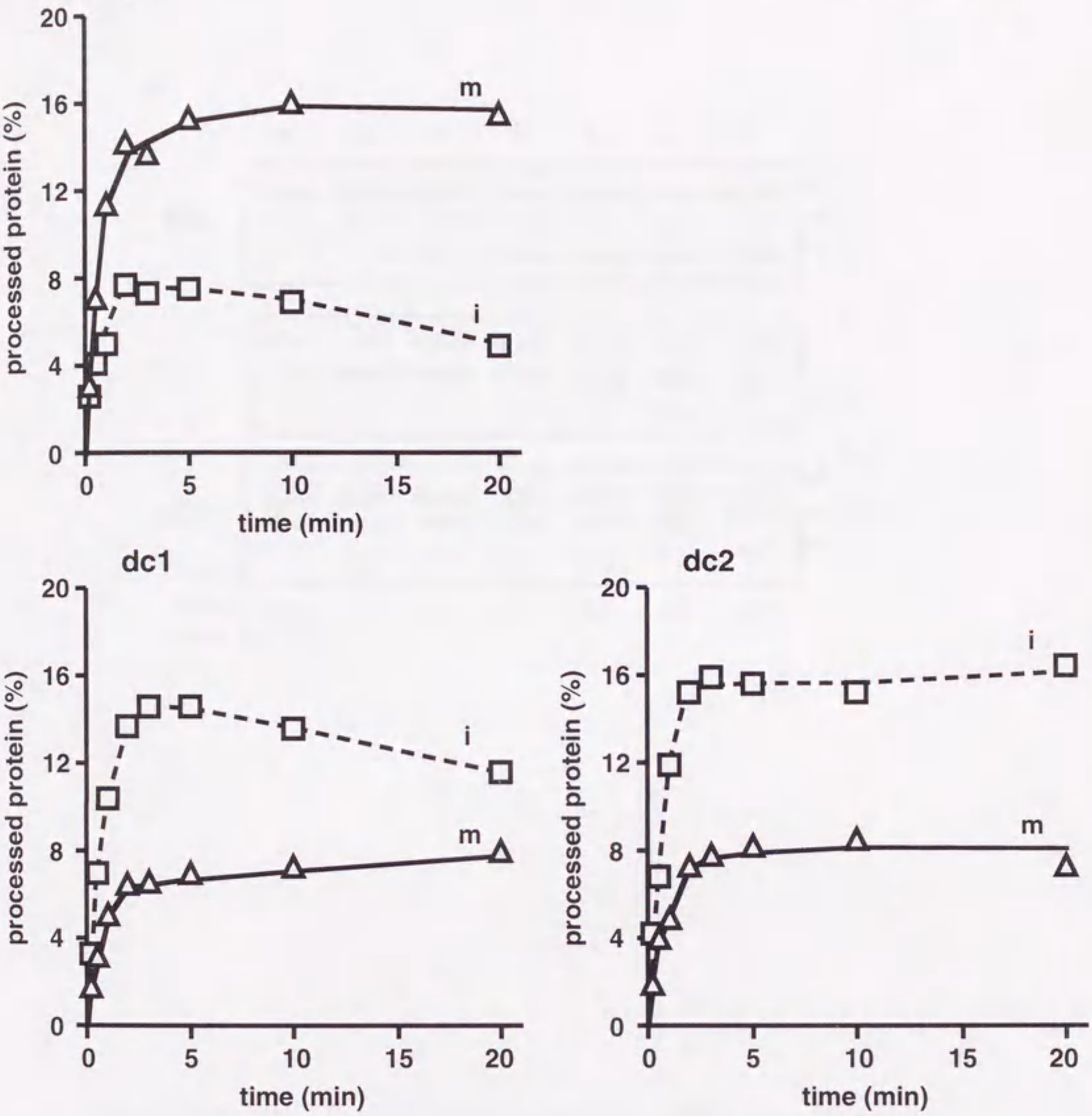

Fig. 2-4 (continued)

C, Amounts of the total intermediate-size form and of the total mature-size form (A, lanes 1-8) are plotted against incubation times. The amounts of the fusion proteins added to each reaction are set to 100%. Squares, intermediate-size form; triangles, mature-size form.

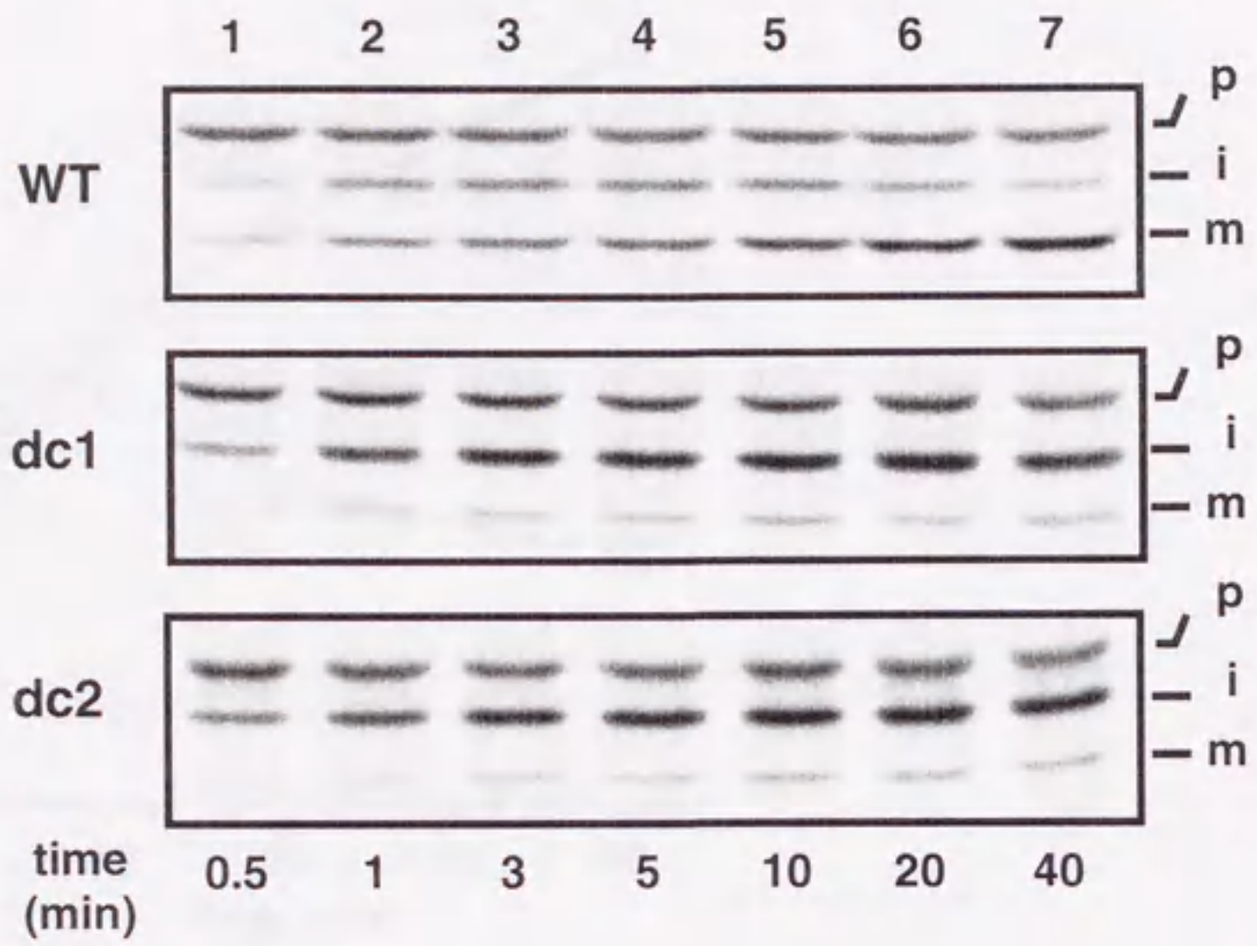

Fig. 2-5 The tight folding of the HBD promotes the Imp1p processing of the MTX-arrested $pb_2(220)$-DHFR fusion proteins

A, Radiolabeled $pb_2(220)^{WT}$-DHFR (WT), $pb_2(220)^{dc1}$-DHFR (dc1), and $pb_2(220)^{dc2}$-DHFR (dc2) were incubated with 1 μM MTX and 1 mM NADPH in import buffer for 15 min on ice, and were subsequently incubated with mitochondria at 25ºC for indicated times. p, precursor; i, intermediate-size form; m, mature-size form.

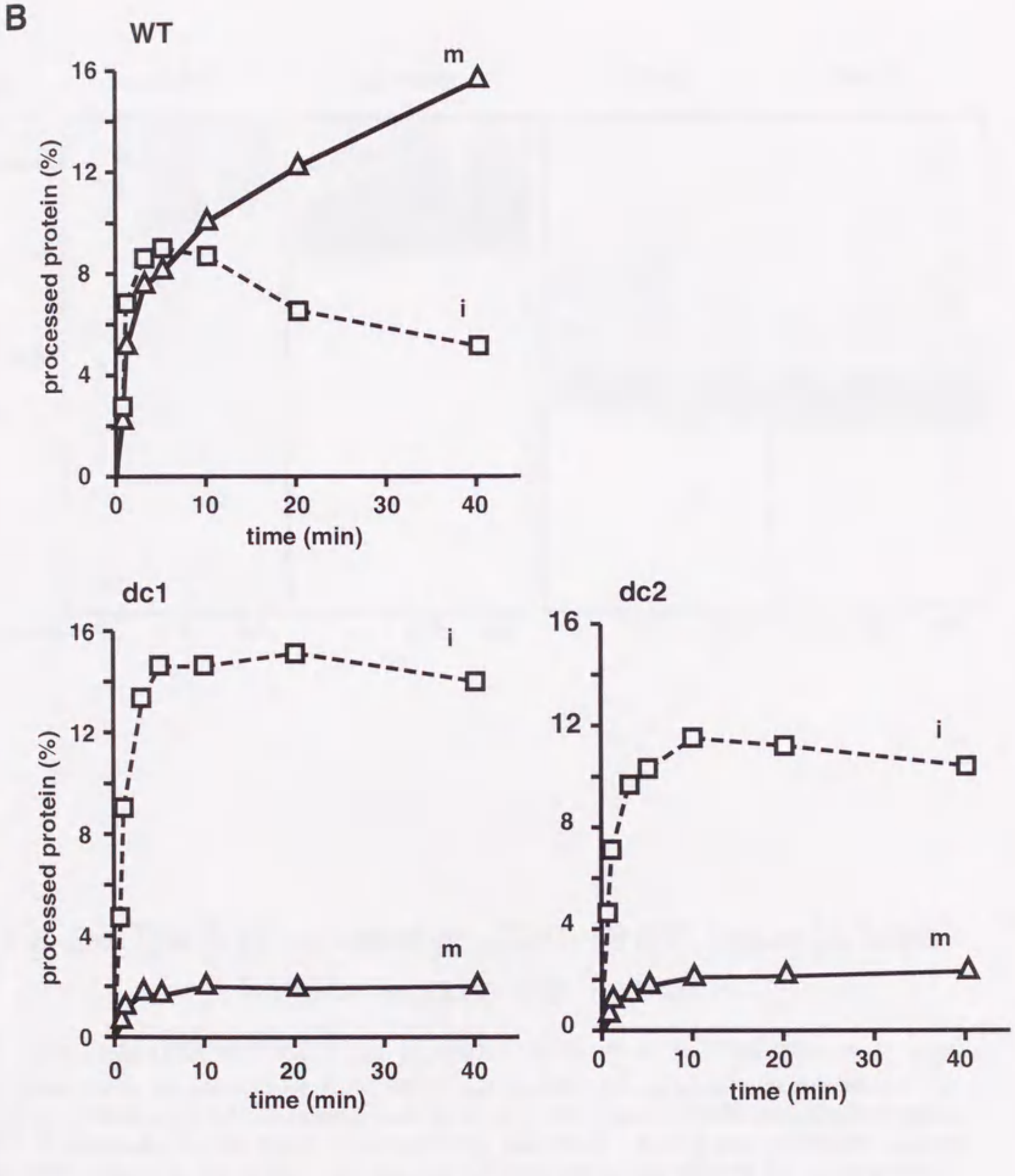

Fig. 2-5 (continued)

B, Amounts of the intermediate-size form (squares) and the mature-size form (triangles) are plotted against incubation times. The amounts of the fusion proteins added to each reaction are set to 100%.

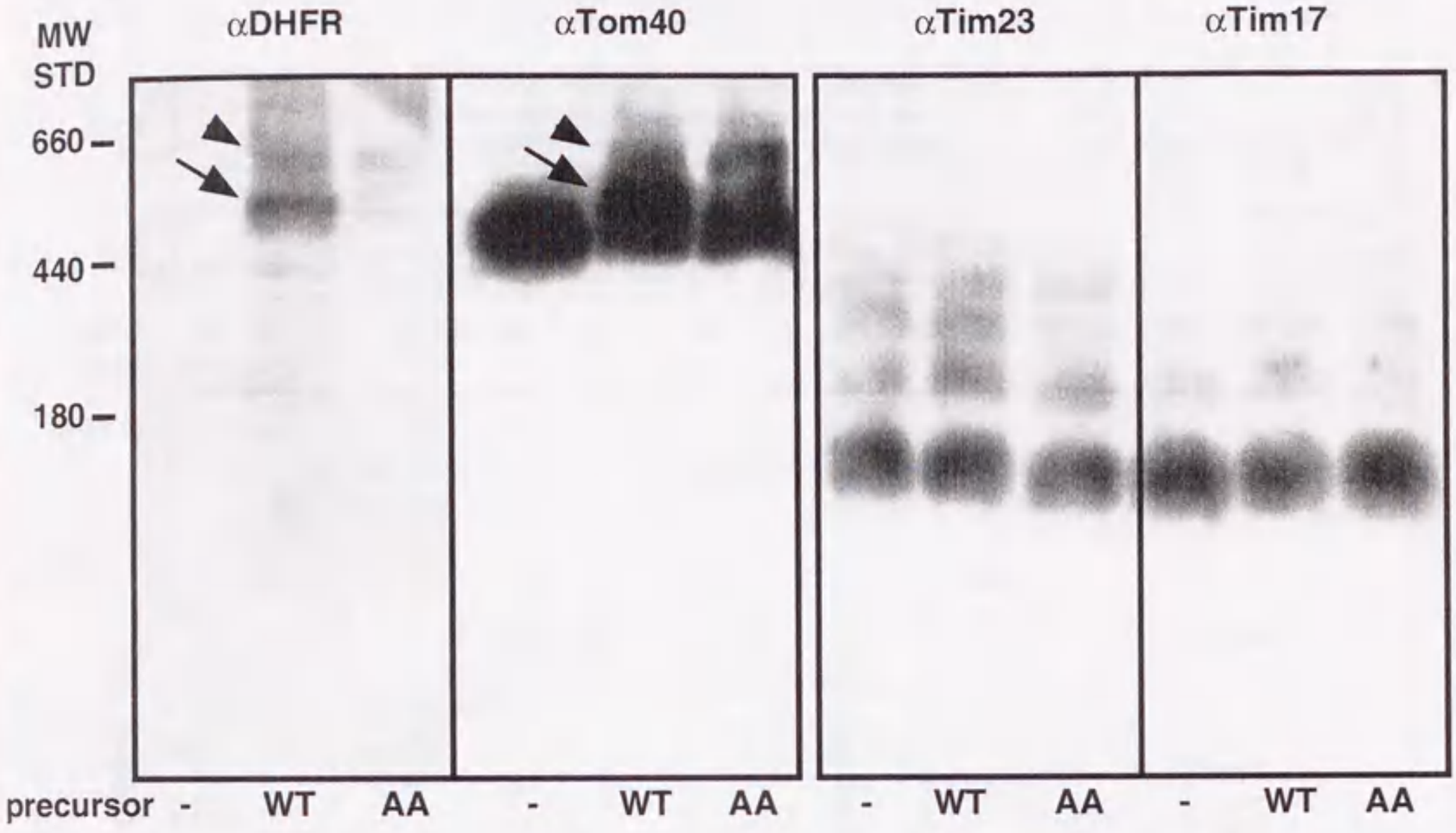

Fig. 2-6 The MTX-arrested pb_2(220)-DHFR fusion proteins form complexes with Tom40

Purified pb_2(220)-DHFR (WT) and pb_2AA(220)-DHFR (AA) were incubated with yeast mitochondria in the presence of 1 μM MTX, and then the mitochondria were solubilized with digitonin buffer. Solubilized proteins were analyzed by blue-native PAGE and immunoblotting with the antibodies against DHFR, Tom40, Tim23, and Tim17. Arrows and arrowheads indicate the bands containing the mature-size form and the intermediate-size form of the fusion proteins, respectively. Thyroglobulin (660 kDa), apoferitin (440 kDa), and carbonic anhydrase (180 kDa) were used as markers for the molecuar weight.

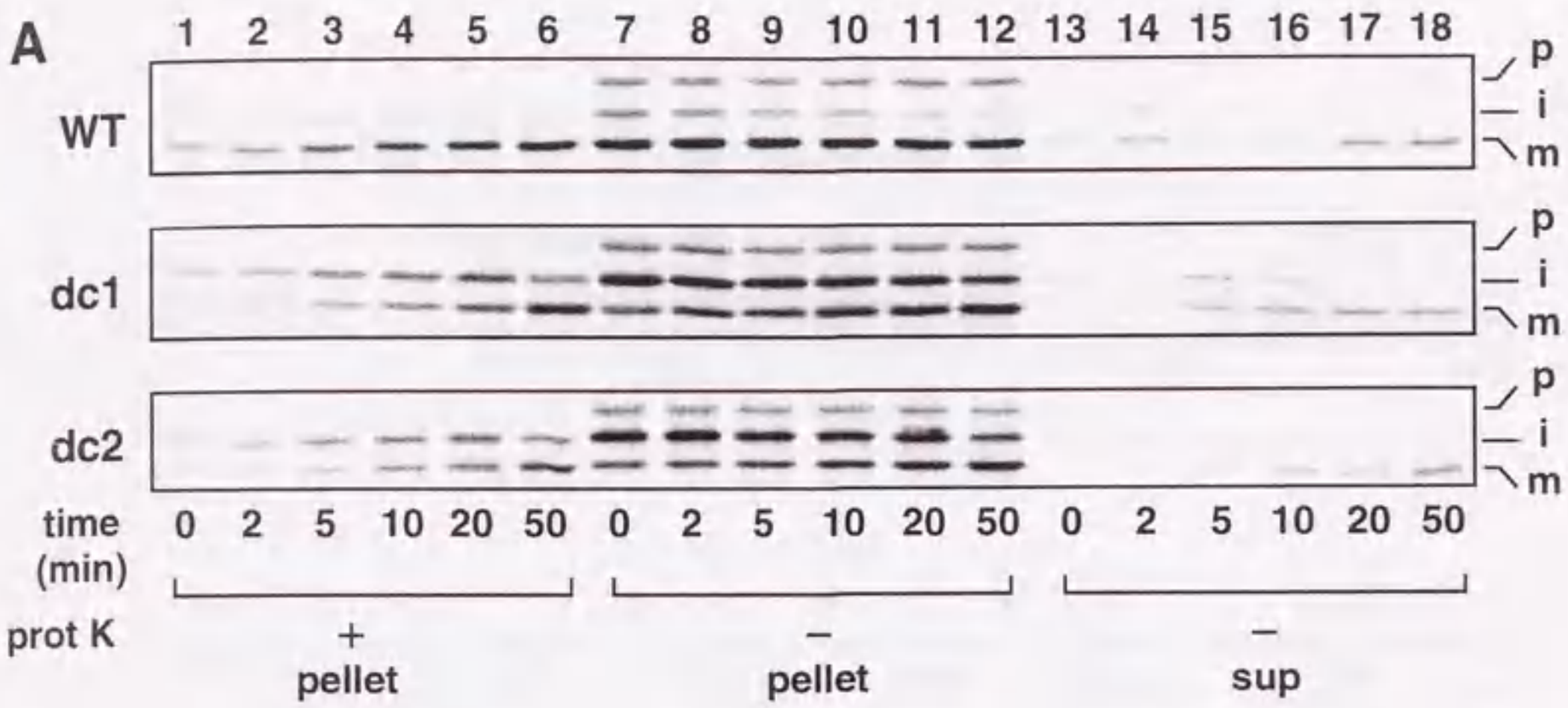

Fig.2-7 The tight folding of the HBD in the IMS promotes the chase of the mature-size forms of the MTX-arrested $pb_2(220)$-DHFR fusion proteins into the IMS.

A, The chase reaction of MTX-arrested $pb_2(220)^{WT}$-DHFR (WT), $pb_2(220)^{dc1}$-DHFR (dc1), and $pb_2(220)^{dc1}$-DHFR (dc2) were performed as described in "Materials and Methods". prot K, proteinase K treatment; sup, post-mitochondrial supernatant; p, precursor; i, intermediate-size form; m, mature-size form.

B, Amounts of the imported proteins (protease-protected mature-size forms (A, lanes 1-6)) are plotted against incubation times in the left panel; the amounts at time 0 are set to 0%. Amounts of the retrotranslocated proteins (the mature-size forms in the post-mitochondrial supernatant (A, lanes 13-18)) are plotted against incubation times in the right panel; the amounts at time 0 are set to 0%. The amounts of the MTX-arrested fusion proteins associated with mitochondria after the first incubation are set to 100%. Squares, WT; triangles, dc1; circles, dc2.

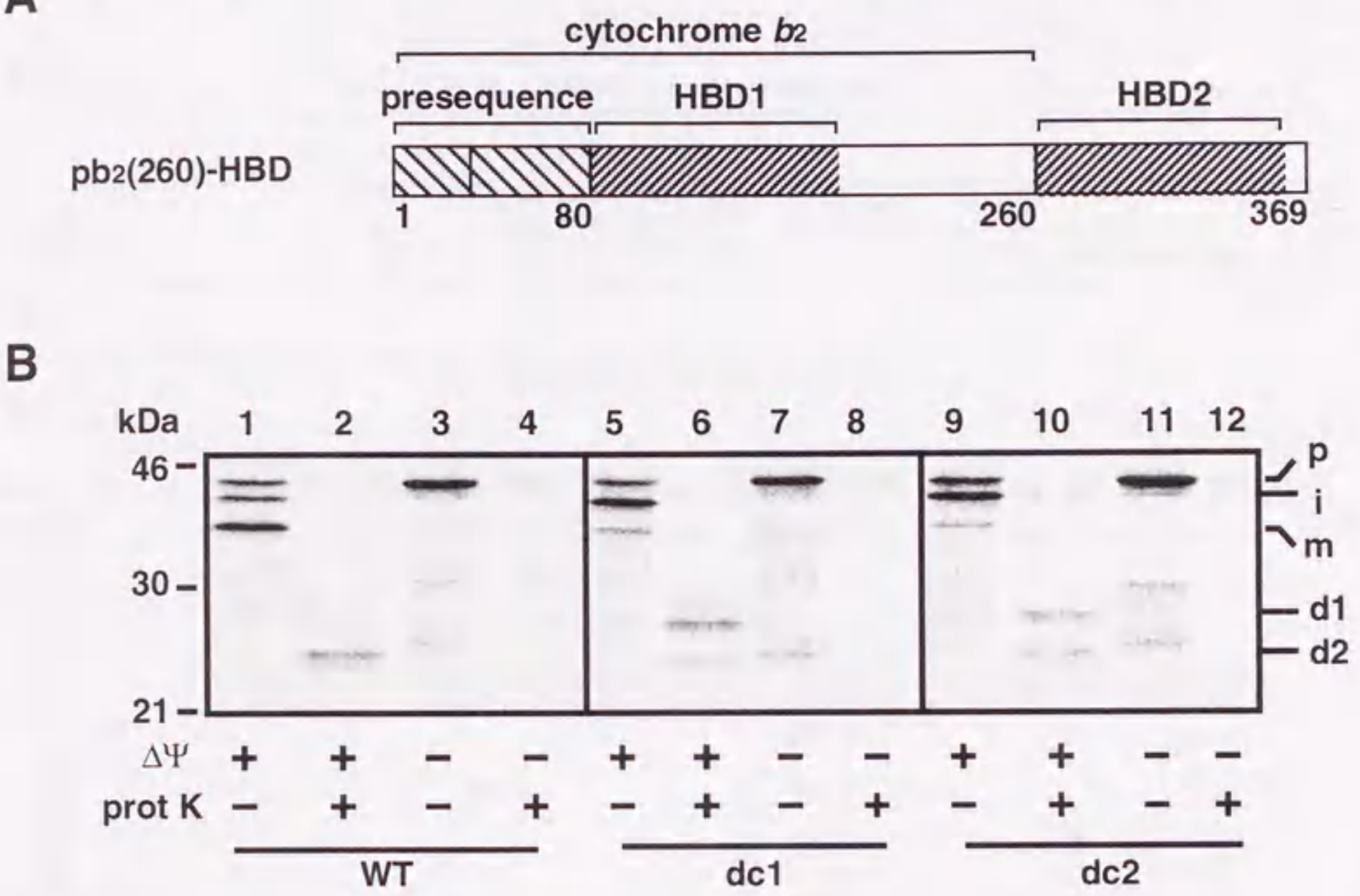

Fig. 2-8 Import of the $pb_2(260)$-HBD fusion proteins is kinetically arrested before translocation of the second HBD across the outer membrane

A, $pb_2(260)$-HBD fusion proteins.

B, Radiolabeled $pb_2(260)^{WT}$-HBD (WT), $pb_2(260)^{dc1}$-HBD (dc1), and $pb_2(260)^{dc2}$-HBD (dc2) were incubated with mitochondria in the presence (lanes 1, 2, 5, 6, 9, 10) or in the absence (lanes 3, 4, 7, 8, 11, 12) of $\Delta\Psi$ across the inner membrane for 30 min at 25°C. The samples were halved, and were incubated with (even lanes) or without (odd lanes) 100 μg/ml proteinase K for 30 min on ice. The mitochondria were reisolated by centrifugation, and were washed once. Proteins were analyzed by SDS-PAGE and radioimaging. p, precursor; i, intermediate-size form; m, mature-size form; d1 and d2, degradation products of 27 kDa and 23 kDa, respectively.

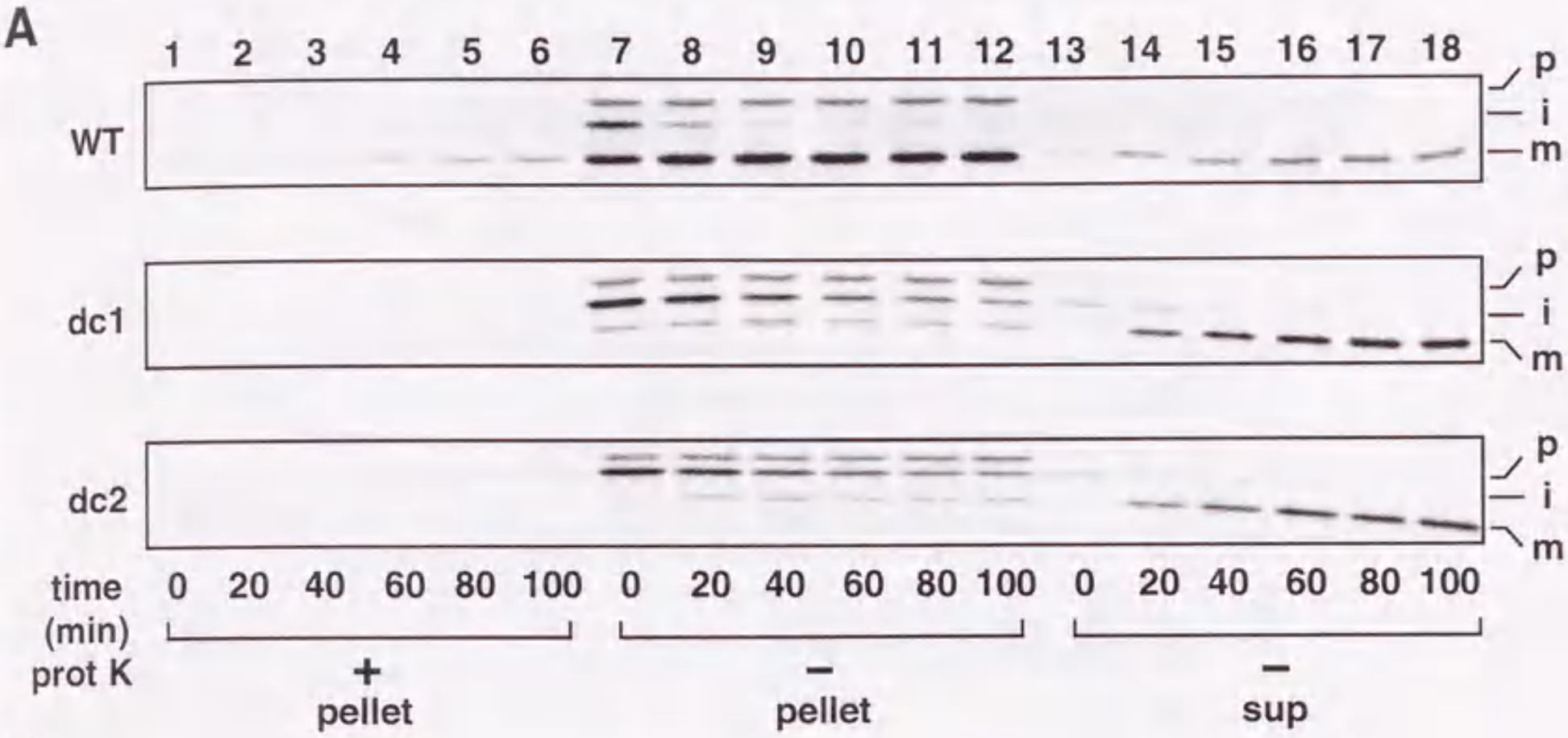

Fig. 2-9 Destabilization of the HBD in the IMS promotes the retrograde translocation of the kinetically arrested translocation intermediates of the pb_2(260)-HBD fusion proteins.

A, The chase reaction of the kinetically arrested $pb_2(260)^{WT}$-HBD (WT), $pb_2(260)^{dc1}$-HBD (dc1), and $pb_2(260)^{dc2}$-HBD (dc2) were performed as described in "Materials and Methods". prot K, protease treatment; sup, post-mitochondrial supernatant; p, precursor; i, intermediate-size form; m, mature-size form.

B, Amounts of the imported proteins and retrotranslocated proteins are plotted against incubation times in the left and the right panels, respectively, as described in the Fig.2-7B. Squares, WT; triangles, dc1; circles, dc2.

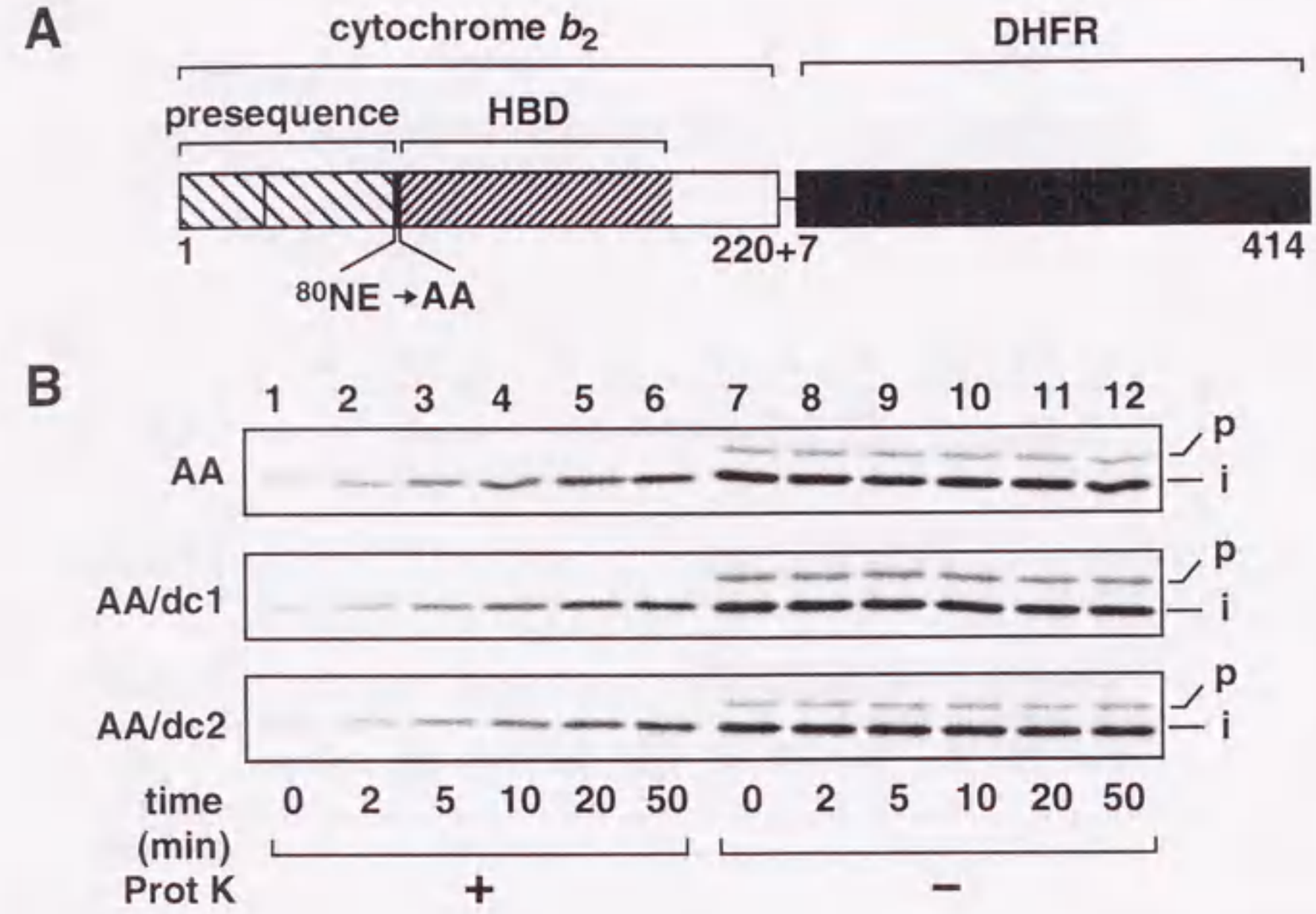

Fig. 2-10 The stability of the tertiary structure of the HBD in the IMS does not affect the chase of the MTX-arrested intermediate-size form

A, The pb_2AA(220)-DHFR fusion protein.

B, The chase reactions of MTX-arrested pb_2AA(220)^{WT}-DHFR (AA), pb_2AA(220)^{dc1}-DHFR (AA/dc1), and pb_2AA(220)^{dc2}-DHFR (AA/dc2) were performed as described in "Materials and Methods". prot K, protease treatment; p, precursor; i, intermediate-size form.

C, Amounts of the protease-protected intermediate-size forms (lanes 1-6) are plotted against incubation times; the amounts at time 0 are set to 0%. The amounts of the fusion proteins added to each reactions are set to 100%. Squares, AA; triangles, AA/dc1; circles, AA/dc2.

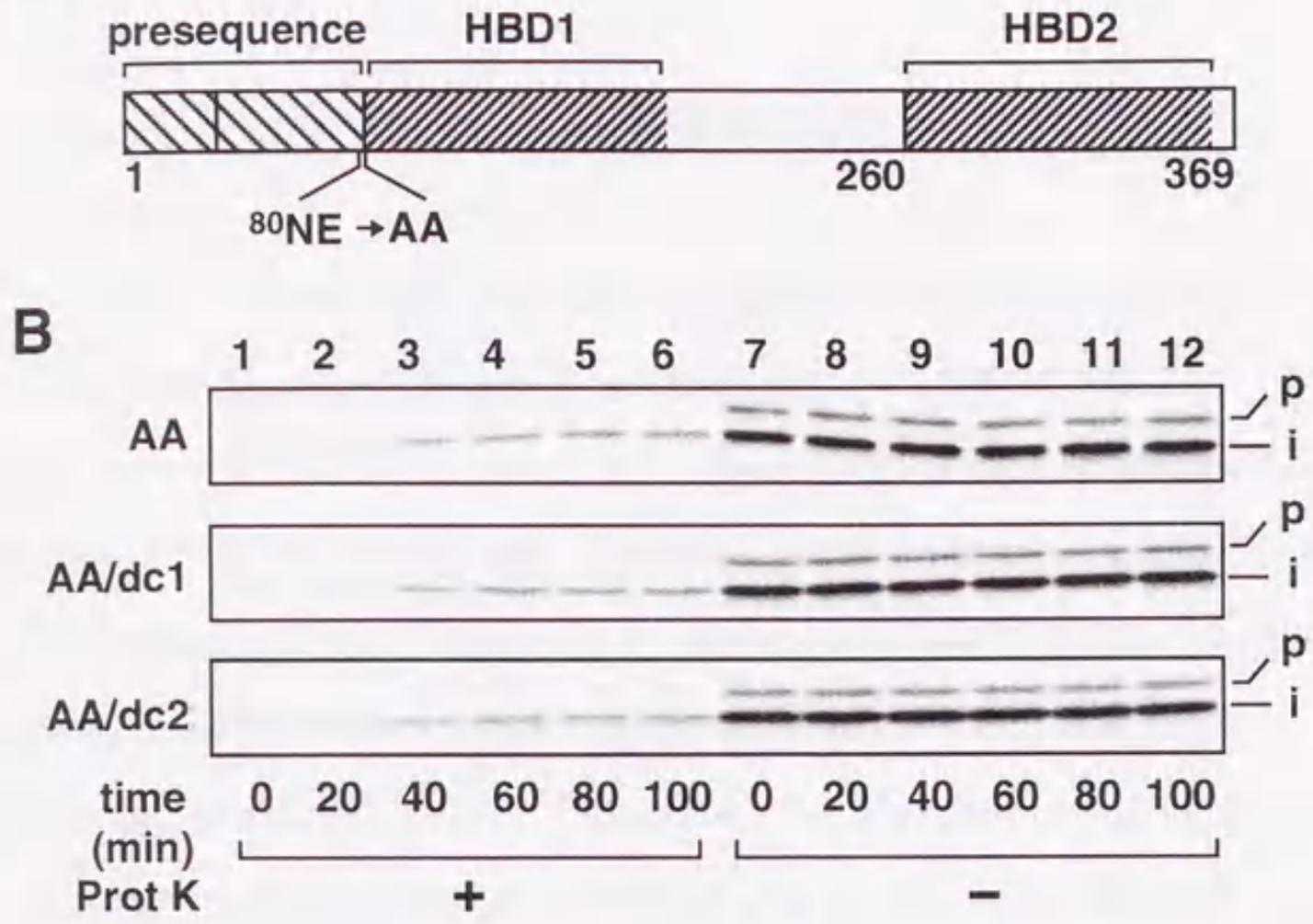

Fig. 2-11 The Stability of the tertiary structure of the HBD in the IMS does not affect the chase of the kinetically arrested intermediate-size form

A, The pb_2AA(260)-HBD fusion protein.

B, The chase reactions of kinetically arrested $pb_2AA(260)^{WT}$-HBD (AA), $pb_2AA(260)^{dc1}$-HBD (AA/dc1), and $pb_2AA(260)^{dc2}$-HBD (AA/dc2) were performed as described in "Materials and Methods". prot K, protease treatment; p, precursor; i, intermediate-size form.

C, Amounts of the protease-protected intermediate-size forms (lanes 1-6) are plotted against incubation times; the amounts at time 0 are set to 0%. The amounts of the fusion proteins added to each reactions are set to 100%. Squares, AA; triangles, AA/dc1; circles, AA/dc2.

2-4 DISCUSSION

The sorting route for proteins including cytochrome b_2 to the mitochondrial IMS has been a matter of debate for several years. To address this issue, I prepared an MTX-arrested translocation intermediate of $pb_2(220)^{WT}$-DHFR in which the N-terminus reached the IMS whereas the C-terminal DHFR domain remained outside the mitochondria. With this intermediate, I showed here that the HBD of the intermediate is stably folded in the IMS, which is consistent with the stop-transfer model but not with the conservative sorting model. This observation is consistent with the previous study, which showed the presence of the folded and protease-resistant HBD in the MTX-arrested $pb_2(219)^{WT}$-DHFR in the IMS by protease digestion after the outer membrane was ruptured (12). Although this earlier approach could not rule out the possibility that the HBD may have folded after cleavage by Imp1p, the present approach avoids such a problem by using Imp1p cleavage itself as an indicator of the HBD folding.

In the stop-transfer model, the MTX-arrested intermediate of the mature-size form of the cytochrome b_2 fusion protein was predicted to be a dead-end intermediate (2, 4). Therefore, the successful chase of the intermediate into the IMS was interpreted as strong evidence for the conservative sorting model (13). However, I have demonstrated here that the chase of the MTX-arrested mature-size intermediate into the IMS can be efficiently achieved in the framework of the stop-transfer model. The present study shows that the late step of the translocation of cytochrome b_2 fusion proteins can be driven by two mechanisms (Fig. 2-12), both of which are uncoupled from the translocation across the inner membrane.

The timing of the second processing by Imp1p switches the mechanism for the late step of the translocation across the outer membrane. When the second processing takes place later and the protein retains the anchorage of its presequence to the inner membrane, the lateral diffusion of the anchored presequence in the plane of

the inner membrane can drive the protein translocation across the outer membrane. Several inner membrane proteins like D-lactate dehydrogenase that are anchored to the inner membrane at their N-terminus and face to the IMS may well use this anchor diffusion mechanism to traverse the outer membrane (17).

When the second processing occurs before the completion of the protein translocation and the protein loses the anchorage to the inner membrane, the Brownian ratchet mechanism can drive the translocation of the rest part of the molecule. The tight folding of the translocating polypeptide chain on the IMS side can function as a ratchet and prevents the back sliding of the polypeptide chain by its Brownian motion. The establishment of the well-defined *in vitro* system to drive protein translocation across the membrane by a Brownian ratchet mechanism allows me to analyze in detail the conditions that affect the rate and direction of the protein translocation. For example as I showed here, the stability of the protein domain on the trans side of the membrane significantly affects the efficiency of the forward translocation vs. the retrograde translocation; the more stably folded trans-side domain could promote the forward translocation of the protein more efficiently. Besides, the rate and the direction of the protein translocation by the Brownian ratchet depend on the stability of the folded domain on the cis side of the membrane. The DHFR domain is less stable than the HBD domain when monitored by protease digestion (Fig. 2-3), suggesting that the global unfolding of the DHFR domain is faster than that of the HBD (18). The translocation intermediate of pb_2(220)^{WT}-DHFR was chased into the IMS more efficiently than that of pb_2(260)^{WT}-HBD. This suggests that the less stable folded domain on the cytosolic side of the membrane leads to more efficient forward translocation of the protein into the IMS than its retrograde translocation to the cytosol. These observations indicate that the global unfolding rates of both cis-side and trans-side domains correlate with the rate of the transmembrane movement driven by the Brownian ratchet.

The present study offered direct evidence for the Brownian ratchet mechanism in operation for protein translocation across the mitochondrial outer membrane. However, the Brownian ratchet mechanism may operate for other membrane systems as well. In such cases, the ratchet may not be necessarily provided by the folding of the translocating protein on the trans side of the membrane. For example, binding of the molecular chaperone Hsp70 to the unfolded translocating polypeptide segment on the trans side of the mitochondrial inner and the ER membranes could function as an efficient ratchet to promote vectorial protein translocation across the membrane. The question of whether the Brownian ratchet by the Hsp70 binding alone is sufficient for driving the protein translocation across the mitochondrial inner and the ER membranes is open to future studies.

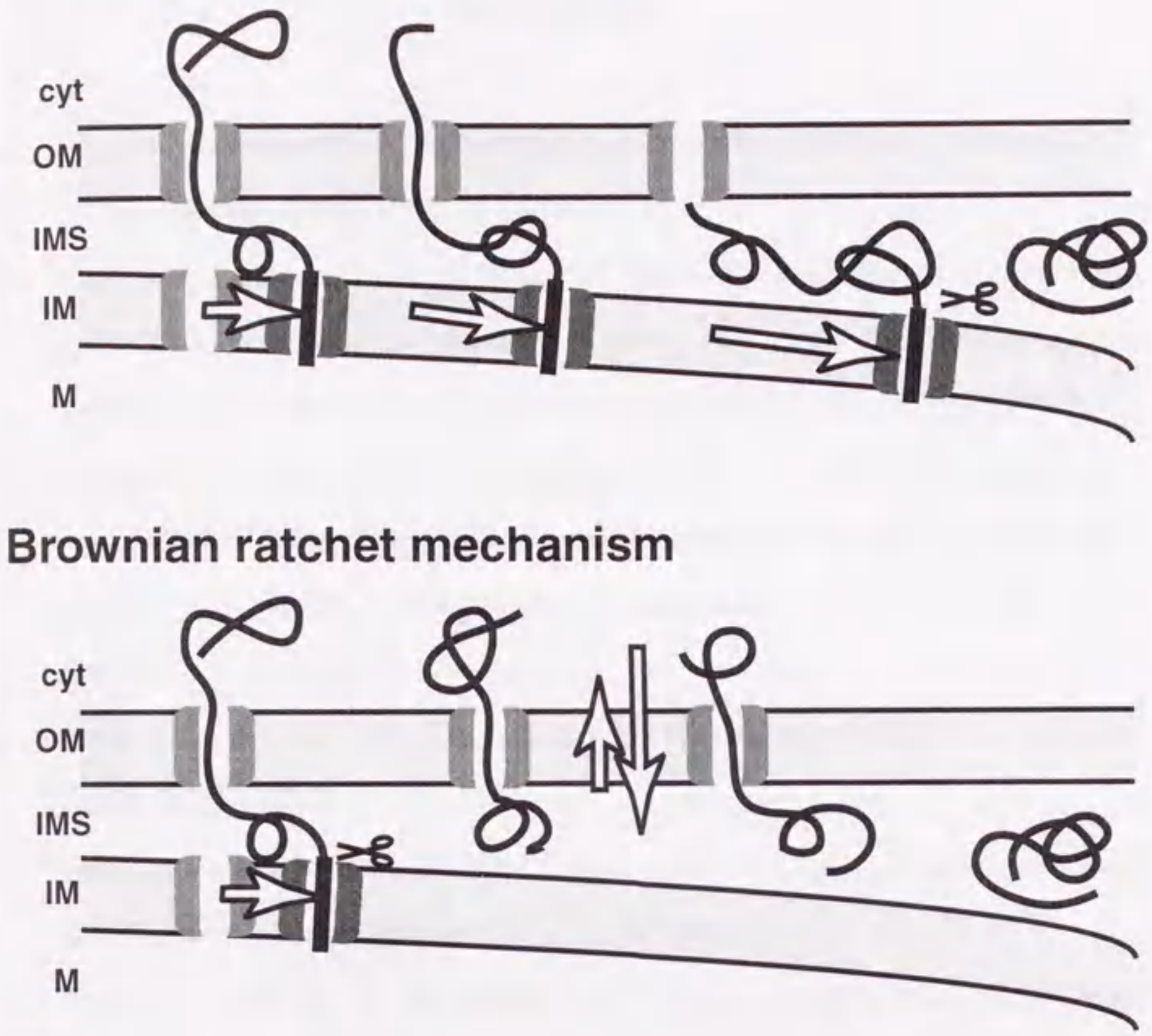

Fig. 2-12 Two distinct mechanisms drive the translocation of cytochrome b_2 across the outer membrane

When cytochrome b_2 has not received the second processing by Imp1p, the driving force for the translocation of cytochrome b_2 across the outer membrane may be provided by the latelal diffusion of the anchorage of the presequence in the inner membrane (anchor diffusion mechanism). Once cytochrome b_2 has received the second processing, the driving force for the translocation of cytochrome b_2 is provided by the Brownian motion biassed by the folding of the HBD on the IMS (Brownian ratchet mechanism). cyt, cytosol; OM, outer membrane; IMS, intermembrane space; IM, inner membrane; M, matrix.

REFERENCES

1. Xia, Z-x. and Mathews, F. S. (1990) Molecular structure of flabocytochrome b_2 at 2.4 Å resolution. *J. Mol. Biol.*, **212**, 837-863
2. Glick, B. S., Wachter, C., Reid, G.A., and Schatz, G. (1993) Import of cytochrome b_2 to the mitochondrial intermembrane space: The tightly folded heme-binding domain makes import dependent upon matrix ATP. *Protein Sci.*, **2**, 1901-1917]
3. Daum, G., Gasser, S. M., and Schatz, G. (1982) Import of proteins into mitochondria: Energy-dependent, two-step processing of the intermembrane space enzyme cytochrome b_2 by isolated yeast mitochondria. *J. Biol. Chem.*, **257**, 13075-13080
4. Glick, B. S., Beasley, E.M., and Schatz, G. (1992) Protein sorting in mitochondria. *Trends Biochem. Sci.*, **17**. 453-459
5. Stuart, R. A. and Neupert, W. (1996) Topogenesis of inner membrane proteins of mitochondria. *Trends Biochem. Sci.*, **21**, 261-267
6. Voos, W., Gambill, B. D., Guiard, B., Pfanner, N., and Craig, E.A. (1993) Presequence and mature part of preproteins strongly influence the dependence of mitochondrial protein import on heat shock protien 70 in the matrix. *J. Cell Biol.*, **123**, 119-126
7. Gärtner, F., Bömer, U., Guiard, B., and Pfanner, N. (1995) The sorting signal of cytochrome b_2 promotes early divergence from the general mitochondrial import pathway and restricts the unfoldase activity of matrix Hsp70. *EMBO J.*, **14**, 6043-6057
8. Kanamori, T., Nishikawa, S., Shin, I., Schultz. P. G., and Endo, T. (1997) Probing the environment along the protein import pathways in yeast mitochondria by site-specific photocrosslinking. *Proc. Natl. Acad. Sci. USA*, **94**, 485-490
9. Kunkel, T. A., Roberts, J. D., and Zakour, R. A. (1987) Rapid and efficient site-

specific mutagenesis without phenotypic selection. *Methods Enzymol.*, **154**, 367-382

10. Daum, G., Böhni, P.C., and Schatz, G. (1982) Import of proteins into mitochondria. Cytochrome b_2 and cytochrome c peroxidase are located in the intermembrane space of yeast mitochondria. *J. Biol. Chem.*, **257**, 13028-13033
11. Dekker, P. J. T., Martin, F., Maarse, A. C., Bömer, U., Müller, H., Guiard B., Meijer, M., Rassow, J., and Pfanner, N. (1997) The Tim core complex defines the number of mitochondrial translocation contact sites and can hold arrested preproteins in the absence of matrix hsp70-Tim44. *EMBO J.*, **16**, 5408-5419
12. Rospert, S., Müller, S., Schatz, G., and Glick, B. S. (1994) Fusion proteins containing the cytochrome b_2 presequence are sorted to the mitochondrial intermembrane space independently of hsp60. *J. Biol. Chem.*, **269**, 17279-17288
13. Gruhler, A., Ono, H., Guiard, B., Neupert, W., and Stuart, R. A. (1995) A novel intermediate on the import pathway of cytochrome b_2 into mitochondria: evidence for conservative sorting. *EMBO J.*, **14**, 1349-1359
14. Neupert, W., Hartl, F. U., Craig, E. A., and Pfanner, N. (1990) How do polypeptides cross the mitochondrial membranes. *Cell*, **63**, 447-450
15. Simon, S. M., Peskin, C. S., and Oster, G. F. (1992) What drives the translocation of proteins? *Proc. Natl. Acad. Sci. USA*, **89**, 3770-3774
16. Herrmann, J. M. and Neupert, W. (2000) What fuel polypeptide translocation? An energetical view on mitochondrial protein sorting. *Biochim. Biophys. Acta*, **1459**, 331-338
17. Rojo, E. E., Guiard, B., Neupert, W., and Stuart, R., A. (1998) Sorting of D-Lactate Dehydrogenase to the inner membrane of mitochondria. *J. Biol Chem.*, **273**, 8040-8047
18. Imoto, T., Yamada, H., and Ueda, T. (1986) Unfolding rates of globular proteins determined by kinetics of proteolysis. *J. Mol. Biol.*, **190**, 647-649

19. Jensen, R. E. and Johnson, A. E. (1999) Protein translocation: Is Hsp70 pulling my chain? *Curr. Biol.*, **9**, R779-782

Chapter 3

Site-specific photocrosslinking revealed that Tom40 has a chaperone-like function

3-1 INTRODUCTION

Newly synthesized proteins must traverse biological membranes when the sites of their synthesis and of their functions are separated by cellular membranes. In order to allow the protein to go across the hydrophobic barrier of the lipid bilayer, the bacterial cytoplasmic membrane and the eukaryotic mitochondrial, ER, and chloroplast membranes possess protein-conducting channels. The electron microscopy showed the presence of pores with diameters of 15-20 Å, 19-23 Å, and 16-20 Å for the SecYEG channel in the bacterial cytoplasmic membrane, the Sec61 channel in the ER membrane, and the TOM channel in the mitochondrial outer membrane, respectively (1-3). Since the diameters of these pores are smaller than globular protein domains, proteins have to become unfolded to thread through the pores. Treatment of the unfolded translocation intermediates spanning the membrane with various reagents revealed hydrophilic environments for the translocating polypeptides (4, 5). Analyses of the stability of the MTX-arrested DHFR fusion protein in a complex with the translocation pores in the mitochondrial membranes showed that the TOM and TIM complexes provide passive channels through which the translocating protein can slide back and forth efficiently (see Chapter 2, ref. 6). These results underscore the limited interactions between the inner wall of the translocation pores and the translocating unfolded polypeptide chains. Recently, X-ray structures have been determined for both the large and small subunits of ribosome (7, 8). The polypeptide exit tunnel in the large ribosomal subunit has an average diameter of 15 Å and its inner wall exhibits a nonstick character to avoid any stable interactions with the unfolded nascent chain. However, the question of if the protein translocation pore has a similar nonstick inner wall and is prevented from interactions with the translocating protein remains unresolved.

The site-specific photocrosslinking offers a powerful tool to analyze the environment around the translocating protein in the protein-conducting channel. A

photoreactive unnatural amino acid is incorporated into the protein site-specifically by using the suppressor tRNA method (9). Briefly, the codon for the amino acid of interest is replaced with the amber nonsense codon by conventional oligonucleotide-directed mutagenesis and the resulting DNA is subjected to *in vitro* transcription. A suppressor tRNA which recognizes the amber nonsense codon is chemically aminoacylated with the desired unnatural amino acid and is added to an *in vitro* translation system that contains the mutant mRNA. This results in the specific incorporation of the unnatural amino acid at the position corresponding to the amber mutation (Fig. 3-1).

By using this approach, Kanamori et al. have analyzed the interactions of the translocation intermediates of pb_2(220)-DHFR and $pb_2\Delta$19(220)-DHFR, which are destined for the matrix and for the intermembrane space (IMS), respectively, with the TOM and TIM complexes (10). Although the MTX-bound DHFR domain of both pb_2(220)-DHFR and $pb_2\Delta$19(220)-DHFR remained outside the mitochondria, the segment interacting with the TOM channel, Tom40, differ each other significantly in their lengths; a 50-residue segment of pb_2(220)-DHFR is crosslinked with Tom40 whereas a 30-residue one of $pb_2\Delta$19(220)-DHFR is close to Tom40 (Fig. 3-2). The reason for this difference could reflect the difference in the pulling force for the N-terminus of the fusion proteins by the translocation system between the matrix and the IMS. However, the precise mechanism for Tom40 to accommodate different lengths of the polypeptide segments of the translocating protein has been still vague.

In the present study, I analyzed the interaction of the translocation intermediate of pb_2(330)-DHFR with Tom40 by site-specific photocrosslinking. The obtained results suggest that Tom40 accommodate a segment of as long as 120 amino-acid residues if it is unfolded. This suggests that Tom40 is a sort of molecular chaperone for translocating proteins by associating with the unfolded polypeptide segment to prevent its misfolding or undesirable interactions leading to aggregation. In other

words, Tom40 provides a protein-conducting channel that is not a simple passive pore but offers an optimized environment for translocating unfolded proteins.

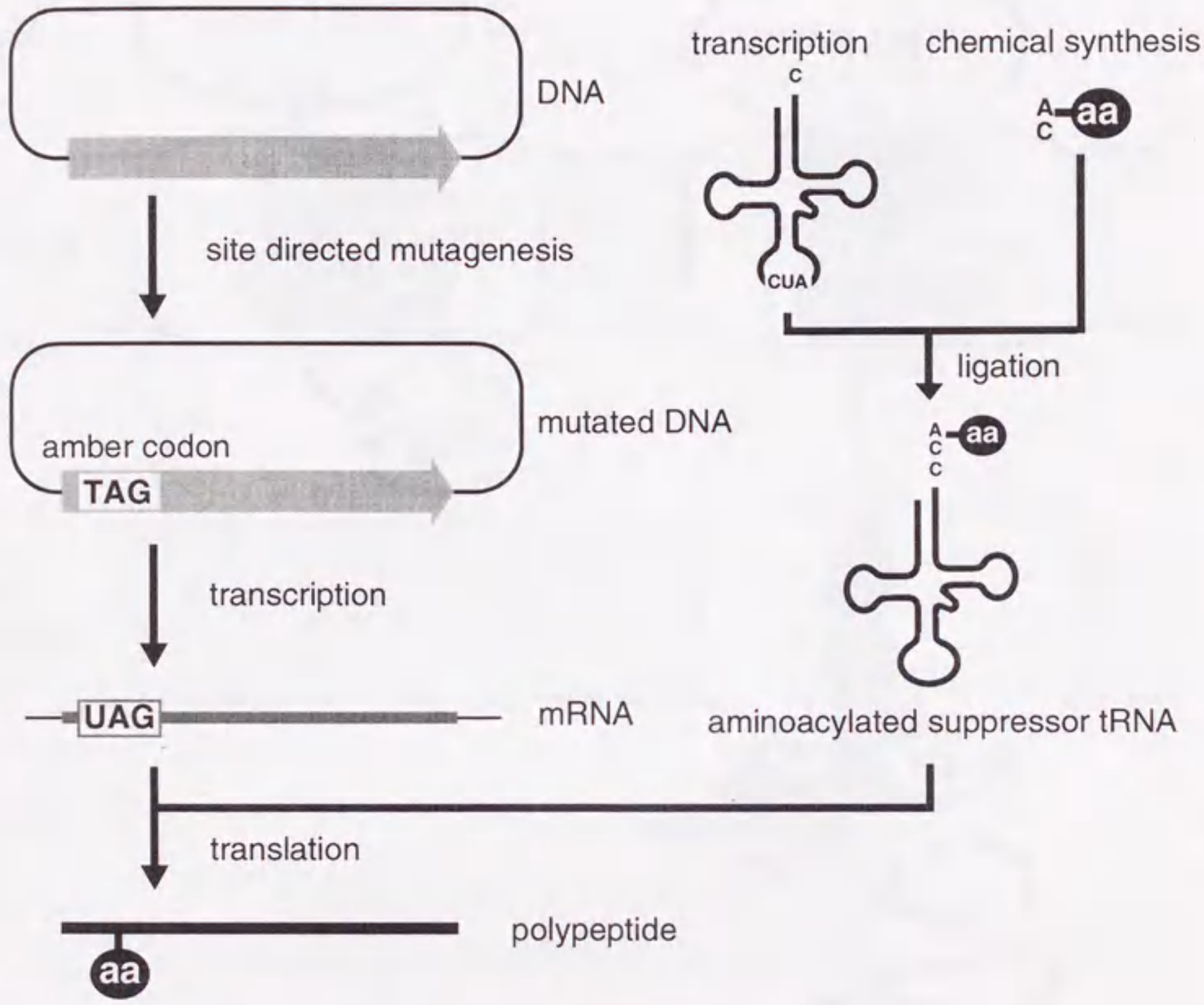

Fig. 3-1 Suppressor tRNA method

The codon for the amino acid of interest is replaced with the amber nonsense codon by conventional oligonucleotide-directed mutagenesis. Then a suppressor tRNA, which recognizes the amber nonsense codon, is constructed. The suppressor tRNA is chemically aminoacylated with a desired unnatural amino acid and is added to an *in vitro* translation system. This results in the specific incorporation of the unnatural amino acid at the position corresponding to the amber mutation

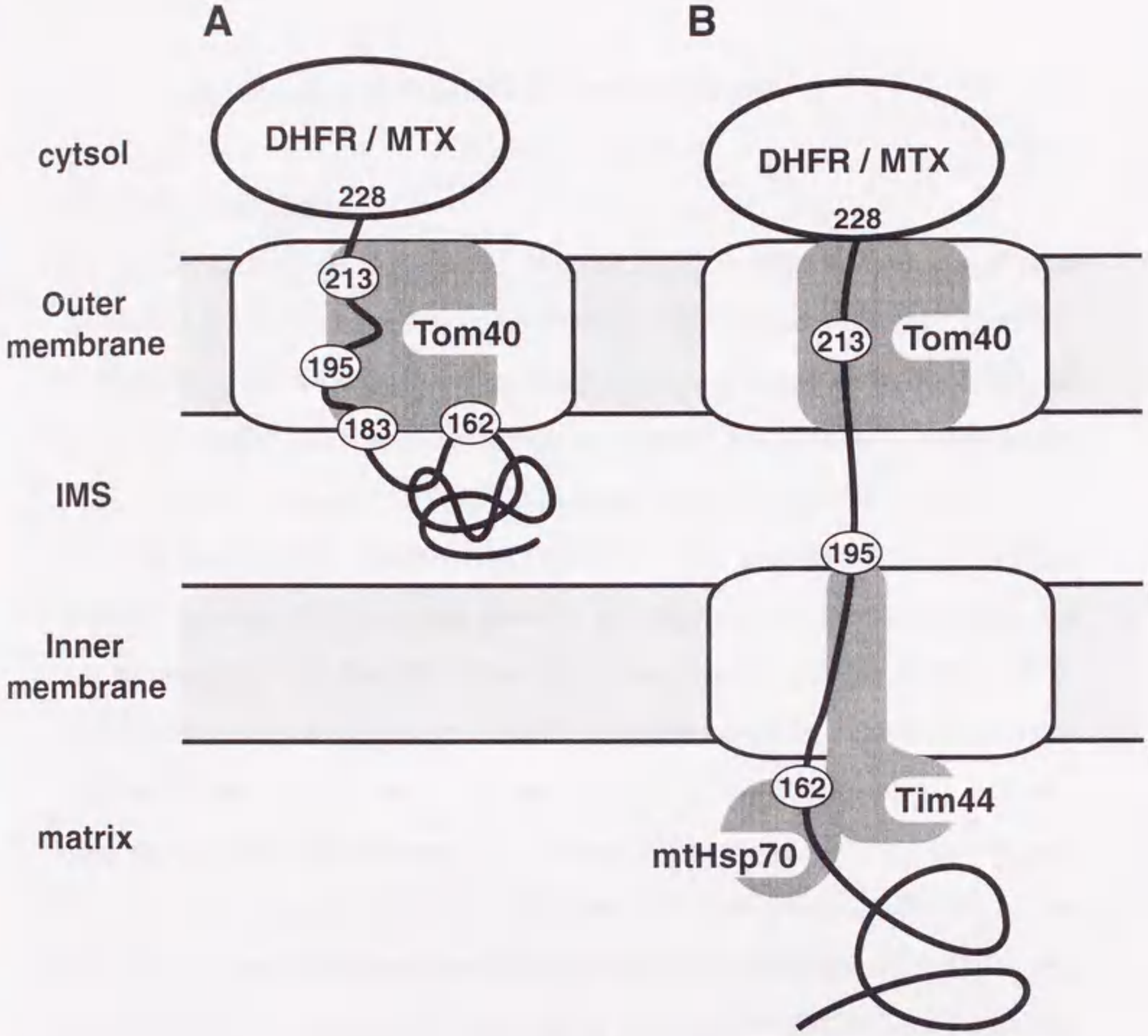

Fig. 3-2 Site-specific photocrosslinking reveals the interaction of the translocating protein with the component of the translocator complexes

The previous study showed that MTX-arrested pb_2(220)-DHFR (A; sorted to the IMS) and $pb_2\Delta19$(220)-DHFR (B; sorted to the matrix) were crosslinked to Tom40, Tim44, and mtHsp70 (10). The numbers indicate the residues crosslinked to the proteins.

3-2 MATERIALS and METHODS

Construction of plasmids

The gene encoding pb_2(330)-DHFR, the first 330 amino acid residues of yeast cytochrome b_2 precursor fused to mouse DHFR, in which codons for Asp^{85} and Met^{86} are replaced by those for Glu^{85} and Leu^{86} and seven extra amino acids, DLSRSGI, are inserted as a linker, was constructed as follows; pHW1 (10) was used as a template for PCR with primers 5'-CCTTCAAGGATCCATGCCTCC-3' and 5'-GGATCTCGAGAGATCCCATTGAATTTGTT-3'. The amplified 0.5 kbp fragment encoding residues 167-330 of cytochrome b_2 was digested with *Bam*HI and *Xho*I, and was introduced into the *Bam*HI and *Xho*I sites of the plasmid encoding pb_2(220)-DHFR (10). The gene for pb_2AA(330)-DHFR was constructed by replacing the DNA fragment for the first 167 amino acid residues of pb_2(330)-DHFR with the one taken from pb_2AA(220)-DHFR (Chapter 2). The codon for residue 94, 114, 132, 154, 162, 174, 183, 195, 204, 213, 224, 233, 252, 264, 272, 284, 293, 305, 314, or 323 of pb_2(330)-DHFR and of pb_2AA(330)-DHFR and the codon for residue 94, 114, 132, 154, 162, 183, or 213 of pb_2AA(220)-DHFR and of $pb_2AA(220)^{dc2}$-DHFR were replaced by the TAG codons by oligonucleotide-directed mutagenesis using appropriate oligonucleotides (11).

MTX-arrest of the protein translocation and photocrosslinking

The fusion proteins containing BPA at positions of interest were synthesized in the presence of [^{35}S]methionine by the suppressor tRNA method as described previously (10). Mitochondria were isolated from yeast strain D273-10B (12). The translation products (5%) were incubated with 1 μM MTX and 1 mM NADPH in import buffer (250 mM sucrose, 10 mM Mops-KOH, pH 7.2, 80 mM KCl, 5 mM $MgCl_2$, 2.5 mM KPi, 5 mM DTT, 2 mM methionine, 1% BSA, 2 mM ATP, 2 mM NADH) for 15 min on ice,

and subsequently incubated with mitochondria for 20 min at 30°C. For photocrosslinking, the mitochondria were reisolated by centrifugation, were washed once with 250 mM sucrose, 5 mM EDTA, 10 mM Mops-KOH, pH 7.2, 1 μM MTX, and were resuspended with the same buffer. The samples were halved, and one halves were UV-irradiated for 5 min on ice as described previously (10). Immunoprecipitation with the antibodies raised against Tom40 and Tom20 was performed as described previously (10). Proteins were analyzed by SDS-PAGE and radioimaging with a Storm 860 image analyzer (Amersham Pharmacia Biotech).

Expression and purification of Tom40

The gene encoding Tom40 was subcloned into the vector pET21a (Novagen). The resulting plasmid was transformed into *E. coli* BL21(DE3) strain. The cells were grown in the TB medium (1.2% tryptone, 2.4% yeast extract, 0.4% glycerol, 17 mM KH_2PO_4, 72 mM K_2HPO_4) at 37°C to an Abs_{600} of 0.5. After induction with 1 mM isopropyl-β-D-thiogalactopyranoside (IPTG) for 2 hours, the cells were collected by centrifugation and were suspended with 50 mM Tris-HCl, pH 8.0, 1 mM EDTA, 100 mM NaCl, 100 μg/ml lysozyme. The cell suspension was frozen at -80°C and thawed at room temperature. The cells were disrupted by sonication for 18 min (2 s on/1 s off pulsed periods, 40% duty, Astorason XL2020 sonicator with a micro tip). The cell lysate was centrifuged at 4,300×*g* for 1 hour at 4°C. The precipitated inclusion bodies were washed once with 2% Triton X-100, 2 M urea, 50 mM Tris-HCl, pH 8.0, 10 mM EDTA, 100 mM NaCl, were washed again with the above buffer without Triton X-100, and were subsequently solubilized in 8 M urea, 50 mM Tris-HCl, pH 8.0, 10 mM EDTA, 100 mM DTT. The pH was lowered to 6.5 by adding 0.1M HCl, and the sample was centrifuged at 50,000×*g* for 20 min at 4°C. The supernatant containing Tom40 (~80% purity) was dialyzed against 6 M urea, 50 mM Tris-HCl, pH 8.0, 1 mM EDTA, 2 mM DTT for 2 hours at room temperature.

Aggregation and reactivation of urea-denatured DHFR

Purified recombinant DHFR and pSu9(69)-DHFR, which contains the presequence of Fo-ATPase subunit 9 of *Neurospora crassa* and mouse DHFR (13), were denatured in 7 M urea, 30 mM Tris-HCl, pH 7.4, 50 mM DTT. The denatured proteins were diluted 100-fold (3 μM) with 60 mM Mega-9, 10 mM Mops-Tris, pH 7.0, 1 mM EDTA, and 10 mM DTT in the presence or absence of Tom40. After centrifugation at 15,000×*g* for 15 min, proteins in the supernatant were analyzed by SDS-PAGE and immunoblotting with the antibodies raised against DHFR.

The DHFR activity was measured as described previously (14). Briefly, DHFR was incubated with 50 μM dihydrofolic acid (Sigma) and 100 μM NADPH in 50 mM KPi, pH 7.4 at room temperature, and decrease in the absorbance at 340 nm was measured. In order to confirm that the inhibitory activity for DHFR is not present in the assay solution, the recombinant DHFR was added after 7 min of incubation.

3-3 RESULTS

3-3-1 A part of the cytochrome b_2 domain of the MTX-arrested pb_2(330)-DHFR is exposed to the cytosolic side of mitochondria

pb_2(330)-DHFR, the N-terminal 330 residues of yeast cytochrome b_2 fused to mouse DHFR, contains two tightly folded domains, the HBD and DHFR separated by about 160 amino-acid residues. When incubated with isolated yeast mitochondria, radiolabeled pb_2(330)-DHFR was processed to the mature-size form, which is resistant to externally added protease (Fig. 3-3A, lane 2). The imported mature-size form was sensitive to protease once the outer mitochondrial membrane was ruptured by osmotic shock (Fig. 3-3A, lane 4), indicating that pb_2(330)-DHFR was correctly sorted to the IMS *in vitro*. When incubated with mitochondria in the presence of MTX, pb_2(330)-DHFR was processed to the mature-size form but was still sensitive to externally added protease (Fig. 3-3A, lane 5 and 6). This was due to the inhibition of the translocation of the DHFR domain by binding of MTX. The efficient formation of the mature-size species indicates that the HBD of this MTX-arrested pb_2(330)-DHFR is folded tightly in the IMS since the processing by Imp1p to yield the mature-size form requires the folded HBD (see Chapter 2).

Mitochondria with the MTX-arrested pb_2(330)-DHFR were treated with various concentrations of proteinase K. The mitochondria were reisolated by centrifugation, and the proteins were analyzed by SDS-PAGE. When treated with low concentrations (0.01 μg/ml) of proteinase K, 28 kDa (Fig. 3-4A, p1) and 26 kDa (Fig. 3-4A, s1) fragments were recovered with the mitochondria and in the supernatant, respectively. As the concentration of proteinase K was increased, the amounts of 28-kDa and 26-kDa fragments increased (Fig. 3-4C). The 26-kDa fragment in the supernatant was immunoprecipitated with the anti-cytochrome b_2 antibodies as well as with the anti-DHFR antibodies, whereas the 28-kDa fragment was precipitated only

with the anti-cytochrome b_2 antibodies (Fig. 3-4B). These results suggest that the fragments were produced by a protease cut of the fusion protein around the residue 310 in the cytochrome b_2 domain (Fig. 3-4D). At higher concentrations of proteinase K, the amounts of the 28-kDa and the 26-kDa fragments decreased, and instead, 25-kDa and 21-kDa fragments were generated in the pellet and in the supernatant, respectively (Fig. 3-4A and C, p2 and s2). The apparent molecular masses suggest that the 25-kDa fragment and the 21-kDa fragment correspond to residues 81-280 and the DHFR domain, respectively. This means that the C-terminal 50 residues of the cytochrome b_2 domain and the DHFR domain of the MTX-arrested pb_2(330)-DHFR are exposed to the cytosolic side, although residues 280-310 and residues 310-330 of the cytochrome b_2 domain are sterically protected to some extent against the protease digestion.

On the other hand, when mitochondria with the MTX-arrested pb_2(220)-DHFR were treated with proteinase K, 22-kDa fragments were recovered with the mitochondria (Fig. 3-5A, p1) and in the supernatant (Fig. 3-5A, s1). As the concentration of proteinase K was increased, the 22-kDa fragments (p1 and s1) were converted to slightly smaller molecular-mass species of 21-kDa (Fig. 3-5A, p2 and s2, respectively). The fragments in the pellet were precipitated only with the anti-cytochrome b_2 antibodies while those in the supernatant with the anti-DHFR antibodies (Fig. 3-5B). Therefore, the entire part (residues 80-220) of the cytochrome b_2 domain of the MTX-arrested pb_2(220)-DHFR is sequestered in the mitochondria and is not exposed to the cytosolic side. In other words, the DHFR domain of the MTX-arrested translocation intermediate of pb_2(220)-DHFR is close to the outer membrane, whereas that of pb_2(330)-DHFR is not.

3-3-2 MTX-arrested pb_2(330)-DHFR is crosslinked to Tom20 as well as Tom40

Benzophenone excited by < 360 nm light can react with a hydrolated carbon, resulting in generation of a covalent bond (Fig. 3-6A). DL-2-amino-5-(*p*-

benzoylphenyl)pentanoic acid (BPA) bearing a benzophenone group is useful as a photoreactive amino-acid crosslinker (Fig. 3-6B). In the present study, BPA was systematically incorporated into various positions in pb_2(330)-DHFR by using the suppressor tRNA method (10). pb_2(330)-DHFR mutants containing BPA were incubated with mitochondria in the presence of MTX, and were subjected to UV irradiation for photocrosslinking. BPA introduced at residue 204 yielded a crosslinked product of 115 kDa (Fig. 3-7, lane 10), whereas that at residue 284 yielded those of 114, 85, 76, 65, and 57 kDa (Fig. 3-7, lane 36). Thus, BPA generated crosslinked products , which depend on the UV irradiation and on the positions of BPA. To identify partner proteins of the crosslinked products, the mitochondria were solubilized with detergent and were subjected to immunoprecipitation with antibodies raised against the known components of the mitochondrial translocase (TOM/TIM) complexes. The crosslinking partners of the crosslinked products of 100-130 kDa and of 80-100 kDa were thus identified as Tom40 and as Tom20, respectively (Fig. 3-7, wt). Therefore BPA introduced at residues 284-323 and at residues 183-305 of the MTX-arrested translocation intermediate of pb_2(330)-DHFR was crosslinked to Tom20 and to Tom40, respectively (Fig. 3-11).

3-3-3 MTX-arrested pb_2(330)-DHFR crosslinked to Tom40 or Tom20 is a mature-size form

Tom40 is an integral membrane protein and constitutes a protein translocation channel in the mitochondrial outer membrane (3, 15). On the other hand, Tom20 is anchored to the outer membrane by its N-terminal hydrophobic segment and the large C-terminal domain is exposed to the cytosol, which functions as a receptor for presequences (16). Why were these proteins having different functions crosslinked to the same region (residues 284-305) of the MTX-arrested pb_2(330)-DHFR? Perhaps Tom20 and Tom40 are crosslinked to differently processed forms, the intermediate-size

form and the mature-size form, of pb_2(330)-DHFR.

To test this possibility, I used pb_2AA(330)-DHFR, in which amino-acid residues at the second processing site are mutated so that it does not virtually receive the second processing by Imp1p. When incubated with mitochondria, pb_2AA(330)-DHFR was sorted to the IMS and was processed to the intermediate-size form but not to the mature-size form (Fig. 3-3B). pb_2AA(330)-DHFR containing BPA was incubated with mitochondria in the presence of MTX, and was subsequently UV-irradiated. The crosslinking patterns of MTX-arrested pb_2AA(330)-DHFR with Tom40 and Tom20 were nearly the same as those of pb_2(330)-DHFR (Fig. 3-7, AA and Fig. 3-11). The apparent molecular masses of the crosslinked products of pb_2AA(330)-DHFR were about 5-kDa higher than those of pb_2(330)-DHFR, and this value (5 kDa) corresponds to the difference in the molecular masses between those of the intermediate-size form and of the mature-size form. Therefore most of the crosslinked products with pb_2(330)-DHFR arose from the mature-size form of pb_2(330)-DHFR. Although the translocation intermediates of pb_2(330)-DHFR were the mixture of the intermediate-size and the mature-size forms, both Tom40 and Tom20 were crosslinked preferentially to the mature-size form.

3-3-4 Generation of the crosslinked products of MTX-arrested pb_2(330)-DHFR with Tom40 as well as Tom20 does not reflect different stages of the translocation

Another possibility is that the crosslinked products of the pb_2(330)-DHFR intermediate involving Tom20 and Tom40 reflect different stages of the translocation. Fig. 3-8 shows the time course of the import of pb_2(330)-DHFR into mitochondria in the absence of MTX. The amount of the protease-protected mature-size form gradually increased with incubation times (Fig. 3-8). Do the crosslinking products with Tom20 and with Tom40 appear in a sequential manner during the import of pb_2(330)-DHFR into mitochondria? To answer this question, the time courses of the crosslinking to

Tom20 and Tom40 were compared each other by using pb_2(330)-DHFR containing BPA at residues 284 and 272, respectively (Fig. 3-9). Residue 272 is the most C-terminal residue that is crosslinked only to Tom40, whereas residue 284 is the most N-terminal residue that is crosslinked to Tom20, when incubated for 20 min (Fig. 3-7). When pb_2(330)-DHFR with BPA at residue 272 was incubated with mitochondria for 3 min, crosslinked products with Tom40 of 123, 118, and 112 kDa were generated. Upon further incubation, the amounts of the 123-kDa and 118-kDa crosslinked products decreased, whereas that of 112 kDa increased (Fig. 3-9A). However crosslinked products with Tom20 were not observed for pb_2(330)-DHFR with BPA at residue 272 at any time points of the incubation. In contrast, pb_2(330)-DHFR with BPA at residue 284 generated crosslinked products with Tom20 of 94, 85, and 76 kDa after 3 min of incubation. Upon further incubation, the amounts of the 94-kDa crosslinked products gradually decreased, whereas those of 85 and 76 kDa increased (Fig. 3-9B). The observation that the amounts of the crosslinked products with Tom40 and with Tom20 exhibited similar dependences on the incubation time (Fig. 3-9C) indicates that these crosslinked products do not reflect different stages of the protein translocation. Taken together, I conclude that the MTX-arrested intermediate is in close contact with Tom40 and Tom20 simultaneously.

3-3-5 The unfolded HBD, but not the folded HBD, of $pb_2(220)^{dc2}$-DHFR was crosslinked to Tom40

Next I focused on the segment crosslinked to Tom40 in the translocation intermediate of pb_2(330)-DHFR. Residues 185-305 of the MTX-arrested pb_2(330)-DHFR were crosslinked to Tom40 (this study) while residues 165-213 of the MTX-arrested pb_2(220)-DHFR were crosslinked to Tom40 (10). I noticed that, in both cases, the residues crosslinked to Tom40 are located downstream of the HBD. Although the HBD is tightly folded in the IMS, the following truncated cytochrome b_2 segment may

be unfolded. This raises the possibility that Tom40 tends to interact preferentially with the unfolded segment of the translocating protein. To test this possibility, I analyzed the effects of a mutation that destabilizes the HBD of the cytochrome b_2 fusion proteins on their interactions with Tom40. BPA was introduced into $pb_2AA(220)^{dc2}$-DHFR, a HBD-destabilized mutant of $pb_2AA(220)^{WT}$-DHFR with the second mutation at the Imp1p processing site to prevent release from mitochondria by the Imp1p cleavage (see Chapter 2). The MTX-arrested $pb_2AA(220)^{dc2}$-DHFR and $pb_2AA(220)^{WT}$-DHFR with BPA at various positions were incubated with mitochondria in the presence of MTX and were subsequently UV-irradiated. BPA at residue 213 was crosslinked to Tom40 in $pb_2AA(220)^{WT}$-DHFR, whereas BPA at residue 213 was crosslinked to Tom20 as well as with Tom40 in $pb_2AA(220)^{dc2}$-DHFR (Fig. 3-10). BPA at residue 114 was not crosslinked to Tom40 in $pb_2AA(220)^{WT}$-DHFR, whereas it is crosslinked to Tom40 efficiently in $pb_2AA(220)^{dc2}$-DHFR. The results of crosslinking for $pb_2(220)^{WT}$-DHFR, $pb_2AA(220)^{WT}$-DHFR and $pb_2AA(220)^{dc2}$-DHFR are summarized in Fig. 3-11. Prevention of the second processing by Imp1p does not alter the crosslinking patterns or interactions with Tom40 for $pb_2AA(220)^{WT}$-DHFR as compared with $pb_2(220)^{WT}$-DHFR. On the other hand, destabilization of the HBD in $pb_2AA(220)^{dc2}$-DHFR allowed Tom40 to interact with the segment within the HBD. Therefore, Tom40 appears to interact with an unfolded segment of the translocating protein. These properties of Tom40 resemble those of molecular chaperones.

3-3-6 Purified Tom40 prevents aggregation of unfolded DHFR

Molecular chaperones interact with unfolded proteins, thereby preventing their aggregation to mediate folding, assembly and translocation of proteins (17, 18). The novel ability of Tom40 to bind to unfolded proteins raises the possibility that Tom40 functions as a molecular chaperone for translocating polypeptides. To test if Tom40 functions as a molecular chaperone in a general sense, I examined the ability of Tom40

to suppress aggregation of denatured proteins *in vitro*.

Recombinant Tom40 was purified from *E. coli* overexpresser cells to homogeneity as an inclusion body (>80% purity), which was solubilized with 6 M urea as described previously (15). When diluted into the non-ionic detergent nonanoyl-*N*-methylglucamide (Mega-9), urea-denatured Tom40 folds into its native conformation (15). Purified DHFR was denatured with urea and was diluted into Mega-9 buffer. In the absence of recombinant Tom40, 90% of DHFR was recovered in the pellet fraction after dilution, suggesting that DHFR formed insoluble aggregates (Fig. 3-12A, ref. 19). When Mega-9 buffer containing 47 μM Tom40, ~40% of DHFR was recovered in the supernatant fraction (Fig. 3-12A). Similar results were obtained for urea-denatured pSu9(69)-DHFR (Fig. 3-12A). However, reactivation of urea-denatured DHFR was not observed even in the presence of Tom40 (Fig. 3-12B). Thus, Tom40 could prevent aggregation of urea-denatured DHFR by binding to it, suggesting its chaperone-like activity.

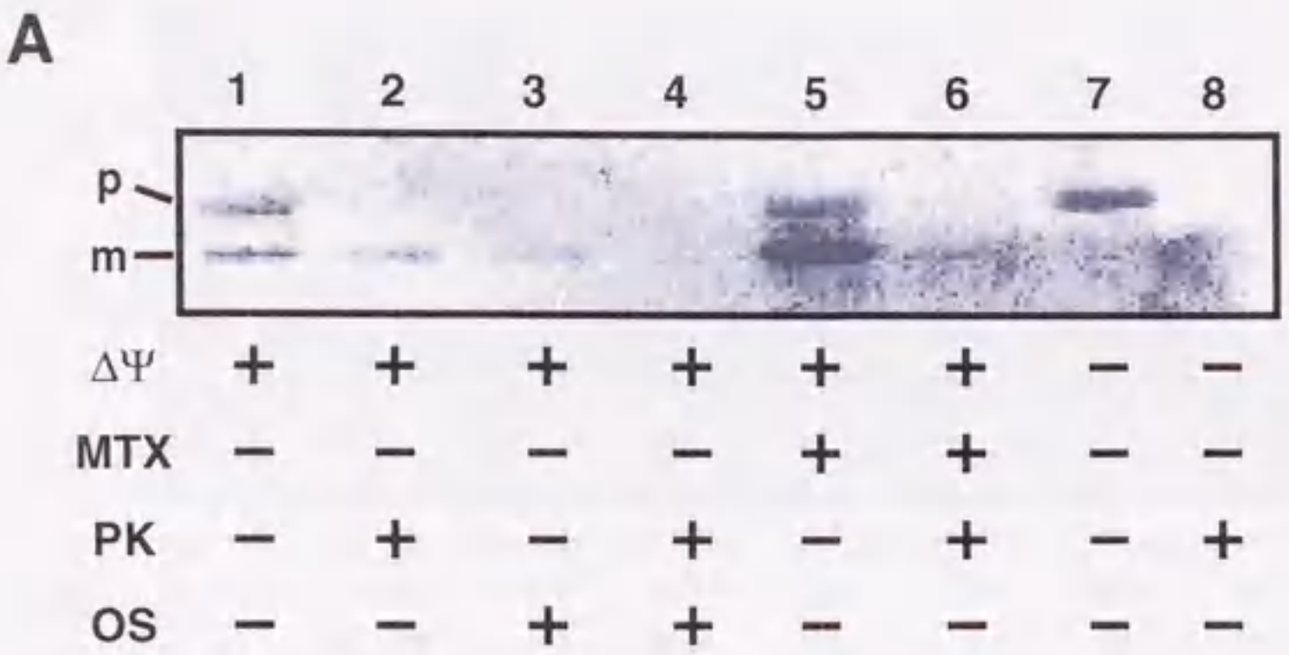

Fig. 3-3 pb_2(330)-DHFR is imported into the IMS

A, Radiolabeled pb_2(330)-DHFR was incubated with (lanes 5 and 6) or without (lanes 1-4, 7, and 8) MTX on ice for 15 min, and was subsequently incubated with mitochondria in the presence (lanes 7 and 8) or in the absence (lanes 1-6) of valinomycin at 30°C for 20 min. The mitochondria were reisolated by centrifugation and were resuspended in 250 mM sucrose, 10 mM Mops-KOH, pH 7.2, 1 mM EDTA. The samples were divided into several aliquots, were diluted 10-fold with the same isotonic buffer (lanes 1, 2, 5-8) or with the hypotonic buffer (10 mM Mops-KOH, pH 7.2) (lanes 3 and 4), and were incubated with (even lanes) or without (odd lanes) 100 μg/ml proteinase K for 30 min on ice. The proteins were analyzed by SDS-PAGE and visualized by X-ray film. OS, osmotic shock; p, precursor; m, mature-size form.

B, Radiolabeled pb_2(330)-DHFR (wt) and pb_2AA(330)-DHFR were incubated with energized mitochondria at 30°C for 20 min. The samples were diluted 10-fold with the isotonic buffer (lanes 1, 2, 4, and 5) or with the hypotonic buffer (lanes 3 and 6), and were incubated with 100 μg/ml proteinase K on ice for 30 min (lanes 2, 3, 5, and 6). The proteins were analyzed by SDS-PAGE and radioimaging. p, precurosor form; i, intermediate-size form; m, mature-size form.

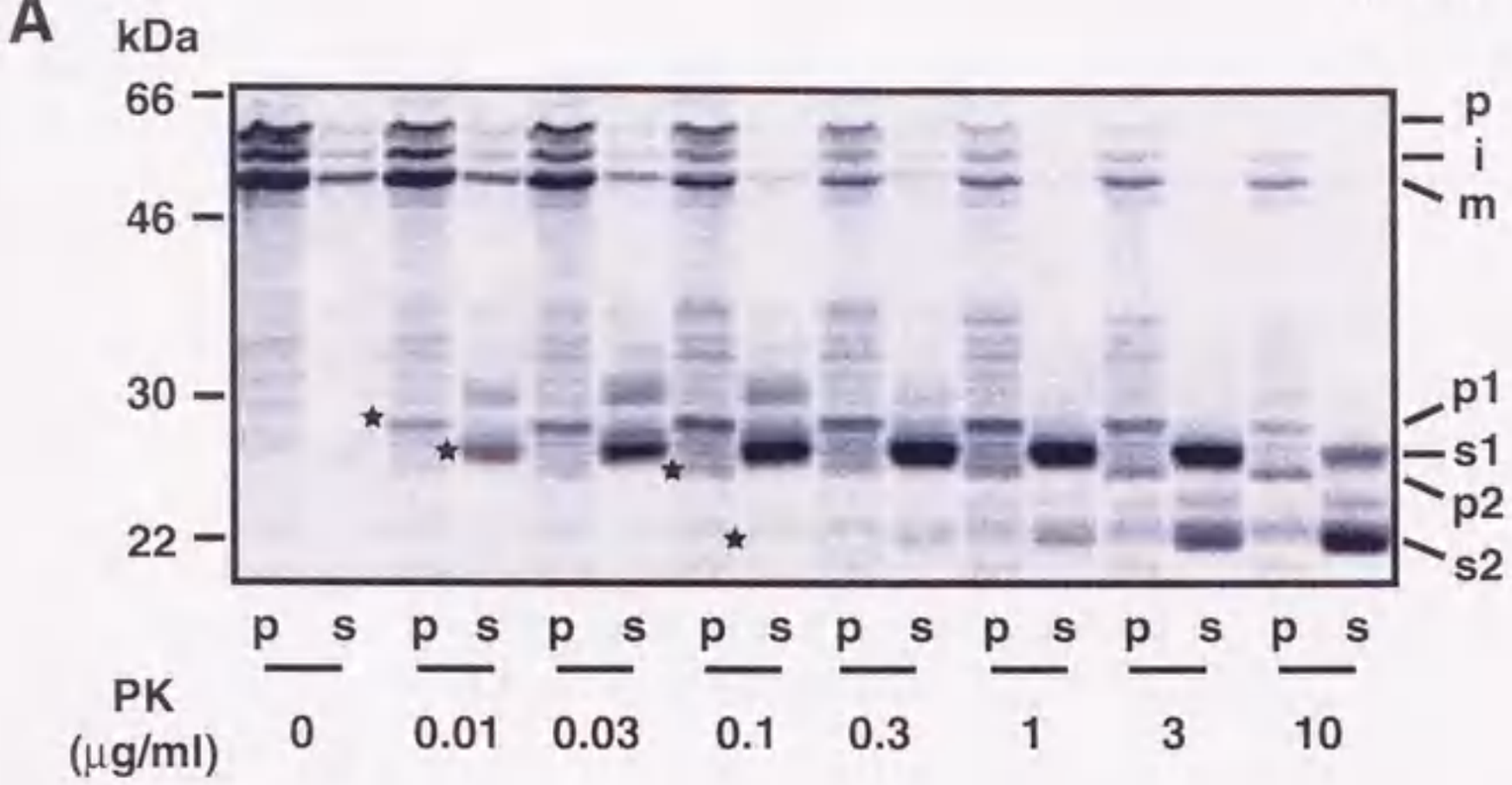

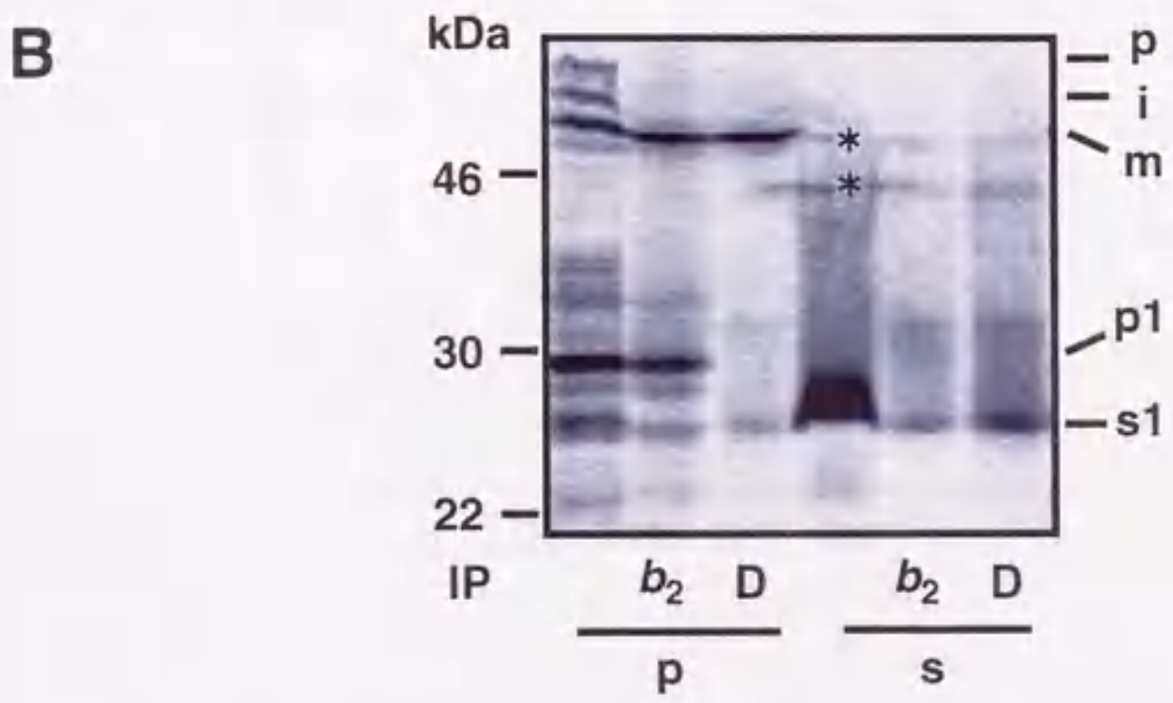

Fig. 3-4 The cytochrome b_2 domain of the MTX-arrested pb_2(330)-DHFR is partly exposed to the cytosolic side

A, Radiolabeled pb_2(330)-DHFR was incubated with MTX and mitochondria at 30ºC for 20 min. The mitochondria were reisolated and were suspended with 250 mM sucrose, 10 mM Mops-KOH, pH 7.2, 1 mM EDTA. The mitochondria were divided into eight aliquots and were treated with 0-10 μg/ml proteinase K (PK) on ice for 30 min. After PMSF was added, the mitochondria were reisolated by centrifugation, and the proteins in the supernatant were precipitated by trichloroacetic acid. The proteins were analyzed by SDS-PAGE and radioimaging. p1 (28 kDa) and p2 (25 kDa) were indicated degragation products collected in the pellet, and s1 (26 kDa) and s2 (21 kDa) were indicated those collected in the supernatant. p, precursor; i, intermediate-size form; m, mature-size form.

B, The MTX-arrested pb_2(330)-DHFR was treated with 0.3 μg/ml proteinase K on ice for 30 min. After PMSF was added, the mitochondria were reisolated by centrifugation. The proteins in the mitohondrial pellet and the supernatant were immunoprecipitated with the antibodies raised aginst cytochrome b_2 (b_2) or DHFR (D). Proteins were analyzed by SDS-PAGE and radioimaging. Asterisks indicate unrelated bands.

C

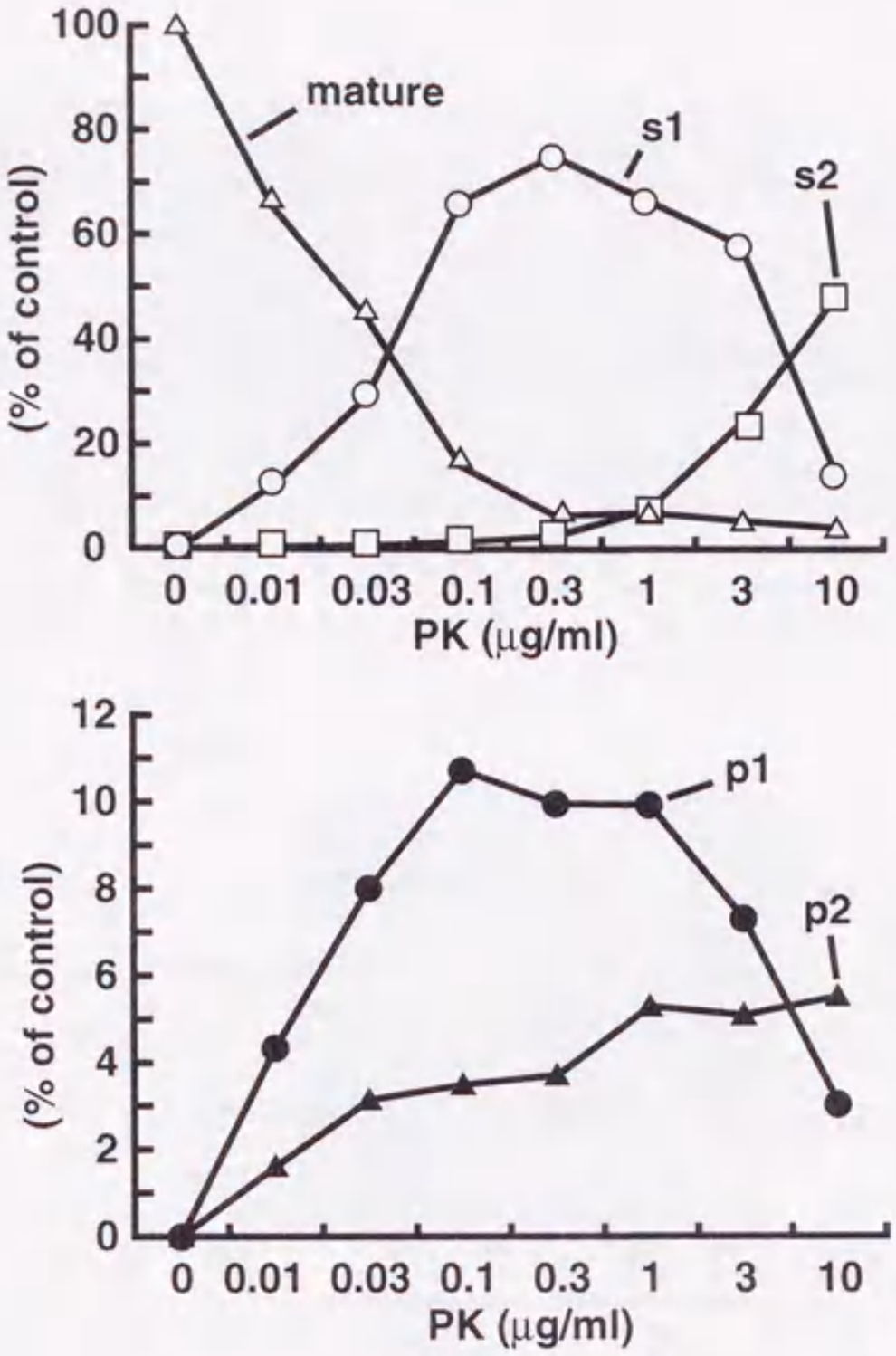

D

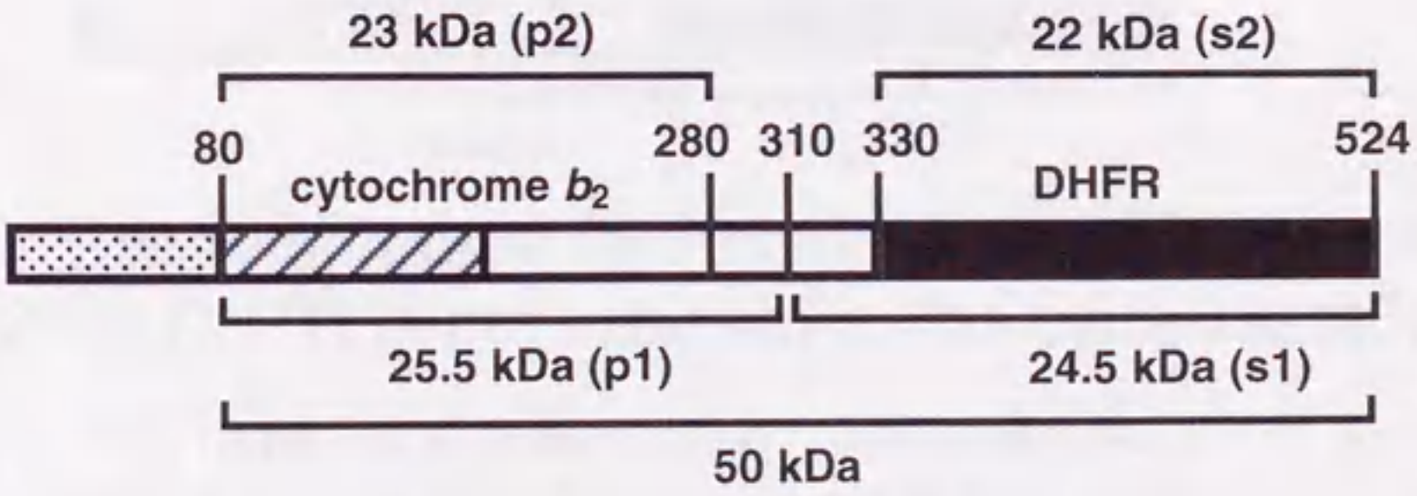

Fig. 3-4 (continued)

C, The amounts of the mature-size form (open triangles), p1 (closed circles), p2 (closed triangles), s1 (open circles), and s2 (open squares) were plotted against concentrations of proteinase K. The amount of the mature-size form without treatment of proteinase K is set to 100%.

D, The segments corresponding to the degradation products are estimated from the apparent molecular masses (A) and from the result of the immunoprecipitation (B). The actual molecular masses are indicated.

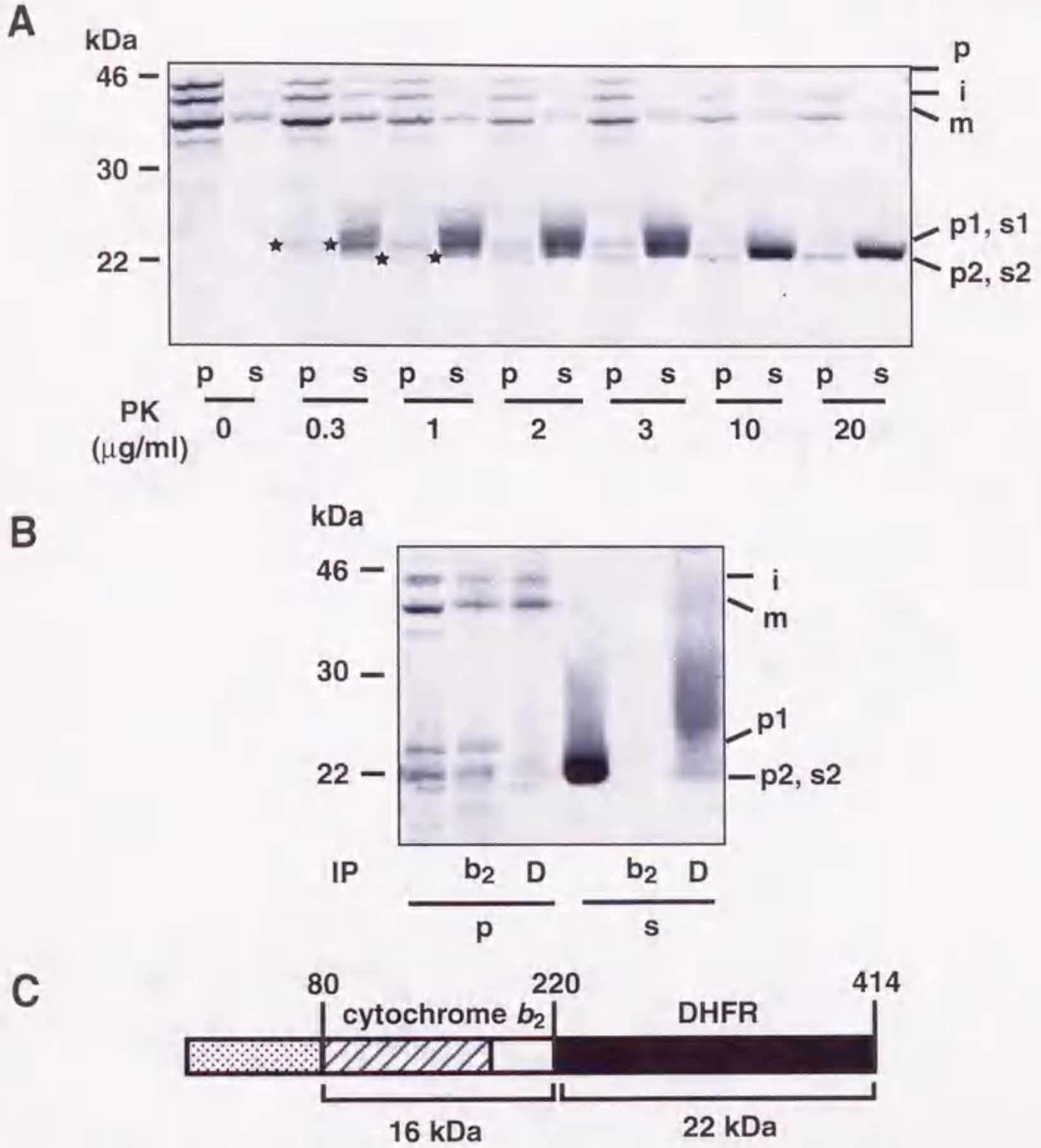

Fig. 3-5 The cytochrome b_2 domain of the MTX-arrested pb_2(220)-DHFR is not exposed to the cytosolic side

A, Radiolabeled pb_2(220)-DHFR was incubated with MTX and mitochondria at 30°C for 20 min. The mitochondria were reisolated, and were suspended with 250 mM sucrose, 10 mM Mops-KOH, pH 7.2, 1 mM EDTA. The mitochondria were divided into seven aliquots and were treated with 0-20 μg/ml proteinase K (PK) on ice for 30 min. After PMSF was added, the mitochondria were reisolated by centrifugation, and the proteins in the supernatant were precipitated by trichloroacetic acid. Proteins were analyzed by SDS-PAGE and radioimaging. p1 (22 kDa) and p2 (21 kDa) were indicated degragation products collected in the pellet, and s1 (22 kDa) and s2 (21 kDa) were indicated those collected in the supernatant. p, precursor; i, intermediate-size form; m, mature-size form.

B, The MTX-arrested pb_2(220)-DHFR was treated with 20 μg/ml proteinase K on ice for 30 min. After PMSF was added, the mitochondria were reisolated by centrifugation. The proteins in the mitohondrial pellet and the supernatant were immunoprecipitated with antibodies raised aginst cytochrome b_2 (b_2) or DHFR (D). The proteins were analyzed by SDS-PAGE and radioimaging.

C, The sizes of the cytochrome b_2 domain and of the DHFR domain of the mature-size form of pb_2(220)-DHFR are 16 kDa and 22 kDa, respectively.

A

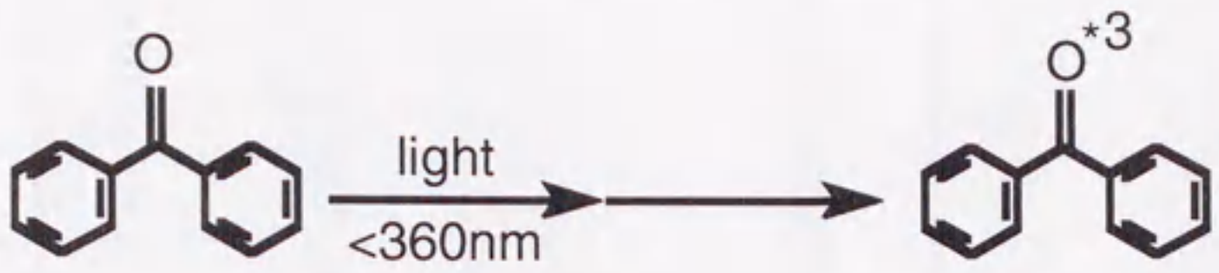

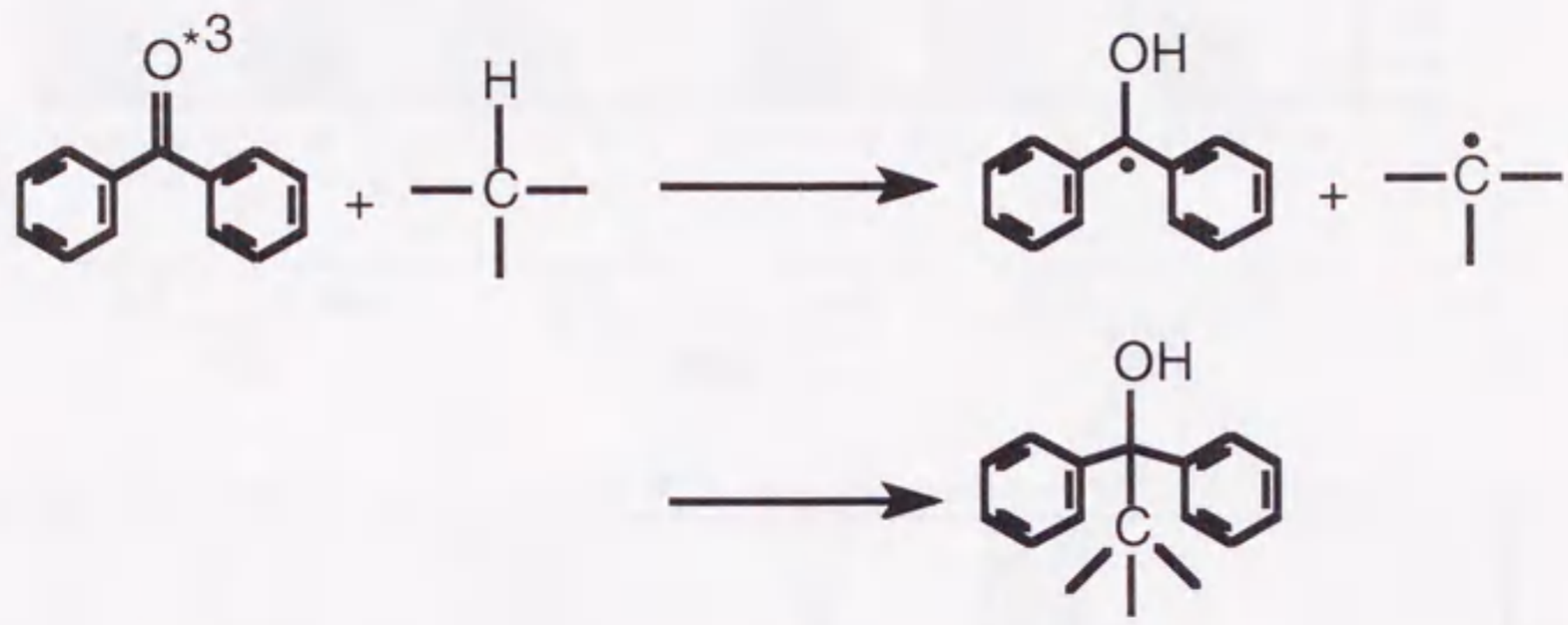

B

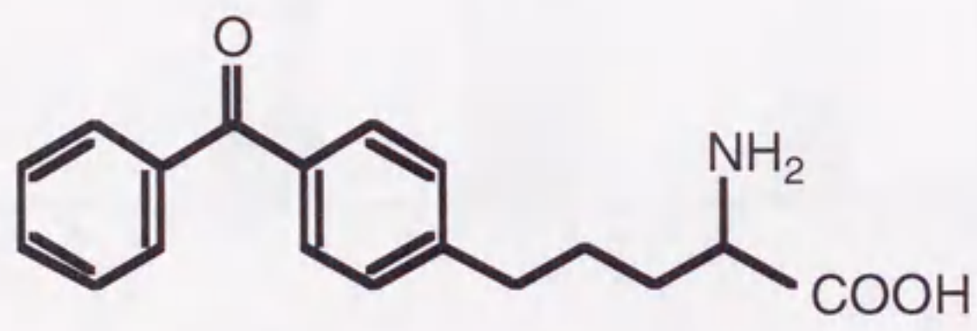

Fig. 3-6 An unnatural amino acid with a photoreactive crosslinker (BPA)

A, Benzophenone excited at <360 nm can react with a hydrogenized carbon.

B, DL-2-amino-5-(*p*-benzoylphenyl)pentanoic acid (BPA).

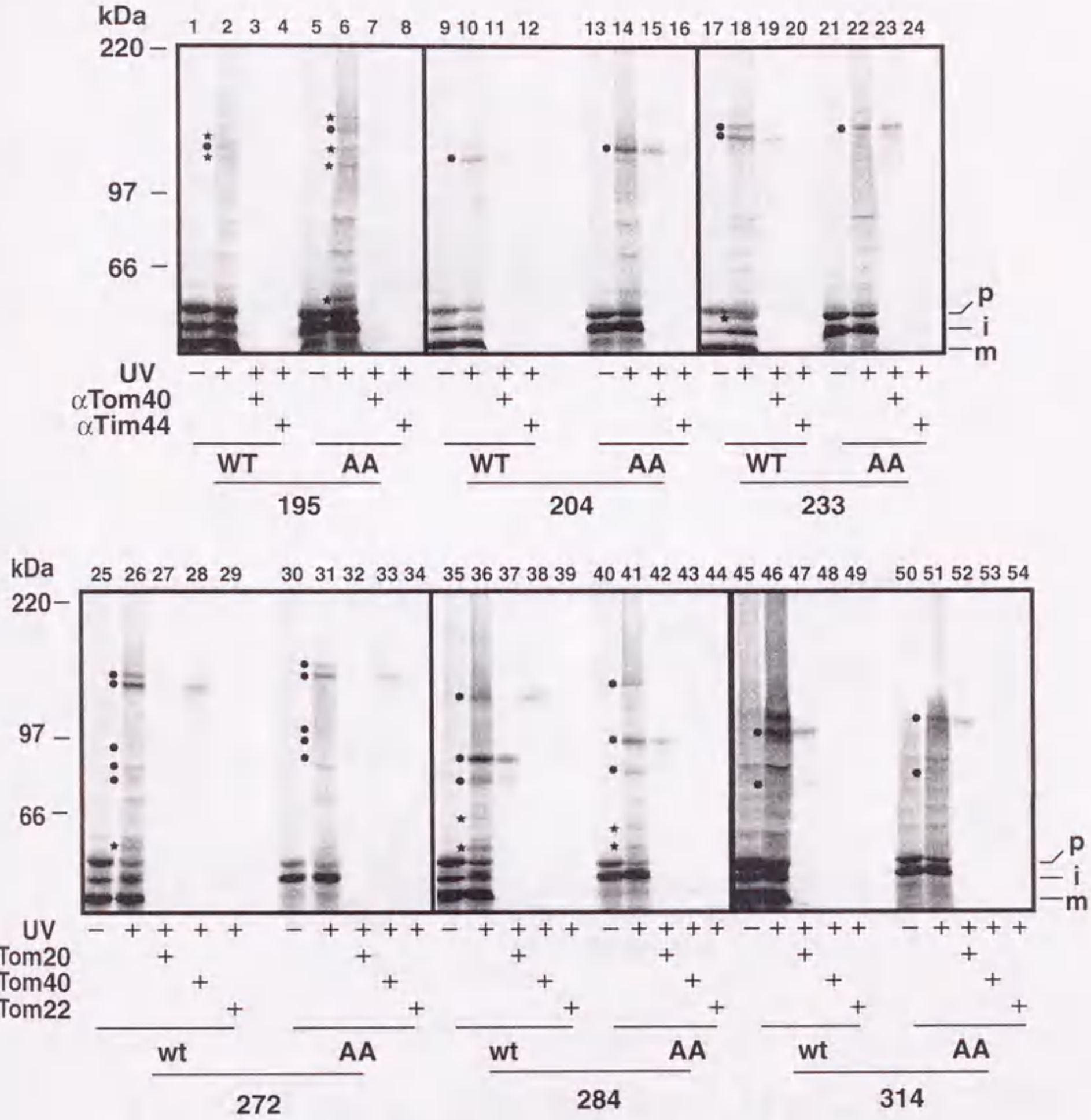

Fig. 3-7 The MTX-arrested intermediates of pb_2(330)-DHFR and pb_2AA(330)-DHFR are crosslinked to Tom40 and Tom20

Radiolabeled pb_2(330)-DHFR (wt) or pb_2AA(330)-DHFR (AA) containing BPA at residues 195, 204, 233, 272, 284, or 314 was incubated with MTX and subsequently incubated with mitochondria. The mitochondria were reisolated by centrifugation and were subjected to UV irradiation. The mitochondria were reisolated by centrifugation and proteins were immunoprecipitated with the antibodies raised against Tom20, Tom22, Tom40, and Tim44. Dots and stars indicate the crosslinked products, whose crosslinking partners were identified or unidentified, respectively. p, precursor; i, intermediate-size form; m, mature-size form

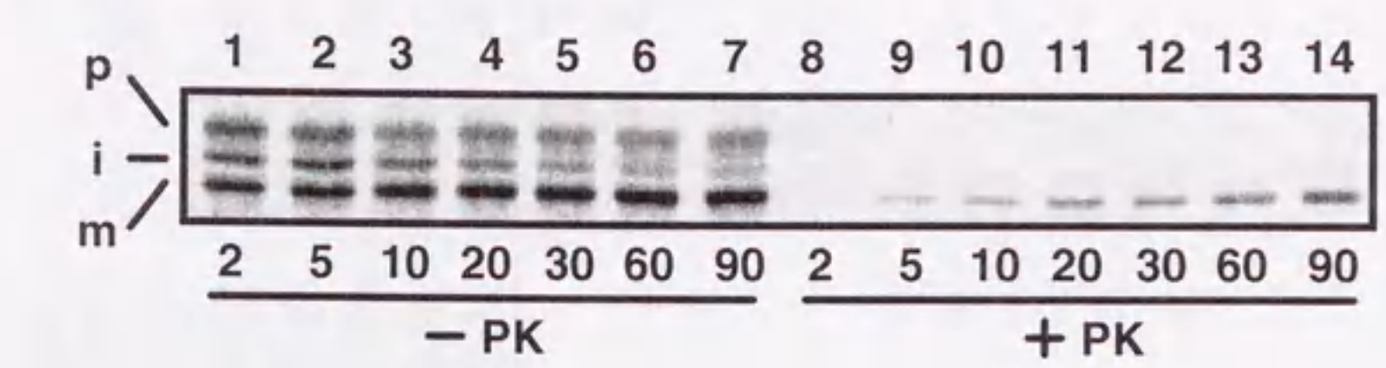

Fig. 3-8 Time course of the import of pb_2(330)-DHFR into mitochondria

A, Radiolabeled pb_2(330)-DHFR was incubated with energized mitochondria at 30°C for indicated times. After addition of valinomycin, samples were halved and were incubated with (lanes 8-14) or without (lanes 1-7) 100 μg/ml proteinase K for 30 min on ice. The mitochondria were reisolated by centrifugation, and proteins were analyzed by SDS-PAGE and radioimaging. p, precursor; i, intermediate-size form; m, mature-size form.

B, The amounts of protease-protected mature-size form were plotted against incubation times. The amount of pb_2(330)-DHFR added to each reaction is set to 100%.

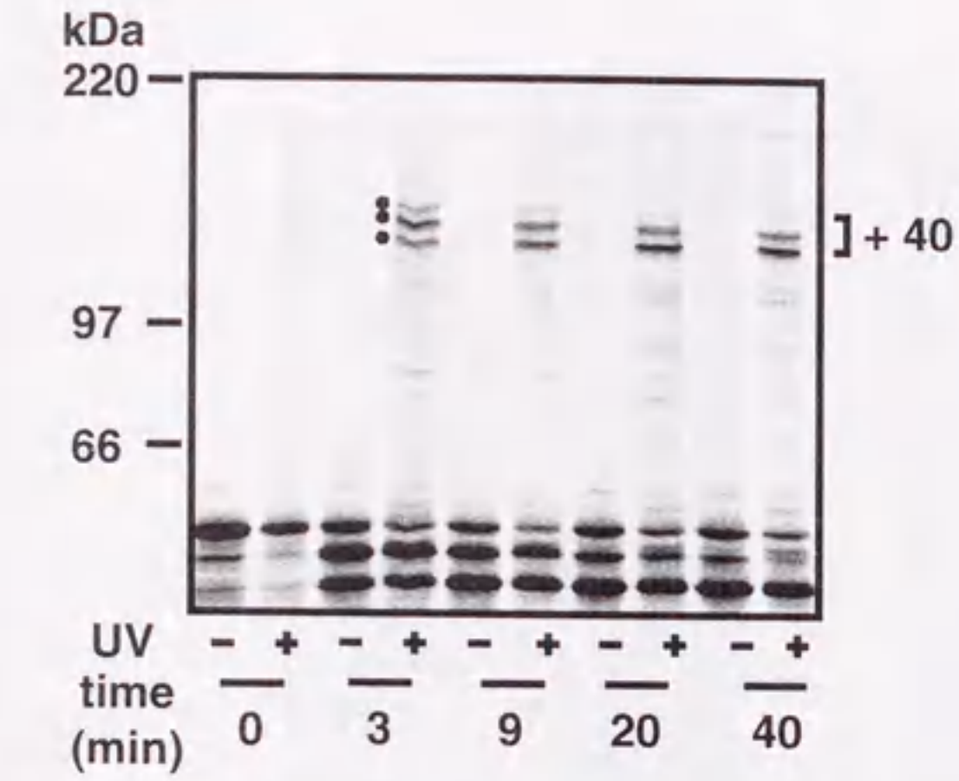

Fig. 3-9 MTX-arrested pb_2(330)-DHFR can be crosslinked to Tom40 and Tom20 simultaneously

A, B, Radiolabeled pb_2(330)-DHFR containing BPA at residues 272 (A) or 284 (B) was incubated with MTX on ice for 15 min, and were subsequently incubated with mitochondria at 30°C for indicated times. The mitochondria were reisolated and were subjected to UV irradiation. +40 and +20 indicate crosslinked products with Tom40 and Tom20, respectively.

C, Total amounts of the crosslinked products with Tom40 (circles) and Tom20 (squares) were plotted against incubation times. The amount of the fusion proteins added to each reaction is set to 100%.

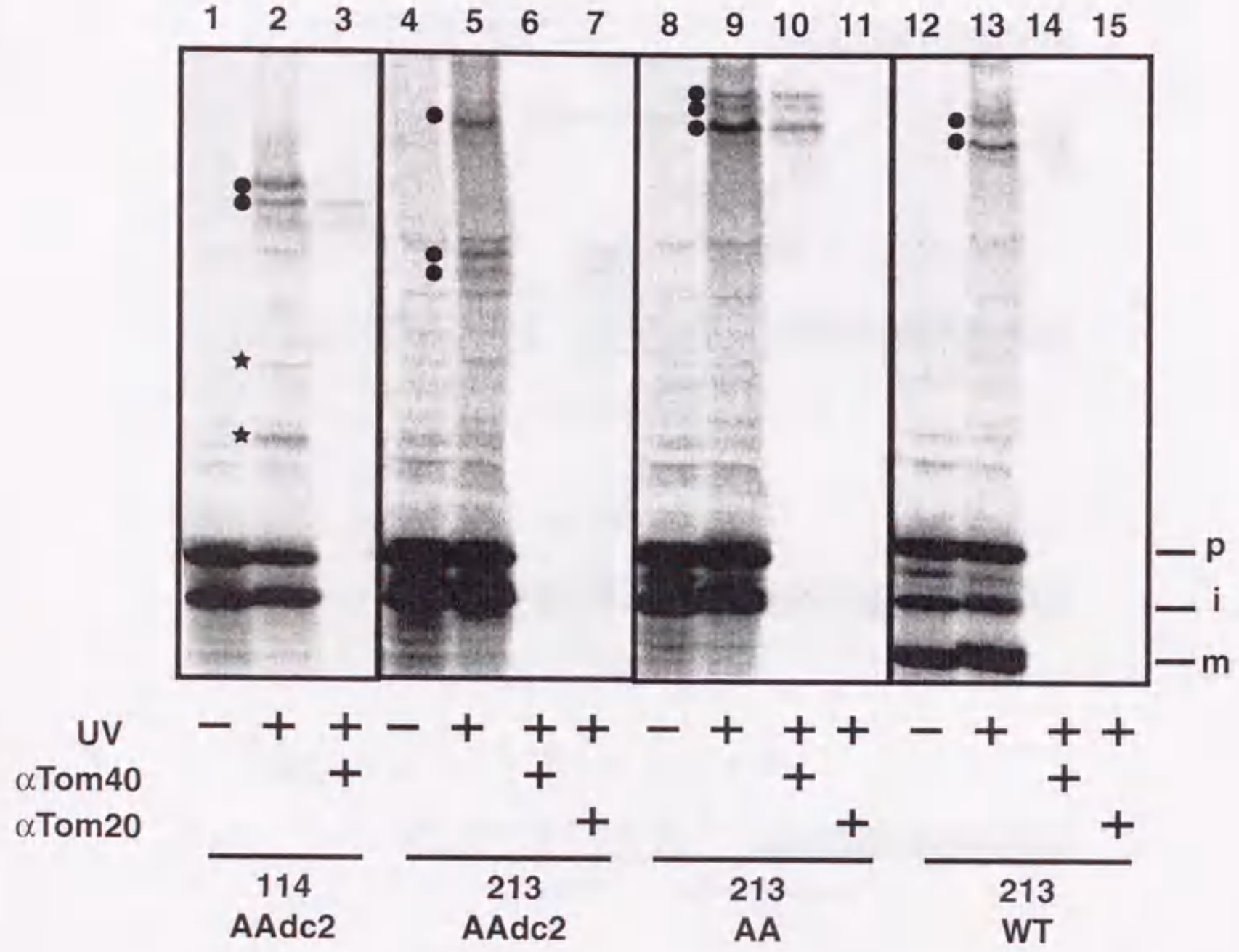

Fig. 3-10 The unfolded HBD of $pb_2AA(220)^{dc2}$-DHFR is crosslinked to Tom40

Radiolabeled $pb_2(220)$-DHFR (WT), $pb_2AA(220)$-DHFR (AA), and $pb_2AA(220)^{dc2}$-DHFR (AAdc2) containing BPA at residues 114 (lanes 1-3) and 213 (lanes 4-15) were incubated with MTX and mitochondria at 30°C for 20 min. The mitochondria were reisolated by centrifugation, and were subjected to UV irradiation (lanes 2, 3, 5-7, 9-11, 13-15). The mitochondria were reisolated by centrifugation, and proteins were immunoprecipitated with the antibodies raised against Tom20 (lanes 7, 11, and 15) and Tom40 (lanes 3, 6, 10, and 14). Dots and stars indicate the crosslinked products, with which the crosslinking partners were identified or unidentified, respectively. The band indicated by star with the highest mobilities in lane 2 was assigned to the crosslinked products with protein X (10). p, precursor; i, intermediate-size form; m, mature-size form.

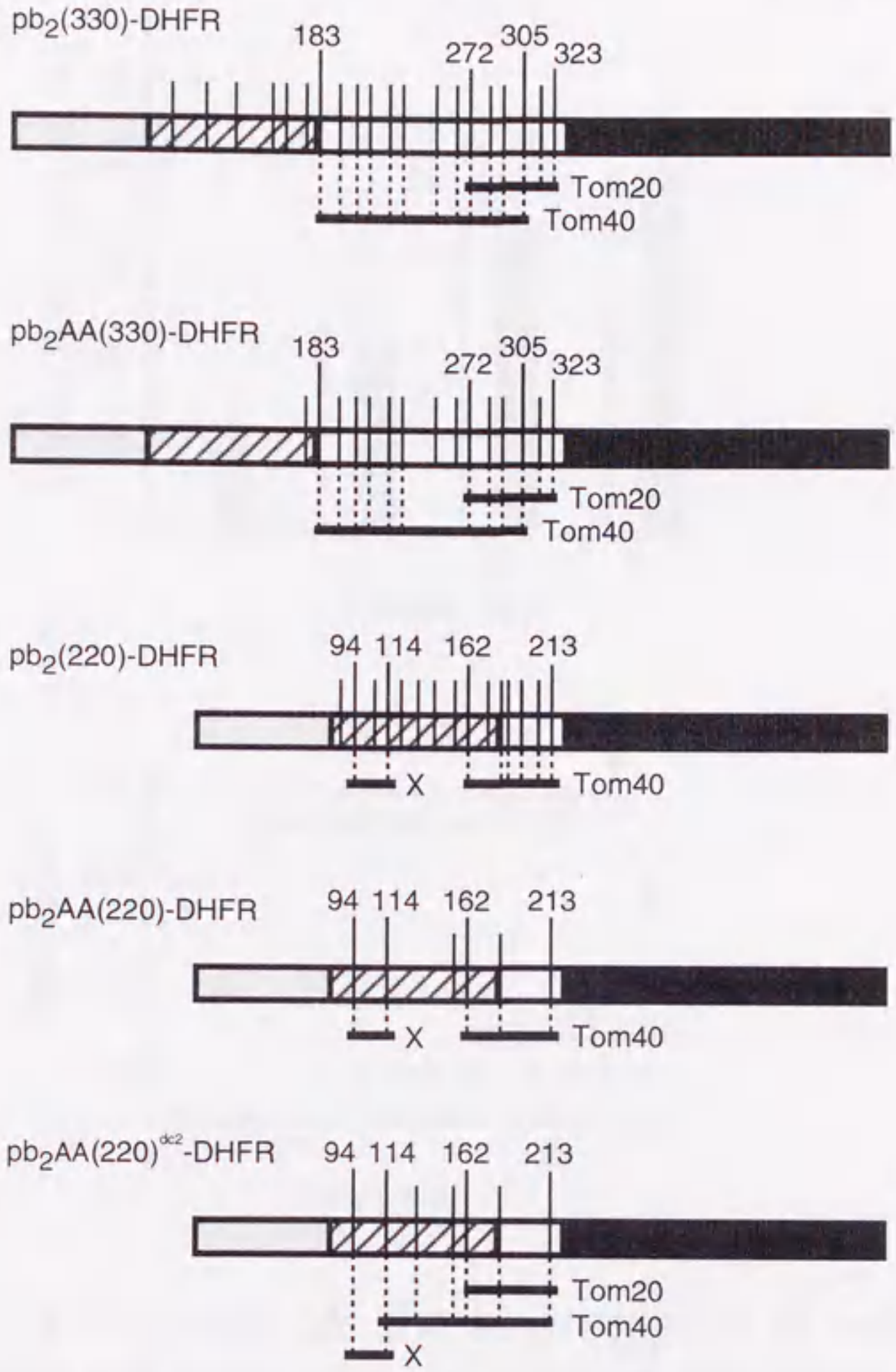

Fig. 3-11 The crosslinking patterns of the MTX-arrested fusion proteins

The crosslinking results of the MTX-arrested pb_2(330)-DHFR, pb_2AA(330)-DHFR, pb_2(220)-DHFR (10), pb_2AA(220)-DHFR, and pb_2AA(220)^{dc2}-DHFR are summarized. The lines and the dashed lines represent the positions of incorporated BPA and those crosslinked to Tom40, Tom20, and/or protein X, respectively. Gray boxes, presequence; shaded boxes, HBD; black boxes, DHFR domain.

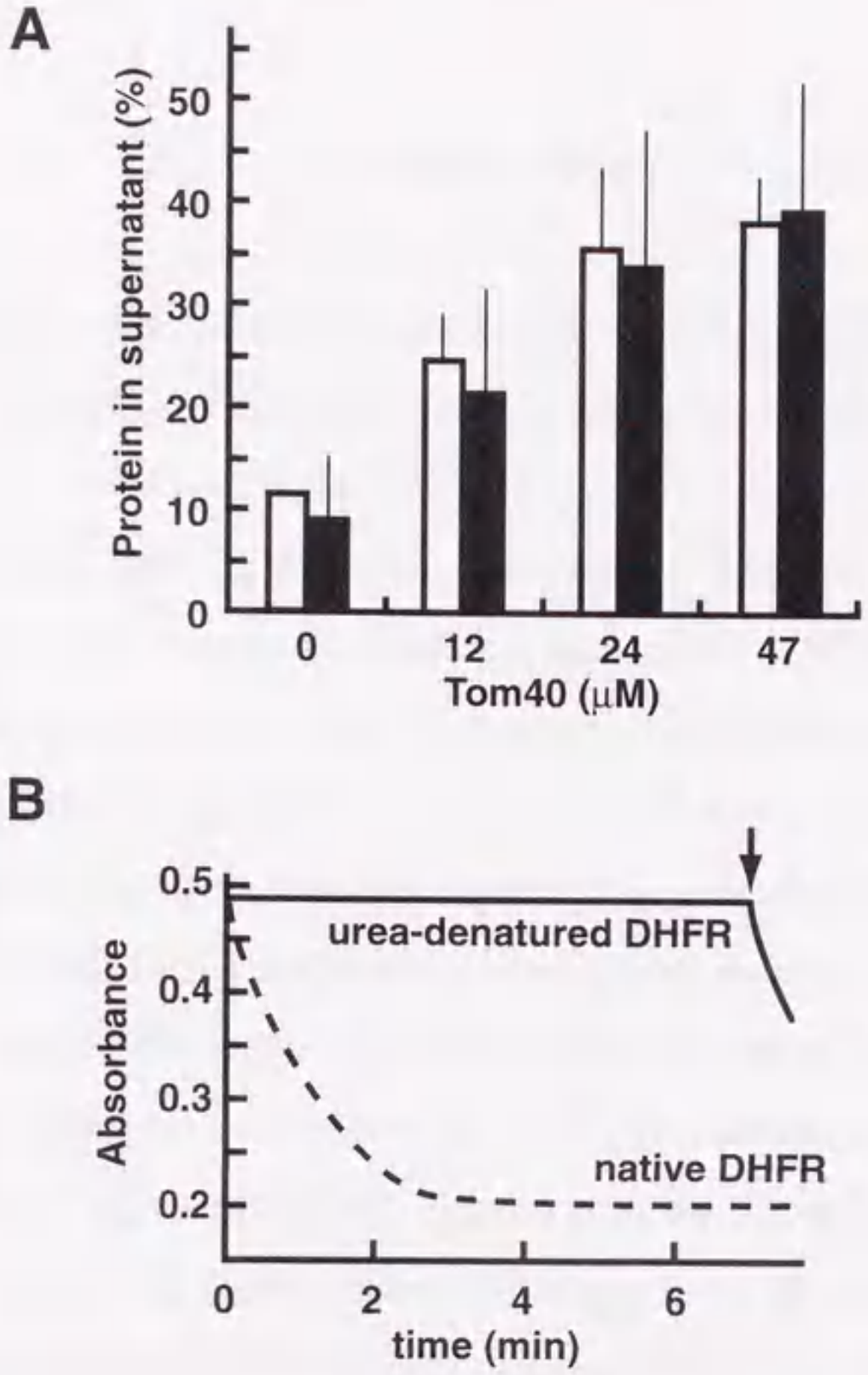

Fig. 3-12 Tom40 prevents the aggregation of unfolded DHFR but does not promote its refolding

A, Purified recombinant Tom40 in urea buffer was diluted 10-fold with 60 mM Mega-9 buffer. Urea-denatured DHFR (white bars) and urea-denatured pSu9(69)-DHFR (black bars) were diluted 100-fold (3 μM) with Mega-9 buffer containing various concentrations of Tom40. After centrifugation at 15,000×*g* for 15 min, the proteins in the supernatant were analyzed by SDS-PAGE and immunoblotting. The fusion proteins added to each reaction are set to 100%.

B, Unfolded DHFR was diluted with Mega-9 buffer containing 47 μM Tom40. After centrifugation, the supernatant was diluted 10-fold with 50 mM KPi, pH 7.4. 50 μM dihydrofolic acid and 100 μM NADPH were added, and absorbance at 340 nm was continuously recorded for indicated times (real line). After 7 min of incubation (indicated by arrow), folded recombinant DHFR was added. Recombinant DHFR, which was not denatured, were diluted with Mega-9 buffer without Tom40, and were further diluted 10-fold with 50 mM KPi, pH 7.4. Dihydrofolic acid and NADPH were added, and absorbance at 340 nm was continuously recorded (broken line).

3-4 DISCUSSION

Cytochrome b_2 is imported into the IMS along the pathway that is consistent with the stop-transfer model. The mature-size form of the MTX-arrested cytochrome b_2-DHFR fusion protein spans only the outer mitochondrial membrane, and its HBD folds tightly in the IMS. In the present study, site-specific photocrosslinking revealed that a segment of as long as 120 amino-acid residues in the MTX-arrested pb_2(330)-DHFR is close to Tom40 (Fig. 3-11). The previous study showed that pb_2(220)-DHFR, in which the HBD and the DHFR are separated by 40 amino-acid residues, interacts with Tom40 only through its 50-residue segment (10). Interestingly, in both pb_2(330)-DHFR and pb_2(220)-DHFR, the Tom40-interacting segments are located in between the folded HBD and the DHFR domain. Besides, destabilization of the HBD by mutation allows Tom40 to interact a segment within the HBD. Taken together, I conclude that Tom40 tends to interact with unfolded segments of the translocating polypeptide chains. Since Tom40 constitutes a protein-conducting channel and a protein moves through the channel in an unfolded state, it may not be surprising that Tom40 preferentially interacts with the unfolded polypeptide chain. However, the capacity of Tom40 to accommodate an unfolded segment of as long as 120 amino-acid residues is somehow unexpected because a ~30-residue segment in an extended conformation is long enough to span a single biological membrane (10).

What is the biological relevance of the ability of Tom40 to interact with an unfolded segment in the translocating protein? It is likely that Tom40 protects the translocating protein against misfolding or undesired interactions with other proteins in the IMS. Such a chaperone-like function of Tom40 may be particularly important for the proteins destined for the IMS. Since the matrix contains significant amounts of chaperones including mitochondrial Hsp70 and Hsp60, the segment of the matrix-targeting protein that enters the matrix may well be protected against misfolding or

undesirable interactions by these matrix-resident chaperones (17). On the other hand, the IMS lacks ATP-dependent chaperones like Hsp70 and Hsp60, the segment of the IMS-targeting protein that enters the IMS should be protected against misfolding or inappropriate association with other proteins. In this respect, it is interesting that Tom40 indeed prevents aggregation of unfolded proteins irrespective of the presence of the presequence. Although this is not consistent with the previous observation that Tom40 reconstituted in liposomes can interact with only presequence-containing proteins (15), Tom40 solubilized with detergent and that reconstituted in liposomes may behave differently.

Tom20 was crosslinked to the MTX-arrested pb_2(330)-DHFR on the cytosolic side of the outer membrane (Fig. 3-11). Tom20 function as a general receptor for presequence-containing mitochondrial proteins and may well be located at the entrance of the TOM channel (16). The cytosolic domain of Tom22 likely complements the receptor function of Tom20 and also serves as the docking point for the receptors Tom20 and Tom70 (20). Tom22 and Tom40 as well as Tom5, Tom6, and Tom7 constitute a core complex of TOM (21). However, the translocating pb_2(330)-DHFR was crosslinked only to Tom40 and Tom20, but not to Tom22. This may raise the possibility that Tom20 actively guides the translocating protein into the Tom40 channel during its import. This hypothesis should be tested in future studies.

REFERENCES

1. Meyer, T. H., Ménétret, J.-F., Breitling, R., Miller, K. R., Akey, C. W., and Rapoport, T. A. (1999) The bacterial SecY/E translocation complex forms channel-like structures similar to those of the eukaryotic Sec61p complex. *J. Mol. Biol.*, **285**, 1789-1800
2. Hanein, D., Matlack, K. E. S., Jungnickel, B., Plath, K., Kalies, K.-U., Miller, K. R., Rapoport, T. A., and Akey, C. W. (1996) Oligomeric rings of the Sec61p complex induced by ligands required for protein translocation. *Cell*, **87**, 721-732
3. Künkele, K-P., Heins, S., Dembowski, M., Nargang, F. E., Benz, R., Thieffry, M., Walz, J., Lill, R., Nussberger, S., and Neupert, W. (1998) The preprotein translocation channel of the outer membrane of mitochondria. *Cell*, **93**, 1009-1019
4. Pfanner, N., Hartl, F-U., Guiard, B., and Neupert, W. (1987) Mitochondrial precursor proteins are imported through a hydrophilic membrane environment. *Eur. J. Biochem.*,**169**, 289-293
5. Glimore, R. and Blobel, G. (1985) Translocation of secretory proteins across the microsomal membrane occurs through an environment accessible to aqueous perturbants. *Cell*, **42**, 497-505
6. Ungermann, C., Neupert, W., and Cyr, D. M. (1994) The role of Hsp70 conferring unidirectionality on protein translocation into mitochondria. *Science*, **266**, 1250-1253
7. Wimberly, B. T., Brodersen, D. E., Clemons Jr, W. M., Morgan-warren, R. J., Carter, A. P., Vonrhein, C., Hartsch, T., and Rammakrishnan, V. (2000) Structure of the 30S ribosomal subunit. *Nature*, **407**, 327-339
8. Ban,N., Nissen, P., Hansen, J., Moore, P. B., and Steitz, T. A. (2000) The complete atomic structure of the large ribosomal subunit at 2.4 Å resolution. *Science*, **289**, 905-920

9. Ellman, J., Mendel, D., Anthony-Cahill, S., Noren, C. J., and Schultz, P. G. (1991) Biosynthetic method for introducing unnatural amino acids site-specifically into proteins. *Methods Enzymol.*, **202**, 301-337

10. Kanamori, T., Nishikawa, S., Shin, I., Schultz, P. G., and Endo, T. (1997) Probing the environment along the protein import pathways in yeast mitochondria by site-specific photocrosslinking. *Proc. Natl. Acad. Sci. USA*, **94**, 485-490

11. Kunkel, T. A., Roberts, J. D., and Zakour, R. A. (1987) Rapid and efficient site-specific mutagenesis without phenotypic selection. *Methods Enzymol.*, **154**, 367-382

12. Daum, G., Böhni, P.C., and Schatz, G. (1982) Import of proteins into mitochondria. Cytochrome b_2 and cytochrome c peroxidase are located in the intermembrane space of yeast mitochondria. *J. Biol. Chem.*, **257**, 13028-13033

13. Kanamori, T., Nishikawa, S., Nakai, M., Shin, I., Schultz, P. G., and Endo, T. (1999) Uncoupling of transfer of the presequence and unfolding of the mature domain in precursor translocation across the mitochondrial outer membrane. *Proc. Natl. Acad. Sci. USA*, **96**, 3634-3639

14. Huang, S., Delcamp, T. J., Tan, X., Smith, P. L., Prendergast, N. J., and Freisheim, J. H. (1989) Effects of conversion of an invariant tryptophan residue to phenylalanine on the function of human dihydrofolate reductase. *Biochemistry*, **28**, 471-478

15. Hill, K., Model, K., Ryan, M. T., Dietmeier, K., Martin, F., Wagner, R., and Pfanner, N. (1998) Tom40 forms the hydrophilic channel of the mitochondrial import pore for preproteins. Nature, 395, 516-521

16. Söllner, T., Griffiths, G., Pfaller, R., Pfanner, N., and Neupert, W. (1989) MOM19, an import receptor for mitochondrial precursor proteins. *Cell*, **59**, 1061-1070

17. Bukau, B. and Horwich, A. L. (1998) The Hsp70 and Hsp60 chaperone machines. *Cell*, **92**, 351-366

18. Jensen, R. E. and Johnson, A. E. (1999) Protein translocation: Is Hsp70 pulling my chain? *Curr. Biol.*, **9**, R779-R782

19. Leonhard, K., Stiegler, A., Neupert, W., and Langer, T. (1999) Chaperone-like activity of the AAA domain of the yeast Yme1 AAA protease. *Nature*, **398**, 348-351

20. Kiebler, M., Keil, P., Schneider, H., van der Klei, I. J., Pfanner, N., and Neupert, W. (1993) The mitochondrial receptor complex: A central role of MOM22 in mediating preprotein transfer from receptors to the general insertion pore. *Cell*, **74**, 483-492

21. Dekker, P. J. T., Ryan, M. T., Brix, J., Müller, H., Hönkinger, A., and Pfanner, N. (1998) Preprotein translocase of the outer mitochondrial membrane: Molecular dissection and assembly of the general import pore complex. *Mol. Cell. Biol.*, **18**, 6515-6524

Chapter 4

Tom7 and the C-terminal domain of Tom22 mediate the transfer of the presequence from the TOM complex to the Tim23 complex

4-1 INTRODUCTION

Many mitochondrial proteins are synthesized in the cytosol as precursor proteins with an N-terminal extension, a presequence. The presequence usually contains the mitochondrial matrix targeting signal and is removed off by matrix processing peptidase (MPP) after import into the matrix (1). Translocation of mitochondrial precursor proteins across the mitochondrial outer and the inner membranes requires coordinated actions of the TOM and the TIM complexes, respectively (2, 3). Translocation of the presequence across the inner membrane through the Tim23 complex requires the membrane potential across the inner membrane (positive outside and negative inside), which may mediate translocation of the positively charged presequence into the matrix via an electrophoretic effect (4, 5). On the other hand, since no membrane potential ($\Delta\Psi$) across the outer membrane is found, the translocation of the presequence across the outer membrane must occur by a different mechanism. A model was proposed in which the mitochondrial outer membrane has two binding sites for the presequence, the *cis* site on the cytosolic side and the *trans* site on the IMS side of the outer membrane (6, 7). The presequence initially bound to the cis site may well move to the trans site since the presequence binding to the trans site is estimated to be stronger than that to the cis site (8).

How do precursor proteins move from the TOM complex in the outer membrane to the Tim23 complex in the inner membrane? Since the TOM complex contains the trans binding site on the IMS side of the outer membrane and Tim23 exhibits an affinity for the presequence (8), it is natural to assume that the presequence is transferred from the trans site of the TOM complex to the IMS domain of Tim23. Although Tim23 bridges the outer membrane and the inner membrane through its N-terminal segment inserted into the outer membrane and its C-terminal part integrated in the inner membrane, Tim23 is apparently not associated with the TOM complex (9).

Therefore the mechanism of the transfer of the presequence from the TOM complex to the Tim23 complex remains unclear.

In order to address this question, it is essential to reveal substantial components of the trans site in the TOM complex. In *in vitro* mitochondrial protein import experiments, the block of the entry of the presequence into the TIM channel by dissipating $\Delta\Psi$ across the inner membrane causes arrest of the protein translocation at the TOM complex (Fig. 4-1). The presequence of the generated translocation intermediate of the fusion protein, pSu9-DHFR, has already crossed the outer membrane and is close to Tom40, the C-terminal domain of Tom22 (Tom22C) and an unidentified small protein (10). In the present study, the small protein crosslinked to the presequence of the TOM-bound intermediate has been identified as Tom7. Tom40 is an integral membrane protein and forms a protein translocation channel in the outer membrane (11, 12). The role of the C-terminal domain of Tom22 on the IMS side of the outer membrane is unclear. Defects of deletion of Tom22C in cell growth or in the import ability of the isolated mitochondria are only marginal (13-17). Although fungal Tom22C, which is rich in acidic residues, has been suggested to interact with positively charged presequences through electrostatic interactions (8, 15), mammalian Tom22C does not have a net negative charge (18, 19). Tom7 apparently mediates disassembly of the TOM complex (20, 21).

The results obtained in the present study with mutant mitochondria lacking both Tom22C and Tom7 suggest that Tom22C and Tom7 are involved in the step of the presequence transfer from the trans site of the TOM complex to the Tim23 complex.

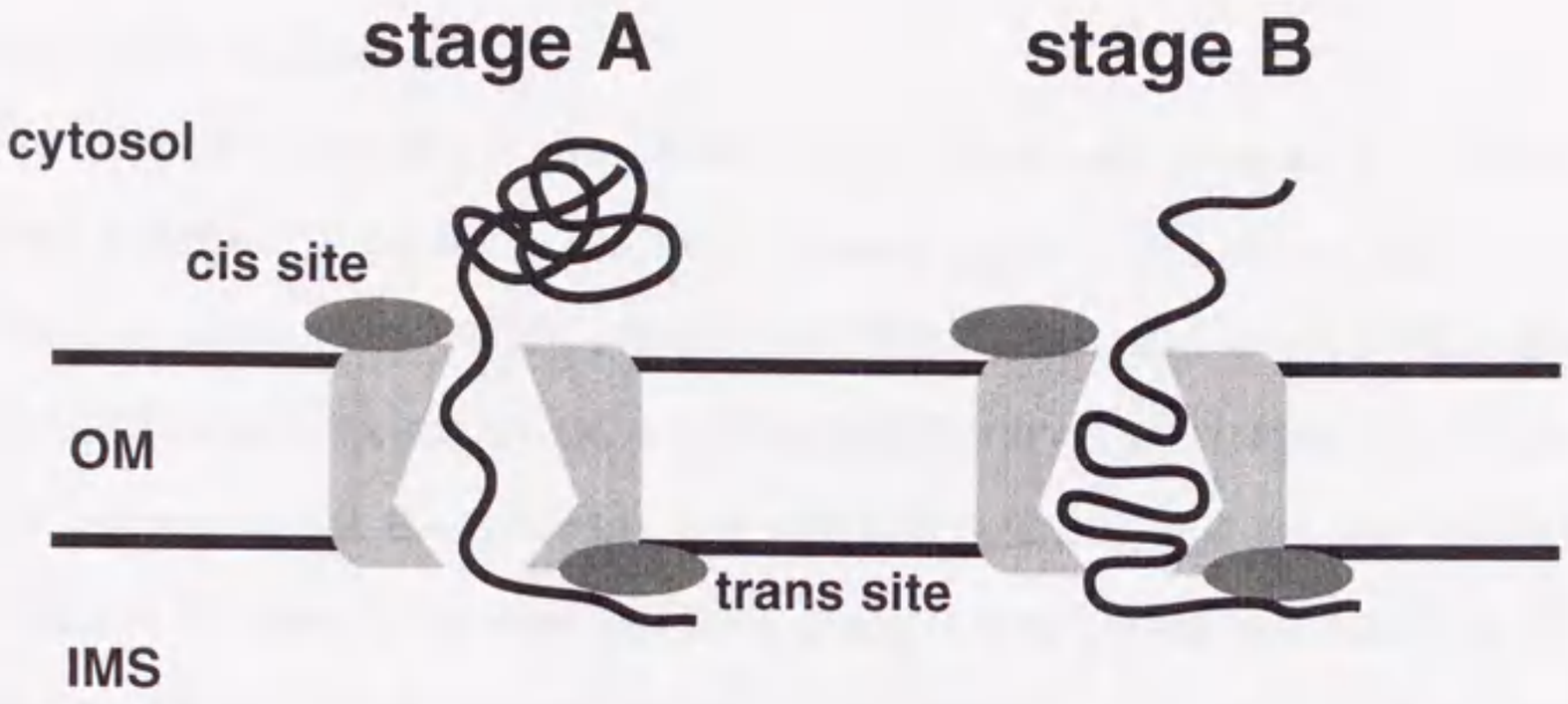

Fig. 4-1 The presequence of the TOM-bound pSu9-DHFR reaches the trans site even when the remaining part is folded on the cytosolic side

Two distinct translocation intermediates across the outer membrane are formed when precursor proteins are incubated with $\Delta\Psi$-dissipated mitochondria (10). In the stage A intermediate, the presequence reaches the trans site although the DHFR part is folded on the cytosolic side. In the stage B intermediate, the presequence reaches the trans site and the unfolded DHFR part interacts with Tom40. OM, outer membrane; IMS, intermembrane space

4-2 MATERIALS and METHODS

Construction of plasmids

A DNA fragment for Tom7 with C-terminally tagged HA epitope YPYDVPDYA (22) and for its upstream noncoding region of 580 bp was amplified by PCR with the primers 5'-TTGGCTCGAGCTACTGTTGAAAGGG-3' and 5'-GCAGCT-CGAGTTA**AGCGTAGTCTGGGACGTCGTATGGGT**AAACACTTGGTAACGG-3' (the segment for the HA epitope is indicated with boldfaces) and the yeast genomic DNA as a template. The amplified DNA fragment was cleaved with *Kpn*I and *Sac*I and was introduced into the *Kpn*I-*Sac*I site of pYO324 (23). The resulting plasmid was transformed into the yeast strain Δtom7 (Table 1).

Photocrosslinking of the TOM-bound intermediate

DL-2-amino-5-(*p*-benzoylphenyl)pentanoic acid (BPA) containing a photoreactive benzophenone side chain was introduced at residue 15 or 18 of pSu9-DHFR labeled with [^{35}S]methionine by the suppressor tRNA method as described previously (24). Mitochondria were isolated from the yeast strain W303-1A (wild-type) or mutant strains (Table 1) as described previously (25). Mitochondria were incubated in binding buffer (10 mM Mops-KOH, pH 7.2, 250 mM sucrose, 10 mM KCl, 5 mM $MgCl_2$, 2 mM cold methionine, 40 μM carbonyl cyanide *m*-chlorophenylhydrazone (CCCP)) for 5 min on ice to dissipate $\Delta\Psi$, and were subsequently incubated with radiolabeled pSu9-DHFR for 10 min on ice. The mitochondria were reisolated by centrifugation, were resuspended with MSC buffer (10 mM Mops-KOH, pH 7.2, 250 mM sucrose, 10 mM KCl, 10 μM CCCP), and were subjected to UV-irradiation for 5 min on ice as described previously (24). Immunoprecipitation with the anti-HA antibody (Boehringer Mannheim) was performed as described previously (24). Proteins were analyzed by SDS-PAGE and radioimaging

with a Storm 860 image analyzer (Amersham Pharmacia Biotech).

Protein import into mitochondria

Mitochondria were isolated from the yeast strains listed in table 4-1, which were grown in a medium containing 2% galactose and 0.1% glucose instead of lactate at 23°C, as described previously (25). Radiolabeled precursor proteins were incubated with energized mitochondria in 10 mM Mops-KOH, pH 7.2, 250 mM sucrose, 80 mM KCl, 5 mM $MgCl_2$, 5 mM DTT, 1% BSA, 2 mM methionine, 2 mM ATP, 2 mM NADH at 23°C. The samples were divided into halves and were treated with or without 100 µg/ml proteinase K for 30 min on ice. The mitochondria were reisolated by centrifugation, and were washed once with MSC buffer. Proteins were analyzed by SDS-PAGE and radioimaging.

Two-step import of pSu9-DHFR

Isolated mitochondria were incubated in binding buffer for 5 min on ice and were subsequently incubated with radiolabeled pSu9-DHFR for 10 min on ice or at 30°C (first incubation). The samples were halved and were diluted 2-fold with MSC buffer containing 10 mM KCl or 300 mM KCl. After incubation on ice for 10 min, the samples were divided into three aliquots and the mitochondria were reisolated by centrifugation. To test whether the intermediates are arrested at *stage A* or at *stage B* (10), the mitochondria were resuspended in MSC buffer (10 mM KCl), and were treated with 100 µg/ml proteinase K. After addition of 1 mM PMSF, proteins were precipitated by trichloroacetic acid. For the chase reaction, the mitochondria without protease treatment were resuspended in chase buffer (250 mM sucrose, 10 mM Mops-KOH, pH 7.2, 10 mM KCl, 5 mM $MgCl_2$, 10 mM DTT, 2% BSA, 2 mM ATP, 2 mM KPi, 5 mM sodium malate, 2 mM NADH) and were incubated at 30°C for 10 min. The mitochondria were reisolated by centrifugation and proteins were analyzed by SDS-

PAGE and radioimaging.

Table 1 *S. cerevisiae* strains used in this study

Strains	Genotype	References
W303-1A	*MAT***a** *ade2-1 his3-11,15 ura3-1 leu2-3,112 trp1-1 can1-100*	26
Δtom5	*MAT***a** *ade2-1 his3-11,15 ura3-1 leu2-3,112 trp1-1 can1-100 Δtom5::cgHIS3*	Yamamoto, H. unpublished
Δtom6	*MAT***a** *ade2-1 his3-11,15 ura3-1 leu2-3,112 trp1-1 can1-100 Δtom6::cgHIS3*	Yamamoto, H. unpublished
Δtom7	*MAT***a** *ade2-1 his3-11,15 ura3-1 leu2-3,112 trp1-1 can1-100 Δtom7::cgHIS3*	Yamamoto, H. unpublished
tom22ΔC	*MAT***a** *ade2-1 his3-11,15 ura3-1 leu2-3,112 trp1-1 can1-100 tom22(Δ120-152)*	Ono, T. unpublished
Δc/Δ6	*MAT***a** *ade2-1 his3-11,15 ura3-1 leu2-3,112 trp1-1 can1-100 tom22(Δ120-152) tom6::cgHIS3*	Ono, T. unpublished
Δc/Δ7	*MAT***a** *ade2-1 his3-11,15 ura3-1 leu2-3,112 trp1-1 can1-100 tom22(Δ120-152) tom7::cgHIS3*	Ono, T. unpublished
7-HA	*MAT***a** *ade2-1 his3-11,15 ura3-1 leu2-3,112 trp1-1 can1-100 Δtom7::cgHIS3* pYO324/TOM7-HA	This study

4-3 RESULTS

4-3-1 Presequence of TOM-bound pSu9-DHFR is crosslinked to Tom7 in the IMS

When $\Delta\Psi$ is dissipated by CCCP, pSu9-DHFR, the N-terminal 69 residues of Fo-ATPase subunit 9 precursor protein of *Neurospora crassa* fused to mouse DHFR, is arrested at two distinct stage, stage A (accumulated at 0°C) and stage B (accumulated at 30°C), in the translocation across the outer membrane (10; Fig. 4-1). The mature domain of the intermediate is unfolded and bound to Tom40 at stage B whereas it remains folded on the cytosolic side of the outer membrane at stage A. The presequence of the intermediate of pSu9-DHFR accumulated at both stage A and stage B was crosslinked to Tom40, the C-terminal IMS domain of Tom22 (Tom22C), and an unidentified small protein, which generated a crosslinked product of 34 kDa (X1) (10). The apparent molecular mass of the crosslinking partner of X1 is estimated to be 5 kDa, which is close to those of Tom5, Tom6, or Tom7.

To test which the crosslinking partner of X1 is, Tom5, Tom6 or Tom7, mutant mitochondria lacking Tom5, Tom6, or Tom7 were isolated from the corresponding deletion mutant strains, were incubated with pSu9-DHFR containing BPA at residue 18 in the presequence in the presence of CCCP, and were UV-irradiated. Although the crosslinked product X1 was generated for mutant mitochondria lacking Tom5 or Tom6 as well as for wild-type mitochondria (Fig. 4-2, lanes 5-7), X1 was not found for mitochondria lacking Tom7 (Fig. 4-2, lane 8), suggesting that Tom7 is the crosslinking partner of X1. It is to be noted that the amount of the crosslinked product with Tom22 also decreased for mitochondria without Tom7 (Fig. 4-2, lane 8).

In order to rule out the possibility that deletion of Tom7 indirectly caused change in the crosslinking pattern, a yeast strain that expresses the C-terminally HA-tagged version of Tom7 (22) but not authentic Tom7 was constructed. Mitochondria were prepared form the strain with Tom7-HA and were used for photocrosslinking

experiments. The 34-kDa crosslinked product X1 was gone (Fig. 4-3, lanes 5, 11) and instead, a new crosslinked product (X1') of 35 kDa was generated. X1' was immunoprecipitated with the anti-HA antibody (Fig. 4-3, lanes 6, 12) and the difference in the molecular masses for X1 and X1', ca 1 kDa, is consistent with the calculated molecular mass of the HA tag. These results indicate that Tom7 is the crosslinking partner of X1.

4-3-2 Simultaneous deletion of Tom22C and Tom7 causes a strong defect in the cell growth

The results of photocrosslinking experiments showed that Tom40, Tom22C and Tom7 are close to the presequence on the IMS side of the outer membrane, suggesting that they constitute the trans site for the presequence binding. However on the other hand, single deletion of Tom22C or Tom7 led to only marginal or no defect in the cell growth (14-17; Fig. 4-4). Since deletion of Tom7 affects the crosslinking efficiency of the TOM-bound intermediate with Tom22C, Tom22C and Tom7 may have an overlapping function and single deletion of one of the two protein/domain, Tom22C and Tom7, can be functionally complemented by each other. To test this possibility, a double deletion mutant strain lacking both Tom22C and Tom7 and that lacking Tom22C and Tom6 as a control were constructed. It is to be noted that Tom6 exhibits an antagonistic function against Tom7 (19).

Deletion of *TOM22C* did not affect the cell growth significantly except for the case of the non-fermentable carbon source at 37°C, where the cell stopped growing (Fig. 4-4). Single deletion of one of the two genes, *TOM6* and *TOM7* did not cause significant growth defects in the cell growth either on the non-fermentable carbon source (lactate) or on the fermentable carbon source (glucose) at 23-37°C (Fig. 4-4). On the other hand, cells lacking both *TOM22C* and *TOM6* showed a moderate defect in the growth on non-fermentable carbon source at low temperature and did not grow on

fermentable or non-fermentable carbon sources at 37°C (Fig. 4-4). Cells lacking both *TOM22C* and *TOM7* did not grow on the fermentable carbon source at 37°C and on the non-fermentable carbon source at 23-37°C (Fig. 4-4). These results indicate the genetic interaction between *TOM22C* and *TOM6* and that between *TOM22C* and *TOM7*, which escaped detection in the previous studies.

4-3-3 Tom22C promotes assembly of the TOM complex in a similar manner to Tom6

Synthetic growth defects of the double mutants tom22ΔC/Δtom6 and tom22ΔC/Δtom7 provide genetic evidence for the functional relationship of Tom22C with Tom6 and Tom7. Tom6 and Tom7 were proposed to modulate the dynamics of the assembly of the TOM complex (21). I thus examined the effects of the simultaneous deletions of Tom22C with Tom6 or Tom7 on the stability of the TOM complex. Mitochondria were isolated from the mutant strains lacking Tom22C, Tom6, and/or Tom7, which were grown in a medium containing 2% galactose and 0.1% glucose at 23°C. The mitochondria were solubilized with non-ionic detergent digitonin, and were subjected to blue-native PAGE (21). When wild-type mitochondria were stained with the anti-Tom40 or anti-Tom23 antibodies, Tom40 was detected in a 400-kDa complex (400K complex) whereas Tim23 in a 90-kDa complex (Fig. 4-5, lanes 1, 7). The previous study showed that the 400K TOM complex contains Tom40, Tom22, Tom5, Tom6, and Tom7 (21). In mitochondria from the Δtom7 strain, Tom40 was detected in the 400K complex (Fig. 4-5, lane 3). On the other hand, a fraction of Tom40 was found in a 100-kDa complex (100K complex) when mitochondria from the Δtom6 or tom22ΔC strains were analyzed by BN-PAGE (Fig. 4-5, lane 2, 4), indicating that deletion of Tom22C as well as Tom6 results in destabilization of the 400K complex. Simultaneous deletion of Tom22C and Tom7 led to a complete loss of the 400K complex and Tom40 was mainly shifted to the 100K complex and partly to a 250-kDa

complex (250K complex) (Fig. 4-5, lane 6). These assembly defects are similar to those for mitochondria lacking both Tom6 and Tom7, in which Tom40 was found in the 200-kDa complex as well as in the 100K complex, but not in the 400K complex (19). Tom40 was observed exclusively in the 100K complex in mutant mitochondria lacking both Tom22C and Tom6 (Fig. 4-6, lane 5). These results indicate that Tom22C and Tom6 exhibit overlapping functions to promote assembly of the TOM complex so that simultaneous deletion of both Tom22C and Tom6 leads to complete destabilization of the 400K TOM complex.

4-3-4 Mitochondria lacking Tom22C together with Tom6 or Tom7 are defective in import of the protein with a cleavable presequence

Next, I examined the effect of simultaneous deletion of Tom22C together with Tom6 or Tom7 on the import of presequence-containing proteins into mitochondria. pSu9-DHFR containing a cleavable presequence was imported into the matrix and received the processing by MPP to yield a mature-size form (Fig. 4-6A). Radiolabeled pSu9-DHFR was efficiently imported into energized mitochondria from tom22ΔC, Δtom6, or Δtom7 strains *in vitro* and was processed to the mature-size form with a similar kinetics to that for wild-type mitochondria (Fig. 4-6B). In contrast, when incubated with energized mutant mitochondria from ΔC/Δ6 or ΔC/Δ7 strains, pSu9-DHFR was imported into mitochondria much less efficiently than that into the wild-type mitochondria (Fig. 4-6B).

Next, I tested the effect of the double deletions of Tom22C together with Tom6 or Tom7 on the import of proteins without a cleavable presequence. ADP/ATP carrier (AAC), which is an integral inner membrane protein, is synthesized in the cytosol without a cleavable presequence. AAC traverses the outer membrane through the Tom40 complex and are inserted into the inner membrane in a ΔΨ-dependent manner *in vitro* (2, 3; Fig. 4-7). When incubated with energized mutant mitochondria from

ΔC/Δ6 or ΔC/Δ7 strains, AAC was imported into mitochondria as efficiently as wild-type mitochondria (Fig. 4-7). This is in contrast to the case of pSu9-DHFR and suggests that the TOM complex lacking Tom22C together with Tom6 or Tom7 has an ability to mediate translocation of presequence-less proteins across the outer membrane. In summary, these results indicate the functional relationships between Tom22C and Tom6 or Tom7 in the import of presequence-containing proteins, but not of presequence-less proteins, into mitochondria.

4-3-5 The lack of Tom22C together with Tom6 or Tom7 causes a defect at the step after the presequence translocation across the outer membrane

Which step of the import of presequence-containing proteins into the matrix is impaired by the double deletions of Tom22C together with Tom6 or Tom7? I thus analyzed the two-step import of pSu9-DHFR into mitochondria lacking Tom22C together with Tom6 or Tom7 by the protein accumulation at the outer membrane in the absence of $\Delta\Psi$ and subsequent chase after the re-establishment of $\Delta\Psi$. When radiolabeled pSu9-DHFR was incubated with wild-type mitochondria on ice in the presence of CCCP, the stage A intermediate was generated. Protease treatment of the re-isolated mitochondria released a protease-resistant fragment from the mitochondria, suggesting that the DHFR domain of the stage A intermediate is folded outside mitochondria (10; Fig. 4-8A and B, WT). The stage A intermediate was easily released from the mitochondria by washing with 150 mM KCl (10; Fig. 4-8A and B, WT). When pSu9-DHFR was incubated with wild-type mitochondria at 30°C in the presence of CCCP, the stage B intermediate was generated. The intermediate is sensitive to protease digestion, suggesting that the DHFR domain of the stage B intermediate is unfolded (Fig. 4-8A and C, WT). The stage B intermediate was stable even when the mitochondria were washed with 150 mM KCl. Since the protease resistant fragment was generated only from the stage A intermediate, the amounts of the

stage A intermediate and the stage B intermediate can be estimated by quantification of the protease-resistant fragment (Fig. 4-8B and C).

When radiolabeled pSu9-DHFR was incubated with the mutant mitochondria lacking Tom22C, Tom6, and/or Tom7 on ice or at 30°C in the presence of CCCP, the amounts of both stage A and stage B intermediates are not significantly reduced as compared with those for wild-type mitochondria (Fig. 4-8B and C). Most of the stage A intermediates, not the stage B intermediates, accumulated in the deletion mutant mitochondria were released from the mitochondria by washing with 150 mM KCl, indicating that the intermediates in the mutant mitochondria share characteristics with that in the wild-type mitochondria (Fig. 4-8B and C).

The stage A and stage B intermediates of pSu9-DHFR accumulated at the outer membrane in the $\Delta\Psi$-dissipated mitochondria can be chased into the matrix after re-establishing the $\Delta\Psi$ by the inactivation of CCCP and addition of the energy source. By monitoring the processing of the presequence of the intermediates, the efficiency of the chase reaction can be determined. 68% and 53% of the stage A and the stage B intermediates, respectively, were chased into the matrix of the wild-type mitochondria (Fig, 4-8D and E, WT). 40-50% reduction of the chase efficiency for the stage A intermediate was observed for the mitochondria from Δtom6, Δtom7, or tom22ΔC as compared with that for wild-type mitochondria (Fig. 4-8D, Δ6, Δ7, and ΔC). On the other hand, the chase reaction of the stage B intermediate occurred for these mutant mitochondria as efficiently as for wild-type mitochondria (Fig. 4-8E, Δ6, Δ7, and ΔC). Neither stage A nor stage B intermediates was chased into the matrix of mutant mitochondria from ΔC/Δ6 or ΔC/Δ7 strains (reduction of 80-90%; Fig. 4-8D and E, ΔC/Δ6 and ΔC/Δ7). Since the presequence of pSu9-DHFR at both stage A and stage B intermediates already reached the trans site and the amounts of the stage A and stage B intermediates were not affected by the double deletions of Tom22C together with Tom6 or Tom7, the double deletions most likely impairs the step after binding to the trans site

of the TOM complex.

4-3-6 Tom7 does not function in protein import in the mitochondria lacking both Tom22C and Tom6

The presequences of the translocation intermediates of pSu9-DHFR at both stage A and stage B are crosslinked with Tom22C and Tom7, but not with Tom6 (Fig. 4-3; ref. 10). However, the effect of the deletion of Tom6 together with Tom22C on protein import into the matrix is similar to that of the deletion of both Tom7 and Tom22C. Perhaps, deletion of Tom6 together with Tom22C impairs the function of Tom7, thereby causing a similar defect to that by simultaneous deletions of Tom7 and Tom22C. To test this possibility, site-specific photocrosslinking of the presequence of the stage A translocation intermediate of pSu9-DHFR was performed for mitochondria lacking Tom22C and Tom6. Radiolabeled pSu9-DHFR containing BPA at residue 18 was incubated with wild-type mitochondria or mutant mitochondria from the ΔC/Δ6 or ΔC/Δ7 strains in the presence of CCCP, and were subjected to UV-irradiation. The crosslinked product X1 with Tom7 was not detected for mutant mitochondria lacking Tom22C and Tom6 as well as for those lacking Tom22C and Tom7 (Fig. 4-9, lanes 4 and 6). These results indicate that Tom7 is not close to the presequence in the TOM complex of mitochondria lacking both Tom22C and Tom6.

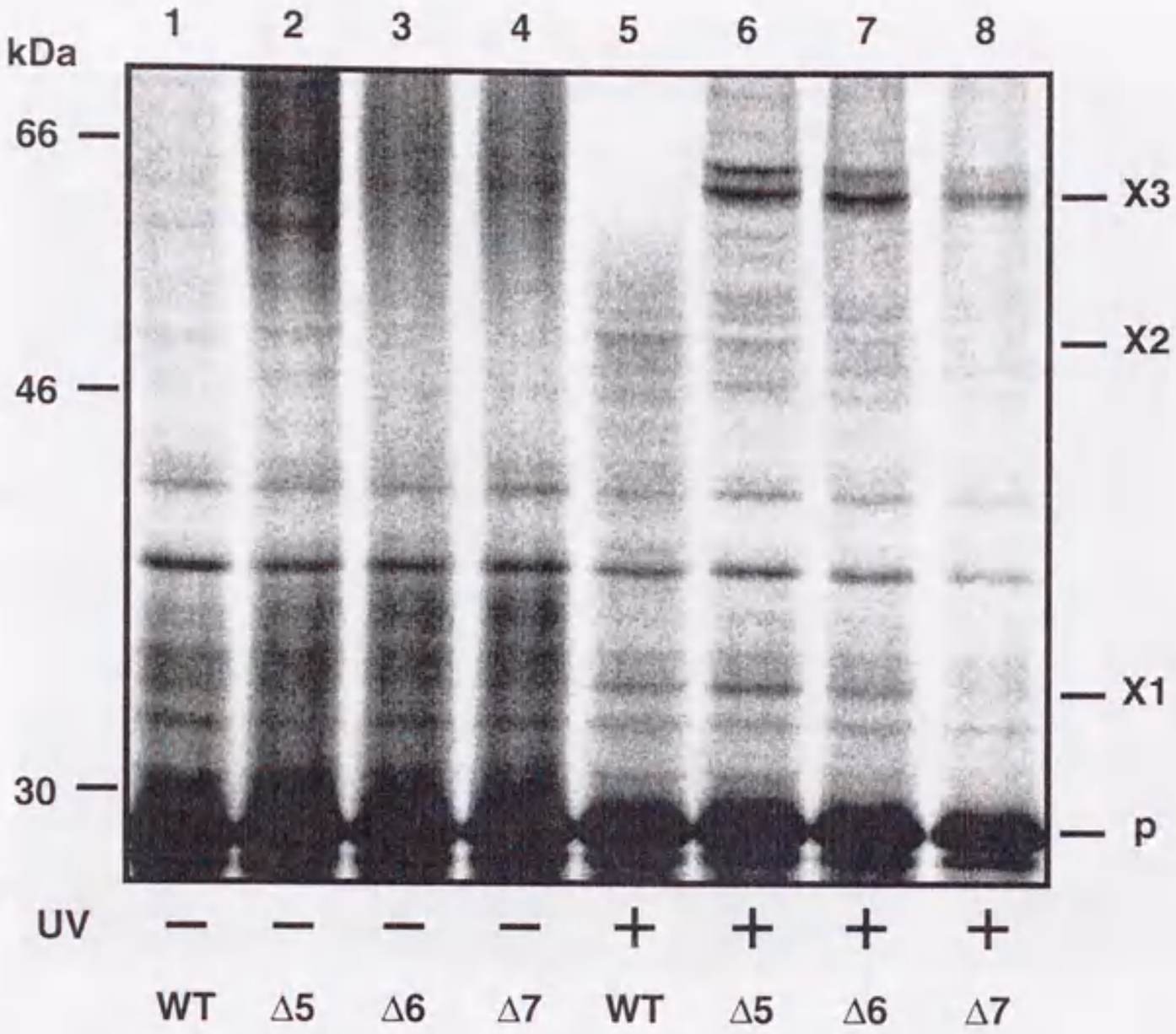

Fig. 4-2 X1 is not generated from mutant mitochondria lacking Tom7

Radiolabeld pSu9-DHFR containing BPA at residue 18 was incubated in the presence of CCCP with mitochondria, which were isolated from yeast strains W303-1A (WT), Δtom5 (Δ5), Δtom6 (Δ6), or Δtom7 (Δ7) for 10 min on ice. The mitochondria were reisolated by centrifugation, were resuspended with SMC buffer, and were subjected to the UV irradiation for 5 min on ice. The mitochondria were reisolated by centrifugation. p, precursor; X1, 34-kDa crosslinked product; X2, crosslinked product with Tom22; X3, crosslinked product with Tom40.

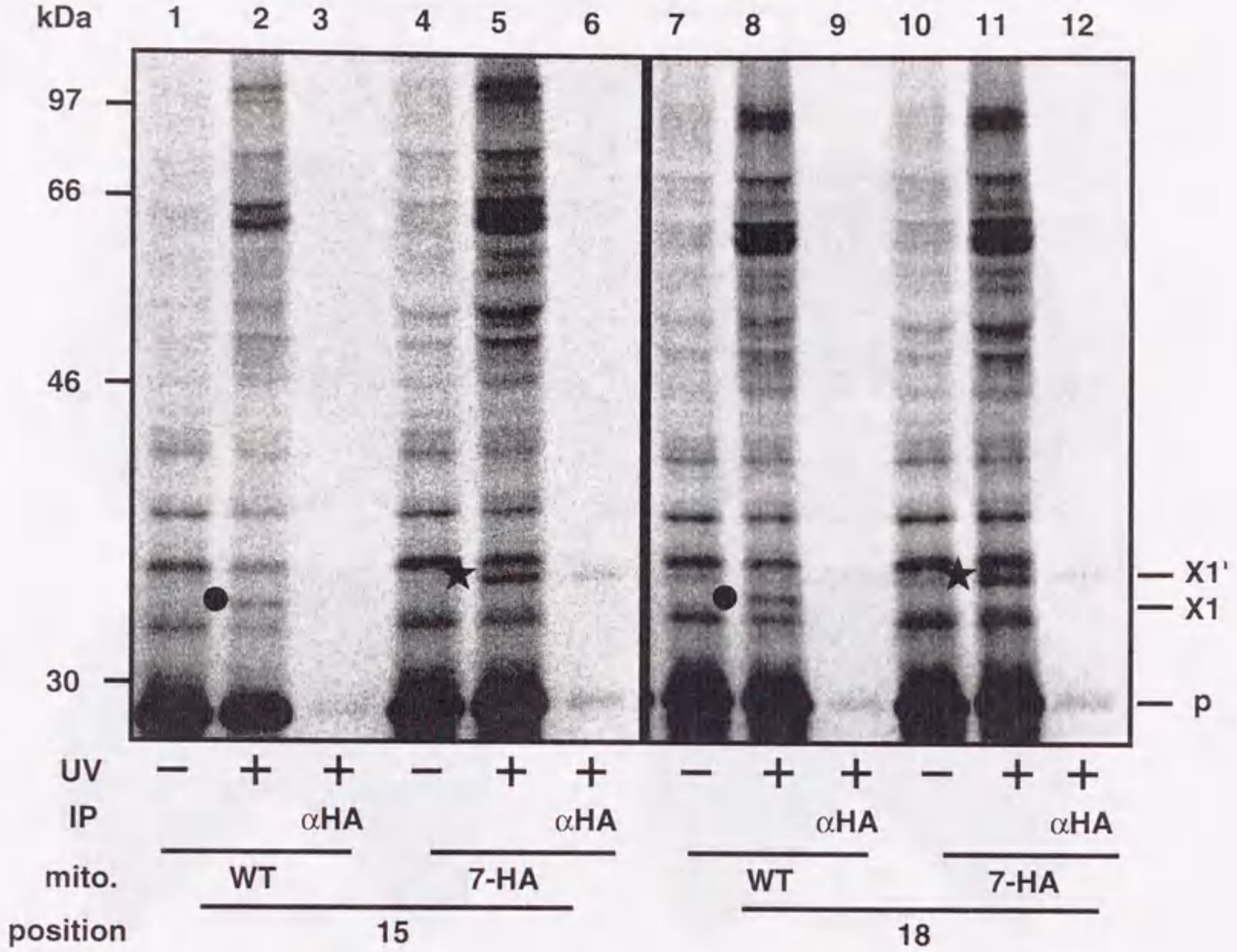

Fig. 4-3 The presequence of the TOM-bound intermediate is crosslinked to Tom7

pSu9-DHFR containing BPA at positions 15 and 18 were incubated in the presence of CCCP with mitochondria isolated from yeast strains W303-1A (WT) and 7-HA. The mitochondria were subjected to UV irradiation (lanes 2, 3, 5, 6, 8, 9, 11, 12). The mitochondria were reisolated by centrifugation and were solubilized with SDS. Proteins were immunoprecipitated with the anti-HA antibody (αHA, lanes 3, 6, 9, and 12). Dots and stars indicate the crosslinked product with Tom7 (X1) and with Tom7-HA (X1'), respectively. p, precursor form.

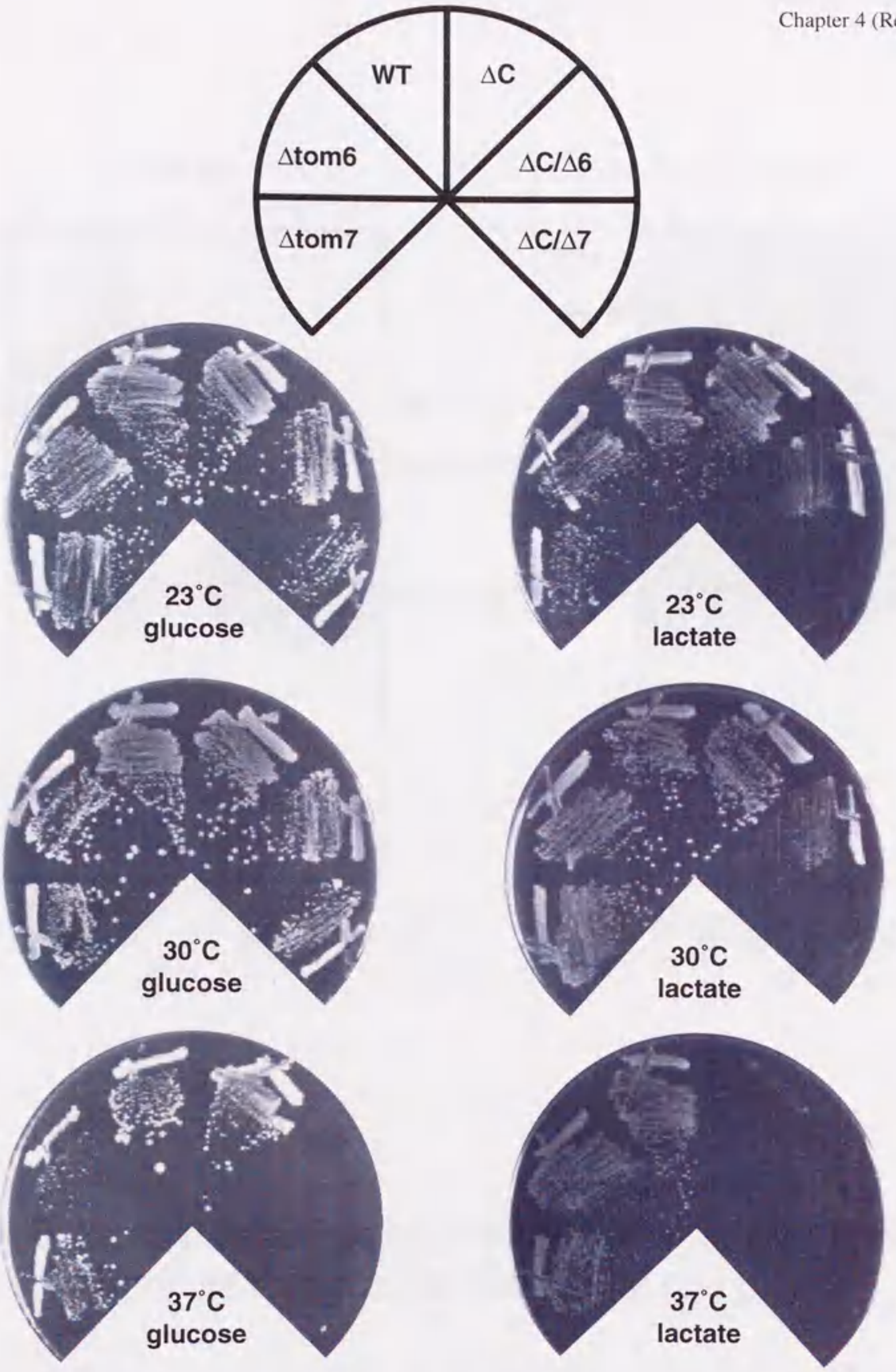

Fig. 4-4 Double deletions of Tom22C together with Tom6 or Tom7 cause respiratory defects and temperature-sensitive phenotype

Yeast strains listed in Table 1 were grown on plates containing glucose (left) or lactate (right) as a sole carbon source at indicated temperature for 4.5 days.

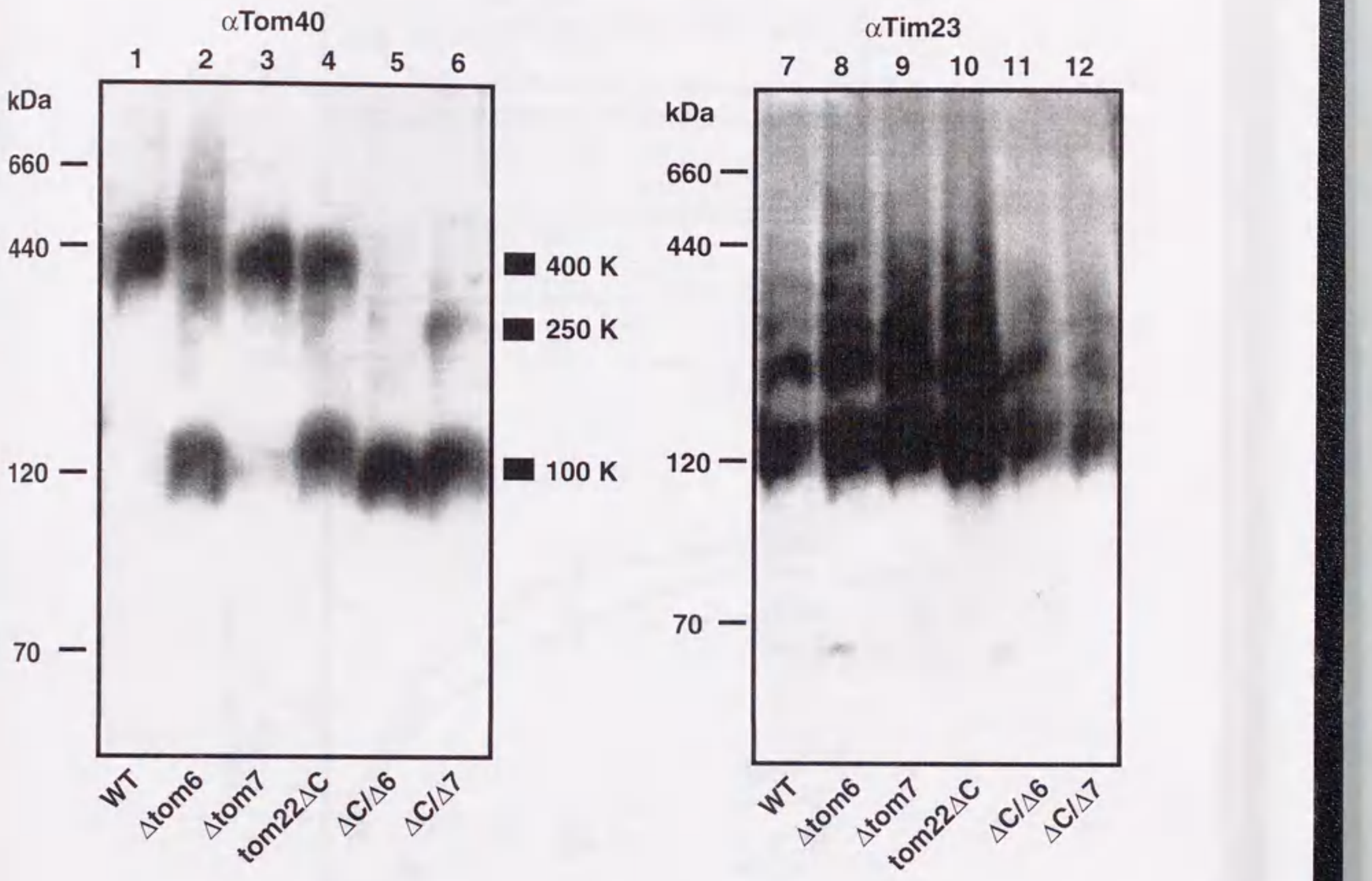

Fig. 4-5 Double deletions of Tom22C together with Tom6 or Tom7 destabilize the 400K TOM complex

Mitochondria isolated from wild type (WT) or the deletion mutant cells listed in Table 1 were solubilized with 1% digitonin and subjected to blue-native PAGE as described previously (21). Proteins were transferred to a PVDF membrane and immunodecorated with the anti-Tom40 (left) or anti-Tim23 (right) antibodies.

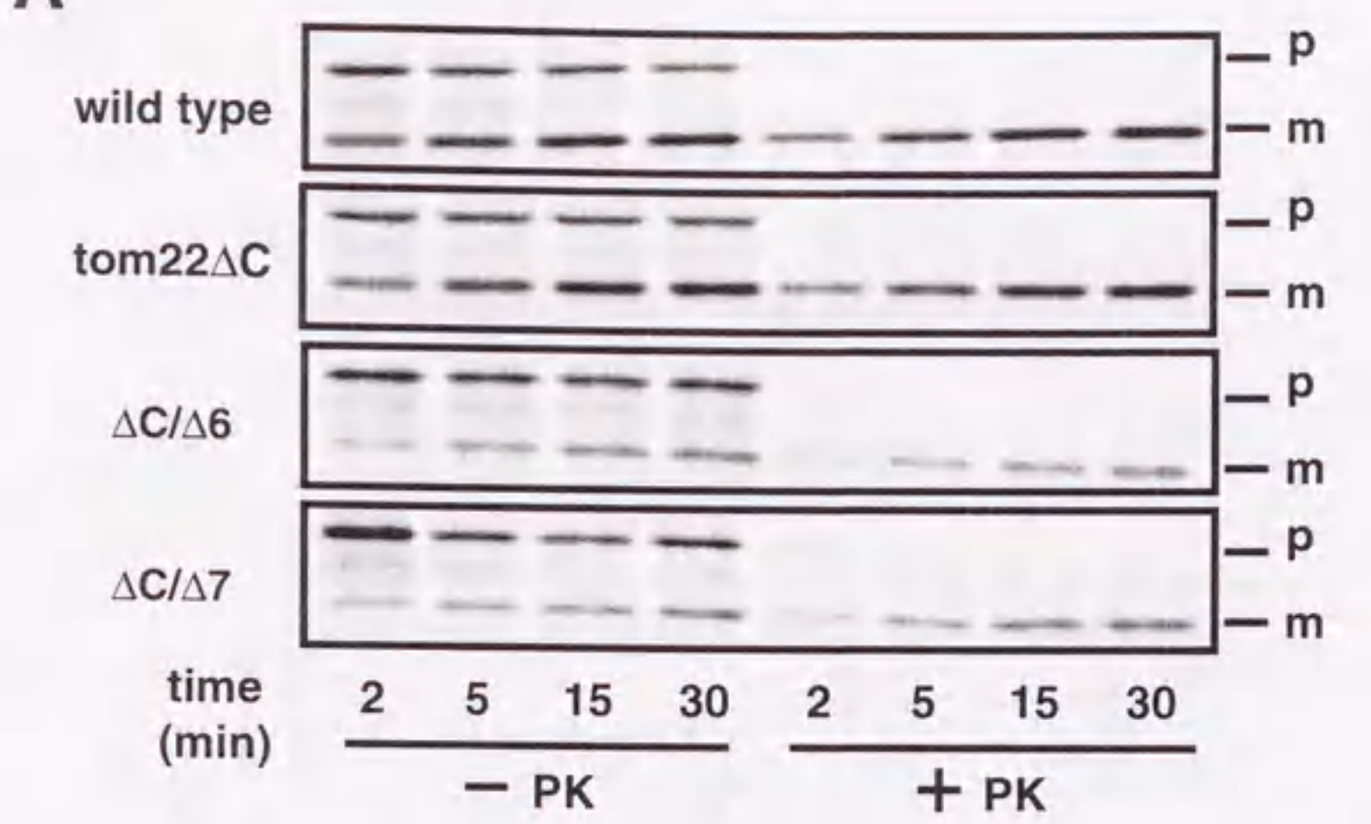

Fig. 4-6 Simultaneous deletions of Tom22C/Tom7 or Tom22C/Tom6 impair the import of pSu9-DHFR into mitochondria

A. Radiolabeled pSu9-DHFR was incubated with energized mitochondria isolated from wild-type cells or the deletion mutant cells for indicated times at 23°C. The samples were divided and were treated with (+PK) or without (-PK) 100 μg/ml proteinase K for 30 min on ice. The mitochndria were reisolated by centrifugation, and proteins were analyzed by SDS-PAGE and radioimaging. p, precursor form; m, mature-size form.

B. The amounts of protease-protected mature-size forms were plotted against the incubation times. The amount of pSu9-DHFR added to each reaction is set to 100%. Open circles, wild-type; open triangles, Δtom7; open squares, Δtom6; closed circles, tom22ΔC; closed triangles, ΔC/Δ7; closed squares, ΔC/Δ6.

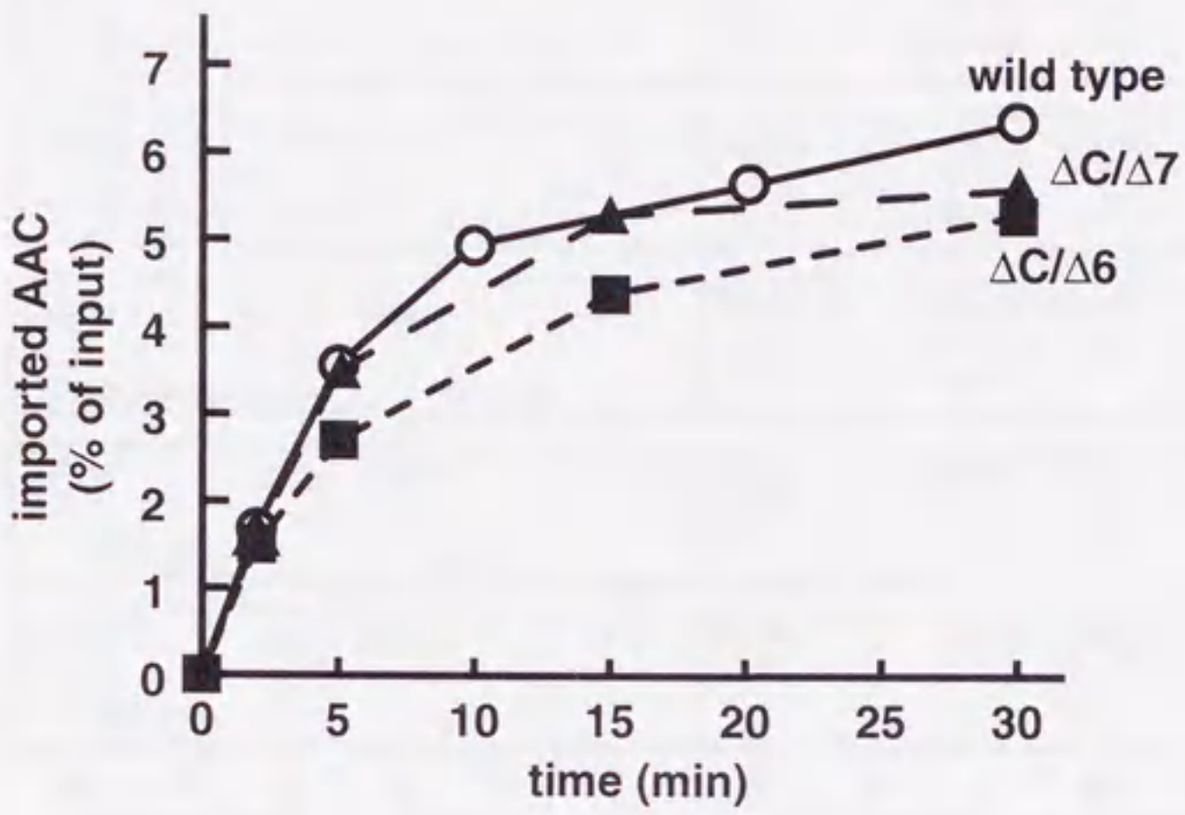

Fig. 4-7 Simultaneous deletions of Tom22C together with Tom6 or Tom7 do not affect the import of AAC

Radiolabeled AAC was incubated with energized mitochondria isolated from wild-type or the deletion mutant cells for indicated times at 23°C. The mitochondria were treated with 100μg/ml proteinase K for 30 min on ice. The mitochondria were reisolated by centrifugation, and the proteins were analyzed by SDS-PAGE and radioimaging. The amounts of protease-protected AAC were plotted against the incubation times. The amount of AAC added to each reaction is set to 100%. open circles, wild-type; closed triangles, ΔC/Δ7; closed squares, ΔC/Δ6.

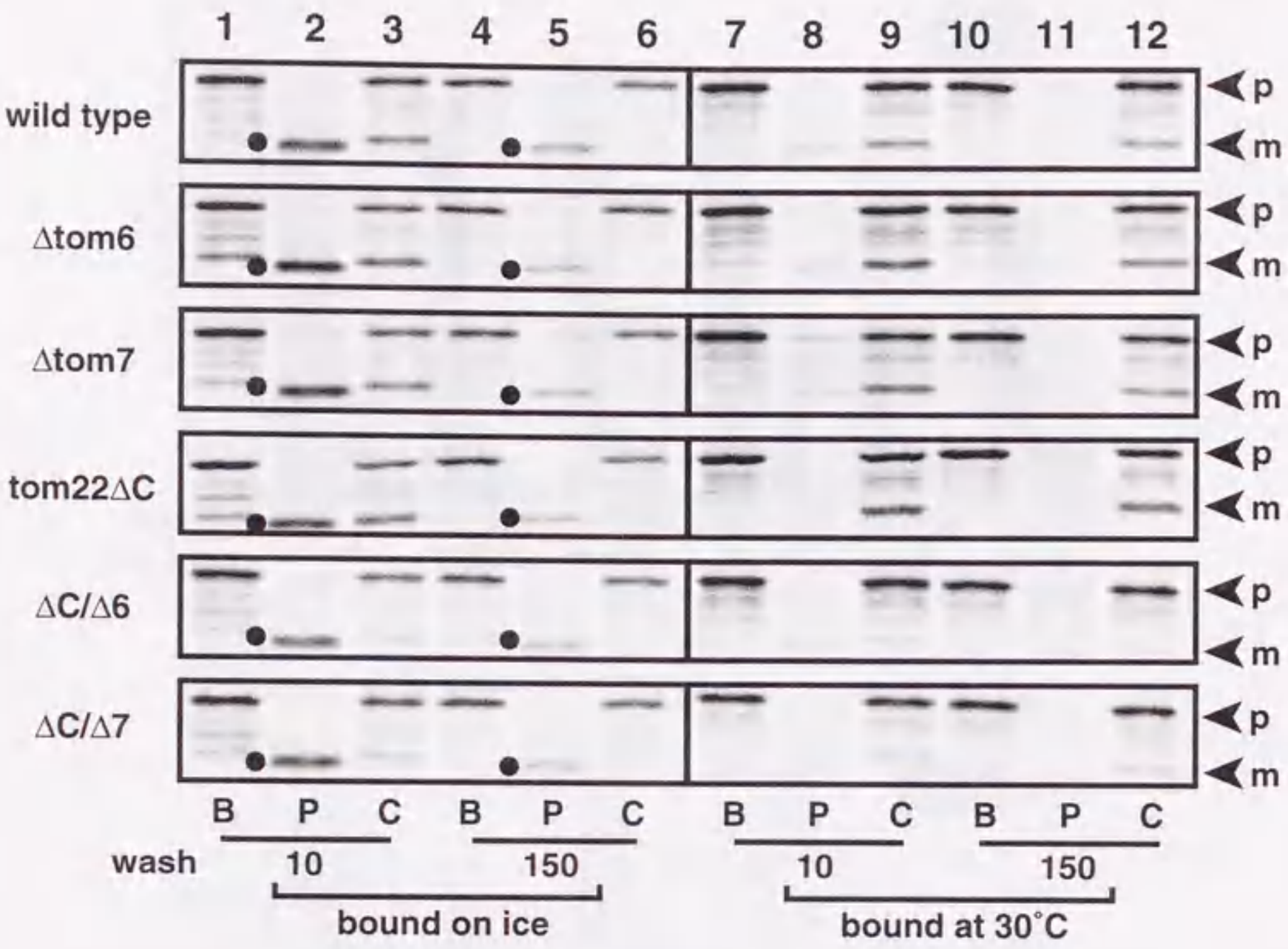

Fig. 4-8 Two-step import of pSu9-DHFR is strongly inhibited by simultaneous deletions of Tom22C together with Tom6 or Tom7

A, Radiolabeled pSu9-DHFR was incubated with the wild-type mitochondria and the mutant mitochodria on ice (lanes 1-6) or at 30ºC (lanes 7-12) for 10 min in the presence of CCCP and 10 mM KCl. The samples were halved and were incubated with 10 mM (lanes 1-3, and 7-9) or 150 mM (lanes 4-6, and 10-12) KCl for 10 min on ice. Each sample was split into three aliquots and the mitochondria were reisolated by centrifugation. The first ones were kept on ice (B, lanes 1, 4, 7, and 10). The second ones were treated with protease for 30 min on ice (P, lanes 2, 5, 8, and 11), and all proteins were precipitated by trichloroacetic acid. In the third samples, mitochondria were resuspended with chase buffer containing 10 mM KCl and were incubated at 30ºC for 10 min (C, lanes 3, 6, 9, and 12). Dots indicate the protease resistant fragments. p, precursor; m, processed mature-size form.

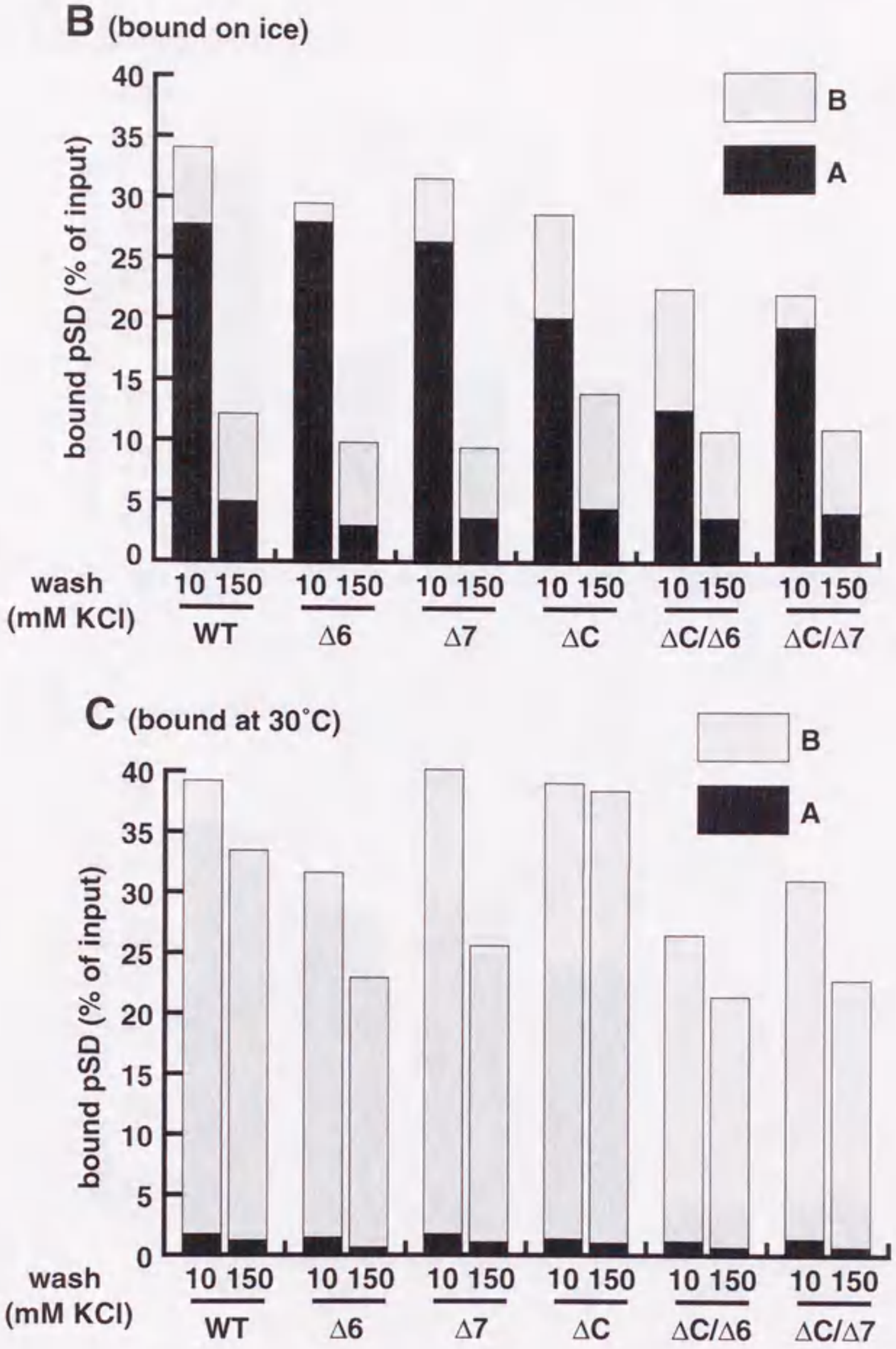

Fig. 4-8 (continued)

B, C, Amounts of bound pSu9-DHFR (lanes 1, 4, 7, and 10) and protease resistant fragments (lane lanes 2, 5, 8, and 11) were quantified. Since the protease resistant fragments were generated only from the stage A intermediates, they reflect the amounts of the stage A intermediates (black bars). The differences between the amounts of bound pSu9-DHFR and those of the protease resistant fragments correspond to those of the stage B intermediates (gray bars). The amount of pSu9-DHFR added to each reaction is set to 100%.

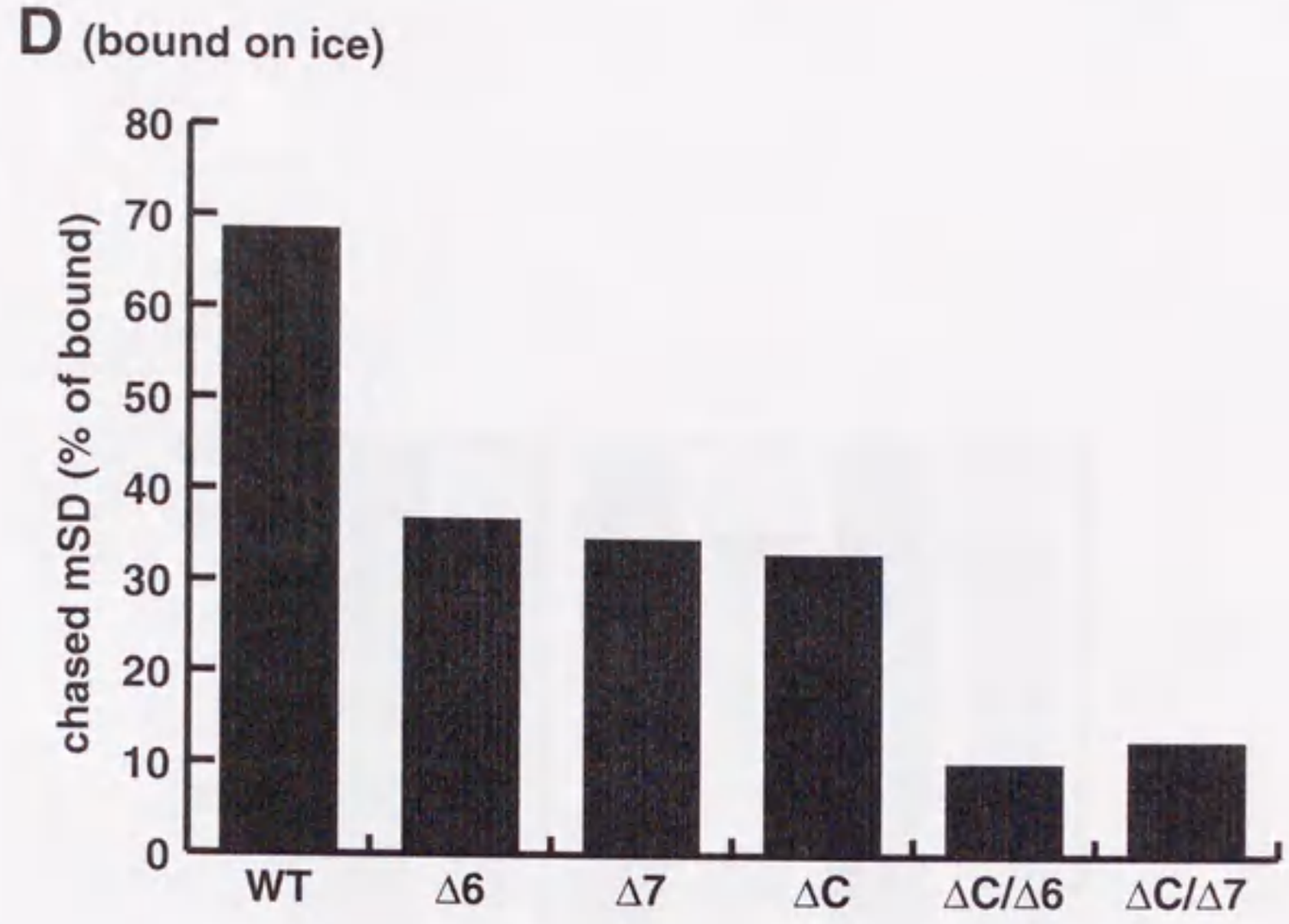

Fig. 4-8 (continued)

D, E, Amounts of the chased mature-size proteins from intermediates washed with 10 mM KCl (lanes 3, 9) were quantified. The amounts of bound pSu9-DHFR in the first incubation are set to 100%.

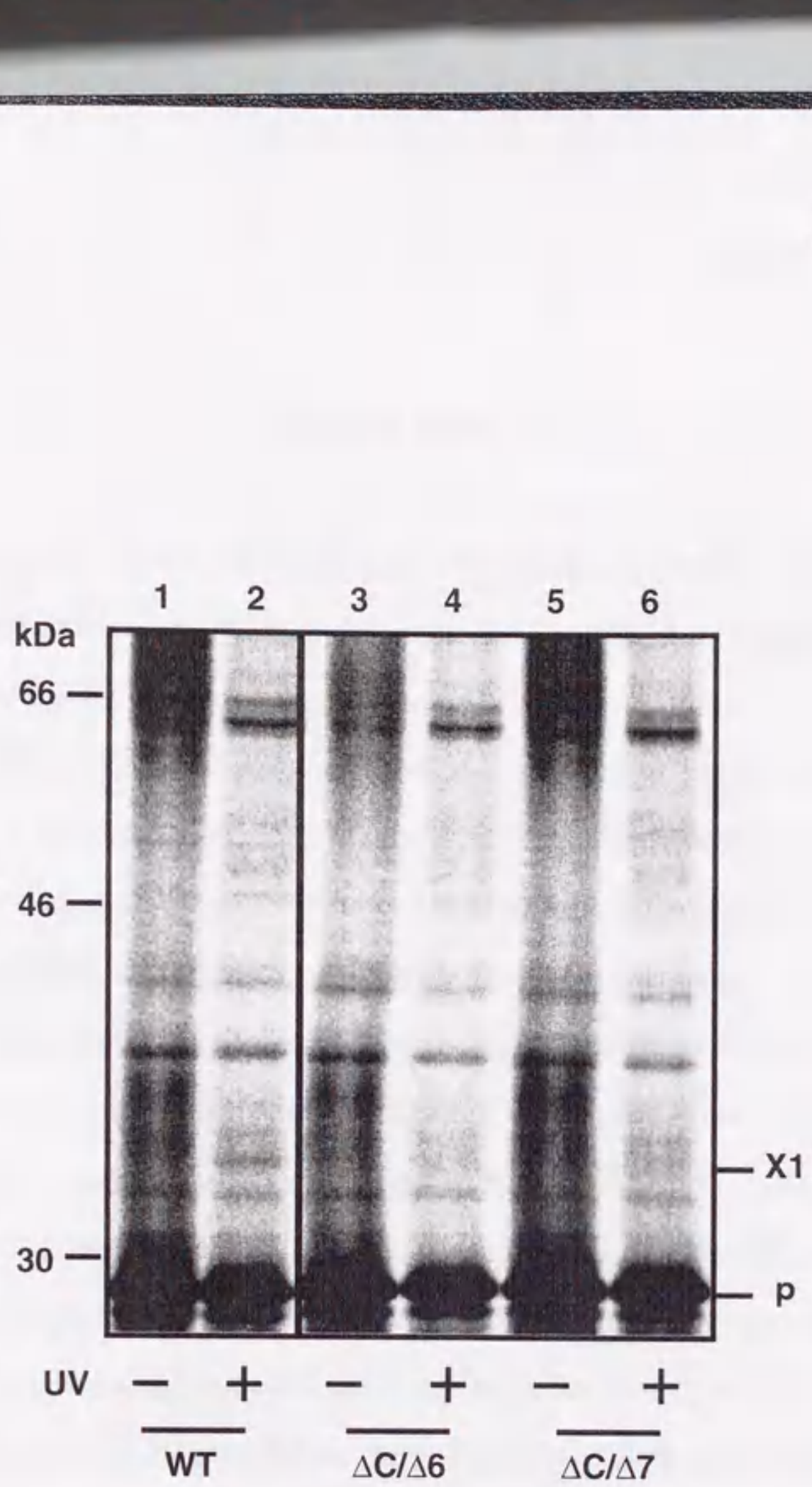

FIg. 4-9 Crosslinked product with Tom7 is not generated from mutant mitochondria lacking both Tom22C and Tom6

Radiolabeld pSu9-DHFR containing BPA at residue 18 were incubated in the binding buffer with mitochondria, which were isolated from yeast strains W303-1A (WT), ΔC/Δ6, or ΔC/Δ7 for 10 min on ice. The mitochondria were reisolated by centrifugation and were resuspended with the SMC buffer. The samples were halved. The first ones were left on ice (odd lanes) and the others were subjected to the UV irradiation for 5 min on ice (even lanes). The mitochondria were reisolated by centrifugation, and proteins were analyzed by SDS-PAGE and radioimaging. p, precursor; X1, crosslinked product with Tom7.

4-4 DISCUSSION

In this chapter, I found that Tom7 and the C-terminal domain of Tom22 play important roles in the import of presequence-containing proteins into the matrix and in the assembly of the TOM complex.

The single deletion of Tom22C or Tom7 did not cause a significant defect in the cell growth or in the protein import. On the other hand, deletions of both Tom22C and Tom7 led to the complete loss of the mitochondrial respiratory function (Fig. 4-4), suggesting that Tom22C and Tom7 play important and complementary roles in the biogenesis of mitochondria. A precursor protein bearing a presequence can bind to the trans site of $\Delta\Psi$-dissipated mitochondria lacking Tom22C and Tom7 in a similar manner to wild-type mitochondria *in vitro*. This indicates that Tom22C and Tom7 are not important for the presequence binding to the trans site, although Tom22C and Tom7 are close to the presequence on the IMS side of the membrane. Therefore, the trans-binding site for presequence is composed mainly of the IMS side region of Tom40.

Two-step import or the chase of the stage A and stage B intermediates of pSu9-DHFR accumulated at the TOM complex revealed that the simultaneous deletion of Tom22C and Tom7 impairs a step after the translocation of the presequence across the outer membrane or presequence binding to the trans site of the TOM complex (Fig. 4-7D and E). It is unlikely that the deletion of the subunits constituting the TOM complex directly affects the protein translocation across the inner membrane. The double deletion of Tom22C and Tom7, therefore, most likely affects transfer of the presequence from the trans site of the TOM complex to the Tim23 complex. Since the strong defect in the cell growth and in the protein import was observed only when Tom22C and Tom7 were simultaneously deleted, Tom22C and Tom7 seem to play overlapping and complementary roles in the presequence transfer from the trans site to the Tim23 complex.

Blue-native PAGE analyses revealed that the deletion of Tom22C caused partial destabilization of the TOM complex (Fig. 4-5), suggesting that Tom22C mediates the assembly of the TOM complex. Dekker et al. reported that Tom6 mediates the assembly of the TOM complex because ~80% of Tom40 was found in the 100K complex in mutant mitochondria lacking Tom6 (21). However in the present study, only moderate destabilization of the TOM complex was observed for mutant mitochondria lacking Tom6 (Fig. 4-5). These apparently divergent results may reflect the difference in the genetic background of the strains used by the two groups. When the deletion of Tom22C is combined with that of Tom6 or Tom7, the 400K TOM complex was completely destabilized to generate mainly the 100K complex. These results suggest that Tom22C and Tom6 or Tom7 play overlapping and complementary roles in the assembly of the 400K TOM complex.

What is the relationship of the roles of Tom22C with Tom6 and Tom7 between the presequence transfer from the trans site of the TOM complex and the assembly of the TOM complex? One possibility is that the 400K complex, which is destabilized by the double deletion of Tom22C together with Tom6 or Tom7, is essential for the presequence transfer. The 100K, and probably 250K, complexes contain the trans site for the presequence and fully function for the transfer of presequence-less proteins from the TOM complex to the Tim22 complex. However, the reason for the difference in the defects in the cell growth between the ΔC/Δ7 and the ΔC/Δ6 strains is not readily explained by the above interpretation and awaits future studies.

REFERENCES

1. Hurt, E. C., Pesold-Hurt, B., and Schatz, G. (1984) The amino-terminal region of an imported mitochondrial precursor polypeptide can direct cytoplasmic dihydrofolate reductase into the mitochondrial matrix. *EMBO J.*, **3**, 3149-3156
2. Pfanner, N., Craig, E. A., and Hönlinger, A. (1997) Mitochondrial preprotein translocase. *Annu. Rev. Cell Dev. Biol.*, **13**, 25-51
3. Neupert, W. (1997) Protein import into mitochondria. *Annu. Rev. Biochem.*, **66**, 863-917
4. Martin, J., Mahlke, K., and Pfanner N. (1991) Role of an Energized inner membrane in mitochondrial protein import. $\Delta\Psi$ drives the movement of presequences. *J. Biol. Chem.*, **266**, 18051-18057
5. Roise, D. (1992) Interaction of a synthetic mitochondrial presequence with isolated yeast mitochondria: Mechanism of binding and kinetics of import. *Proc. Natl. Acad. Sci. USA*, **89**, 608-612
6. Ryan, M. T., Wagner, R., and Pfanner, N. (2000) The transport machinery for the import of preproteins across the outer mitochondrial membrane. *Int. J. Biochem. Cell Biol.*, **32**, 13-21
7. Herrmann, J. M. and Neupert, W. (2000) What fuels polypeptide translocation? An energetical view on mitochondrial protein sorting. *Biochim. Biophys. Acta*, **1459**, 331-338
8. Komiya, T., Rospert, S., Koehler, C., Looser, R., Schatz, G., and Mihara, K. (1998) Interaction of mitochondrial targeting signals with acidic receptor domains along the protein import pathway: evidence for the 'acid chain' hypothesis. *EMBO J.*, **17**, 3886-3898
9. Donzeau, M., Káldi, K., Adam, A., Paschen, S., Wanner, G., guiard, B., Bauer, M. F., Neupert, W., and Brunner, M. (2000) Tim23 links the inner and outer

mitochondrial membrane. *Cell*, **101**, 401-41

10. Kanamori, T., Nishikawa, S., Nakai, M., Shin, I., Schultz, P. G., and Endo, T. (1999) Uncoupling of transfer of the presequence and unfolding of the mature domain in precursor translocation across the mitochondrial outer membrane. *Proc. Natl. Acad. Sci. USA*, **96**, 3634-3639
11. Vestweber, D., Brunner, J., Baker, A., and Schatz, G. (1989) A 42K outer-membrane protein is a component of the yeast mitochondrial protein import site. *Nature*, **341**, 205-209
12. Künkele, K-P., Heins, S., Dembowski, M., Nargang, F. E., Benz, R., Thieffry, M., Walz, J., Lill, R., Nussberger, S., and Neupert, W. (1998) The preprotein translocation channel of the outer membrane of mitochondria. *Cell*, **93**, 1009-1019
13. Mayer, A., Nargang, F. E., Neupert, W., and Lill, R. (1995) MOM22 is a receptor for mitochondrial targeting sequences and cooperates with MOM19. *EMBO J.* **14**, 4204-4211
14. Nakai, M., Kinoshita, K., and Endo, T. (1995) Mitochondrial receptor complex protein. The intermembrane space domain of yeast Mas17 is not essential for its targeting or function. *J. Biol. Chem.*, **270**, 30571-30575
15. Bollinger, L., Junne, T., Schatz, G., and Lithgow, T. (1995) Acidic receptor domains on both sides of the outer membrane mediate translocation of precursor proteins into yeast mitochondria. *EMBO J.*, **14**, 6318-6326
16. Court, D. A., Nargang, F. E., Steiner, H., Hodges, R. S., Neupert, W., and Lill, R. (1996) Role of the intermembrane-space domain of the preprotein receptor Tom22 in protein import into mitochondria. *Mol. Cell. Biol.*, **16**, 4035-4042
17. Moczko, M., Bömer, U., Kübrich, M., Zufall, N., Hönlinger, A., and Pfanner, N. (1997) The intermembrane space domain of mitochondrial Tom22 functions as a *trans* binding site for preproteins with N-terminal targeting sequences. *Mol. Cell. Biol.*, **17**, 6574-6584

18. Saeki, K., Suzuki, H., Tsuneoka, M., Maeda, M., Iwamoto, R., Hasuwa, H., Shida, S., Takahashi, T., Sakaguchi, M., Endo, T., Miura, Y., Mekada, E., and Mihara, K. (2000) Identification of mammalian TOM22 as a subunit of the preprotein translocase of the mitochondrial outer membrane. *J. Biol. Chem.*, **275**, 31996-32002

19. Yano, M., Hoogenraad, N., Terada, K., and Mori, M. (2000) Identification and functional analysis of human Tom22 for protein import into mitochondria. *Mol. Cell. Biol.*, **20**, 7205-7213

20. Hönlinger, A., Bömer, U., Alconada, A., Eckerskorn, C., Lottspeich, F., Dietmeier, K., and Pfanner, N. (1996) Tom7 modulates the dynamics of the mitochondrial outer membrane translocase and plays a pathway-related role in protein import. *EMBO J.*, **15**, 2125-2137

21. Dekker, P. J. T., Ryan, M. T., Brix, J., Müller, H., Hönlinger, A., and Pfanner, N. (1998) Preprotein translocase of the outer mitochondrial membrane: Molecular dissection and assembly of the general import pore complex. *Mol. Cell. Biol.*, **18**, 6515-6524

22. Kolodiziej, P. A. and Young, R. A. (1991) Epitope tagging and protein surveillance. *Methods Enzymol.*, **194**, 508-519

23. Qadota, H., Ishii, I., Fujiyama, A., Ohya, Y., and Anraku, Y. (1992) RHO gene products, putative small GTP-binding proteins, are important for activation of the CAL1/CDC43 gene product, a protein geranylgeranyltransferase in *Saccharomyces cerevisiae*. *Yeast*, **9**, 735-741

24. Kanamori, T., Nishikawa, S., Shin, I., Schultz, P. G., and Endo, T. (1997) Probing the environment along the protein import pathways in yeast mitochondria by site-specific photocrosslinking. *Proc. Natl. Acad. Sci. USA*, **94**, 485-490

25. Daum, G., Böhni, P.C., and Schatz, G. (1982) Import of proteins into mitochondria. Cytochrome b2 and cytochrome c peroxidase are located in the intermembrane space of yeast mitochondria. *J. Biol. Chem.*, **257**, 13028-13033

26. Nakai, M., Endo, T., Hase, T., and Matsubara, H. (1993) Intramitochondrial protein sorting. Isolation and characterixation of the yeast MSP1 gene which belongs to a novel family of putative ATPases. J. Biol. Chem., 268, 24262-24269

Chapter 5

Concluding remarks

In order to reach their destinations, newly synthesized proteins have to traverse several biological membranes when the sites of their synthesis and of their functions are separated by biological membranes. Translocator complexes in the membranes mediate the process of protein translocation across the membranes. The questions of how proteins move across the membrane in a unidirectional manner with the aid of translocator complexes is a key issue in cell biology today.

In the present study, I have resolved the issue of intramitochondrial protein sorting to the intermembrane space (IMS). The question of whether proteins including cytochrome b_2 reach the IMS by crossing only the outer membrane or by entering the matrix first and then being re-exported to the IMS has been a matter of debate. I presented here the solid evidence for the former pathway to the IMS, the stop-transfer pathway. However, this conclusion, in turn, raised another problem. Since neither the energy of ATP hydrolysis nor the membrane potential can be apparently coupled to the protein translocation across the outer membrane, how can the protein go across the outer membrane in a unidirectional manner? I found that the transport of cytochrome b_2 fusion proteins to the IMS is driven by two distinct mechanisms, the Brownian ratchet model and the anchor diffusion model. The establishment of the well-defined *in vitro* system to drive protein translocation across the membrane by a Brownian ratchet mechanism also allows us for the first time to analyze in detail the conditions that affect the rate, direction etc. of the protein translocation.

The current models including the above two models assume limited interactions between the inner wall of the translocation pores and the translocating unfolded polypeptides. However this is not true. By using the site-specific photocrosslinking, I found that Tom40 functions as a membrane chaperone to provide a protein-conducting channel that is not a simple passive pore but offers an optimized environment for translocating unfolded proteins.

In the last, I addressed the question of what links the functions of the two

translocating systems in the two membranes. On the basis of the *in vitro* import analyses with mutant mitochondria lacking one or a few subunit of the TOM complex in the outer membrane, I found that Tom7 and the intermembrane space domain of Tom22 are involved in the transfer of the presequence from the TOM complex to the Tim23 complex in the inner membrane.

With all these new findings, I hope that the fog will be now breaking up around several key issues on mitochondrial protein traffic. The results presented here could also contribute to better understanding of the mechanistic aspects of protein translocation across not only the mitochondrial membranes but also cellular membranes in general.

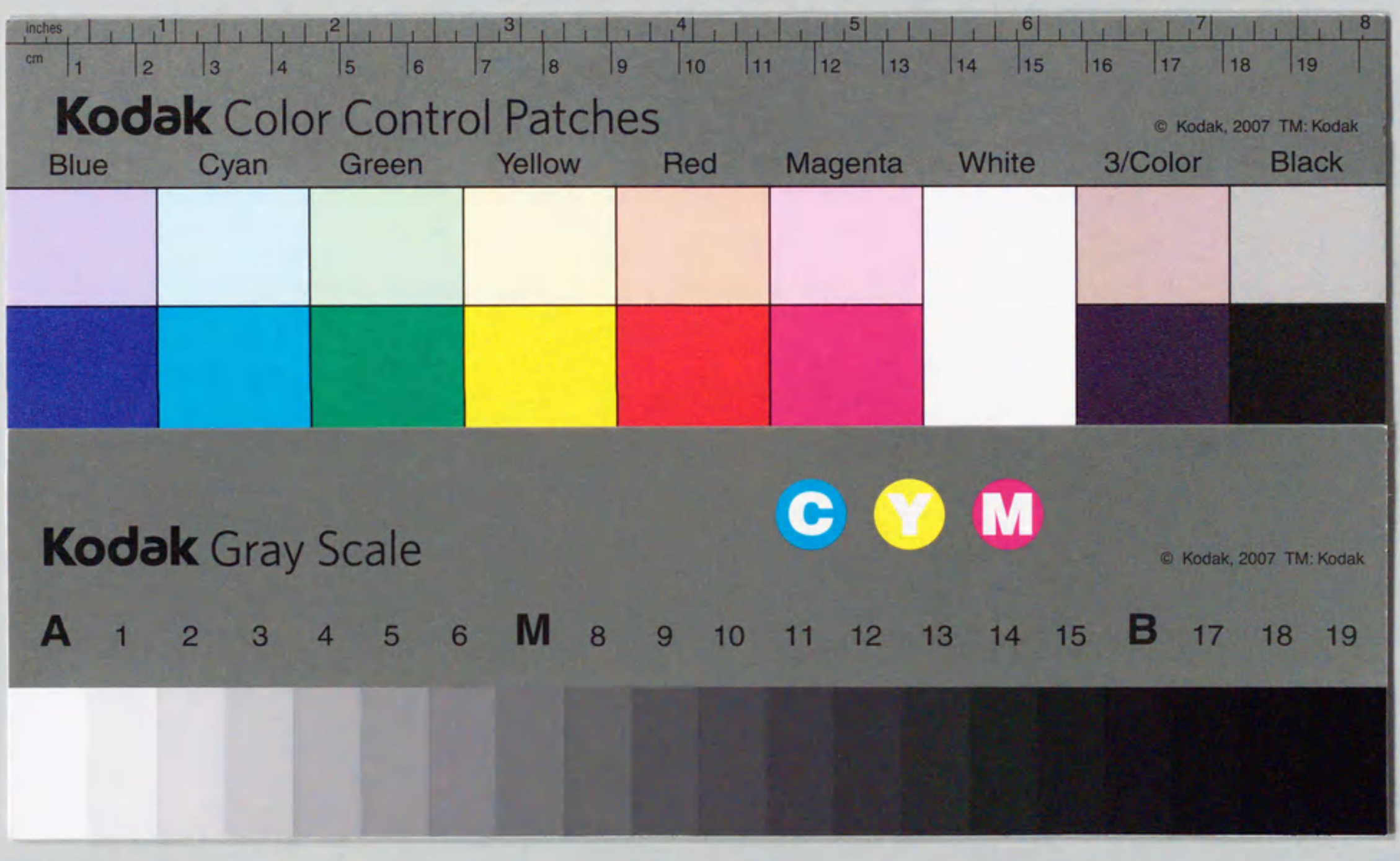
inches
cm
Kodak Color Control Patches
© Kodak, 2007 TM: Kodak
Blue
Cyan
Green
Yellow
Red
Magenta
White
3/Color
Black
Kodak Gray Scale
C
Y
M
© Kodak, 2007 TM: Kodak
A 1 2 3 4 5 6 M 8 9 10 11 12 13 14 15 B 17 18 19